Illinois U Library

The American Mineralogist

Journal of the Mineralogical Society of America

Vol. 35 JULY-AUGUST, 1950 Nos. 7 and 8

Contents

Morphology and structure of endellite and halloysite . . . . Thomas F. Bates, Fred A. Hildebrand, and Ada Swineford 463
Synthesis of some hydrated manganese minerals . . . . A. D. Wadsley 485
An occurrence of natrolite, andradite, and allanite in the Franklin Furnace quadrangle, New Jersey . . . . Charles Milton and Norman Davidson 500
An amplifier for differential thermal analysis . . . . Carl W. Beck 508
Studies of uranium minerals (III): Saléeite from Schneeberg, Saxony . . . . Mary E. Mrose 525
Studies of uranium minerals (IV): Johannite . . . . . . Cornelius S. Hurlbut, Jr. 531
Thermoelectric power and electrical resistivity of minerals . . . . . Maria Telkes 536
An occurrence of jarosite in altered volcanic rocks of Stoddard Mountain, San Bernardino County, California . . C. Osborne Hutton and Oliver E. Bowen 556
The crystal structure of ferroan zincian rhodochrosite . . . . Ernesto E. Galloni 562
Tin and indium in mica, as determined spectrochemically . . . . L. H. Ahrens and W. R. Liebenberg 571
X-ray diffraction patterns of asbestos . . . . Suzanne van Dijke Beatty 579
The alternating layer sequence of rectorite . . . . W. F. Bradley 590
Notes and news: Notes on arcanite, ammonian aphthitalite and oxammite . . . . Clifford Frondel 596
Demonstration of the double refraction of aragonite for rays traveling in the neighborhood of an optic axis . . . . Reynolds M. Denning 598
Mordenite from Tintic, Utah, and the discredited mineral arduinite . . . . Bronson Stringham 601
Book reviews 605
Mineralogical Society (London) 609
Constitution and By-laws of the Mineralogical Society of America 611
Nominations of Officers for 1951 614

MCMXIX

EDITOR
WALTER F. HUNT
ASSOCIATE EDITORS
MICHAEL FLEISCHER, ESPER S. LARSEN,
AUSTIN F. ROGERS, M. N. SHORT AND GEORGE TUNELL

Published bi-monthly by the Society

Mineralogical Society of America

ASSOCIATED WITH THE GEOLOGICAL SOCIETY OF AMERICA

President: **George Tunell**, University of California at Los Angeles, California.
Vice President: **Ralph E. Grim**, Illinois Geological Survey, Urbana, Illinois.
Secretary: **C. S. Hurlbut, Jr.**, Harvard University, Cambridge, Massachusetts.
Treasurer: **Earl Ingerson**, U. S. Geological Survey, Washington 25, D.C.
Editor: **Walter F. Hunt**, University of Michigan, Ann Arbor, Michigan.
Councilors: **H. H. Hess**, Princeton University, Princeton, New Jersey.
Clifford Frondel, Harvard University, Cambridge, Massachusetts.
Lewis S. Ramsdell, University of Michigan, Ann Arbor, Michigan.
E. F. Osborn, School of Mineral Industries, Pennsylvania State College, Pennsylvania.
John W. Gruner, University of Minnesota, Minneapolis, Minnesota.

The enlarged issues of this journal for 1950 are made possible by a grant from the Penrose Fund of the Geological Society of America.

The American Mineralogist—Journal of the Mineralogical Society of America

A journal containing articles on mineralogy, crystallography, petrography, and allied sciences, issued every two months. Contributions are invited from everyone.

Office of Publication, Mineralogical Laboratory, Ann Arbor, Mich.

The general conduct of the journal is in the hands of the Editor, **Walter F. Hunt**, Ann Arbor, Michigan. The council of the Mineralogical Society has appointed the following board of associate editors, to whom should be sent articles dealing with the special subjects indicated:

Michael Fleischer, U. S. Geological Survey, Washington, D.C., *New minerals.*
Esper S. Larsen, U. S. Geological Survey, Washington, D.C., *Optical crystallography.*
Austin F. Rogers, Stanford University, California, *Geometrical crystallography.*
M. N. Short, University of Arizona, Tucson, Arizona, *Mineralography.*
George Tunell, University of California at Los Angeles, *Structural crystallography.*

Contributors of leading articles are given without charge 100 reprints (without covers) of their article. If additional reprints are desired these can be purchased at the following rates:

Pages	*1–4*	*5–8*	*9–12*	*13–16*	*17–20*	*21–24*	*25–28*	*29–32*	*Covers*
Copies									
25	$3.50	$5.00	$ 8.00	$ 9.50	$11.00	$13.00	$15.00	$16.00	$4.90
50	3.80	5.55	8.80	10.40	12.10	14.20	16.40	17.50	5.50
75	4.10	6.10	9.60	11.30	13.20	15.40	17.80	19.00	6.10
100	4.40	6.65	10.40	12.20	14.30	16.60	19.20	20.50	6.70
Addl. C's	1.20	2.20	3.20	3.60	4.40	4.80	5.60	6.00	2.40

Cover Composition $1.55.

Sent to all members and fellows of the Mineralogical Society of America. Subscription price, $4.00 per year (single copies of normal issues, $1.00 plus postage).

Entered as second class matter at the post office at Menasha, Wis., under Act of March 3, 1879. Acceptance for mailing at the special rate of postage provided for in section 1103, Act of Oct. 3, 1917, paragraph 4 section 429 P. L. & R. authorized March 13, 1922.

Notices of change of address, orders, and remittances should be sent to Dr. Earl Ingerson, U.S. Geological Survey, Washington 25, D. C.

Printed by the George Banta Publishing Company, Menasha, Wisconsin

THE AMERICAN MINERALOGIST
JOURNAL OF THE MINERALOGICAL SOCIETY OF AMERICA

Vol. 35 JULY-AUGUST, 1950 Nos. 7 and 8

MORPHOLOGY AND STRUCTURE OF ENDELLITE AND HALLOYSITE

THOMAS F. BATES, FRED A. HILDEBRAND, AND ADA SWINEFORD,
The Pennsylvania State College, State College, Pennsylvania.

CONTENTS

Abstract........ 463
Introduction........ 464
Previous morphological studies........ 465
Morphology........ 466
  Kaolinite........ 466
  Halloysite (metahalloysite) and endellite (halloysite)........ 467
Correlation of experimental data with morphology........ 474
  X-ray........ 474
  Petrographic microscope........ 476
  Crystal growth........ 476
Structure........ 476
  Present concept and proposed structure........ 476
  Significance of the tubular structure........ 479
    Relation of endellite (halloysite) to halloysite (metahalloysite)........ 479
    Random structure in endellite (halloysite) and halloysite (metahalloysite)........ 480
    Effect of tubular structure on optical properties........ 480
    Dehydration characteristics........ 481
Applicability of proposed concept to other minerals........ 481
Conclusion........ 482
Acknowledgment........ 483
References........ 483

ABSTRACT

An electron microscope study of the minerals of the kaolinite group has revealed that halloysite (metahalloysite) crystals consist of hollow tubes which have commonly collapsed, or have split and partially or completely unrolled. There is no apparent morphological transition from these crystals to the pseudohexagonal plates characteristic of kaolinite, dickite, and nacrite. The mineral endellite (halloysite) is believed to consist of well-developed tubes which split upon dehydration to halloysite (metahalloysite). It is suggested that this change in morphology explains the irreversibility of the dehydration process.

Halloysite (metahalloysite) specimens from different localities show notable morphological differences due to original variation in tube size and the degree of subsequent splitting and unrolling. This may be a partial explanation of the discrepancies in optical data on this mineral which exist in the literature.

X-ray, optical, and crystal growth data indicate the relation of the tubular morphology to the sheet structure of the minerals.

The tubular form of endellite (halloysite) is explained by (1) the "misfit" of the silicon-oxygen and aluminum-hydroxyl layers in the 1:1 structural unit, (2) the larger intervening distance between the 1:1 units in endellite (halloysite) as compared with kaolinite, and (3) the presence of water between the units in endellite (halloysite). According to this picture the morphological change which occurs when halloysite (metahalloysite) is formed is a logical result of the removal of interlayer water. Values obtained from the electron micrographs for the inner diameters of the tubes are of the same order of magnitude as those obtained by calculations based on the proposed structure.

The structural interpretation of the morphology indicates that in a given tube the randomness of orientation (in the *a* and *b* crystallographic directions) of successive cylindrical sheets is partial rather than complete.

INTRODUCTION

The application of the electron microscope to the study of the clay minerals has posed a number of interesting problems. In the kaolinite group one of the most perplexing of these is the structural explanation of the morphological relationship between kaolinite and halloysite (metahalloysite).* The so-called laths of halloysite (metahalloysite) contrast markedly with the well-known pseudohexagonal plates of kaolinite despite the chemical similarity of the two minerals (see Table 1).

TABLE 1. PARTICLE SIZE AND HABIT OF THE KAOLIN MINERALS

Minerals of the Kaolin Group			
Mineral	Formula	Habit	Particle Size in Microns
NACRITE	$(OH)_8Al_4Si_4O_{10}$	pseudohexagonal plates	1000–5000
DICKITE	$(OH)_8Al_4Si_4O_{10}$	pseudohexagonal plates	1.0–500
KAOLINITE	$(OH)_8Al_4Si_4O_{10}$	pseudohexagonal plates	0.25–3000
ENDELLITE (HALLOYSITE)	$(OH)_8Al_4Si_4O_{10}\cdot 4H_2O$	tubes	0.01–15
HALLOYSITE (METAHALLOYSITE)	$(OH)_8Al_4Si_4O_{10}$	split tubes	0.01–15
ALLOPHANE	$(OH)_8Al_4Si_4O_{10}\cdot nH_2O$	irregular particles	<1

---

* The writers feel that the nomenclature of the kaolinite group is still problematical and that final solution of the problem should rest with an international committee. To avoid confusion both terms will be used for each of the minerals involved. The American usage is given preference because this article has been published in an American Journal.

The present paper deals with the morphology of kaolinite, halloysite (metahalloysite), and endellite (halloysite) and proposes a structural relationship to explain the physical and chemical properties and behavior of these minerals. The data were obtained by electron microscope and *x*-ray diffraction studies of 83 specimens from 66 localities.

A report of these investigations was presented at the meetings of the Mineralogical Society of America in November 1948 (Bates, Hildebrand, Swineford, 1949). Most data and theory in the following pages were given at that time.

PREVIOUS MORPHOLOGICAL STUDIES

Berthier described and named halloysite (metahalloysite) in 1826, and from that time until 1934 the mineral was regarded as an amorphous substance with no characteristic shape. An early worker (Mellor, 1908) described it in detail as irregularly shaped, amorphous granules, with irregular surfaces and a sponge-like structure. Rogers (1917) as a result of optical studies, listed halloysite (metahalloysite) in his review of the amorphous minerals. *X*-ray studies by Hofmann, Endell, and Wilm in 1934 indicated the crystalline nature of halloysite (metahalloysite). In the same year Ross and Kerr (1934, p. 142) concluded from *x*-ray data that halloysite (metahalloysite) "occupies a state of crystallinity intermediate between the microcrystalline particles of kaolinite and the finely divided, almost completely dispersed allophane." A study of dityndallism of various clay minerals by Marshall (1941) led him to the conclusion that halloysite (metahalloysite) forms platy particles with only slight elongation.

Early study of halloysite (metahalloysite) with the electron microscope (Dittler, 1941) revised the earlier concepts of its morphology. Shaw and Humbert (1941) observed from electron micrographs that the mineral typically occurs as split rods, each rod seemingly composed of twin sections. They concluded: "The marked differences in structure of kaolinite and halloysite are far greater than has been suspected on the basis of other evidence. . . . The split character of halloysite rods is of extreme interest. It is evident that crystal structures that have been proposed for halloysite do not explain its observed features."

In 1942 Kelley and Shaw determined the dimensions of halloysite (metahalloysite) particles from Maiden, Catawba County, N. C., by a combination of electron micrograph studies (for length and breadth) and hydrodynamic theory (for thickness). In calculating the third dimension they assumed that the halloysite (metahalloysite) particles are rod-shaped ellipsoids. They differentiated the two smaller axes on the basis of density in the electron micrograph and concluded that in some particles the breadth, *b*, is much greater than the thickness, *c*, whereas in others the *b* and *c* dimensions are about equal. By calculations from the *a* and *b* dimensions of halloysite (metahalloysite) particles in the 0.56 to 0.22 micron fraction, they found the ratio of $c:b$ to be between 1:5 and 1:1. On the other hand, the mean axial ratio for the 2 to 1 micron fraction of kaolinite was found to be 1:6.7.

In the same year Kelley and Page (1942, p. 176) described halloysite (metahalloysite) as "needle-like crystals." They concluded, as had Shaw and Humbert, that the electron microscope has "revealed peculiarities in the form of halloysite . . . , which do not seem to be explained by our present picture of [its] crystal structure and so may lead to a revision, or, at least, to a reconsideration of the validity of the structures that are accepted at the present time."

Eitel (1943, p. 43) wrote that halloysite (metahalloysite) crystals are not flaky, but show in electron micrographs a pronounced lath-shaped habit resembling that of the serpentine minerals. A later paper (Eitel and Radczewski, 1943) discussed the possibility of a chain structure of the type ($Si_4O_{10-10.5}$) as an explanation for the lath-like appearance of the particles.

Alexander, et al. (1943), observed in electron micrographs of halloysite (metahalloysite) from Lawrence County, Indiana, "geometrical arrangements of laths, serrations on the lath edges, and indentations of lath ends not hitherto noted." They called attention to lath intersections and terminations showing 60° angles and suggested that the halloysite (metahalloysite) fragments are "relic laths" of a larger plate-like unit. In electron microscope studies of morphology of these and other workers (Callaghan, 1948, pp. 20, 32) it has been assumed or stated that the morphology of the particles does not change upon dehydration in the electron microscope. In this connection Alexander, et al., also pointed out that halloysite (metahalloysite) has essentially the same morphological characteristics as endellite (halloysite), and this was considered to be one line of evidence indicating that halloysite (metahalloysite) forms from endellite (halloysite). The dark edges and notched ends of the particles were tentatively attributed by them to "longitudinal division."

Morphology

Kaolinite

Characteristic kaolinite crystals are euhedral pseudohexagonal flakes such as those illustrated in Fig. 1. The range in particle size (long diameter of the hexagonal plate) is given in Table 1. Since the morphological relationship of kaolinite and halloysite (metahalloysite) is of primary concern, particular emphasis in the following discussion is placed upon the departure of kaolinite particles from the ideal pseudohexagonal form. The most outstanding deviations observed in the present study are as follows:

(1) Euhedral crystals with prominent elongation in one direction (Fig. 2*A*);
(2) groups of overlapping oriented plates (Fig. 2*B*);

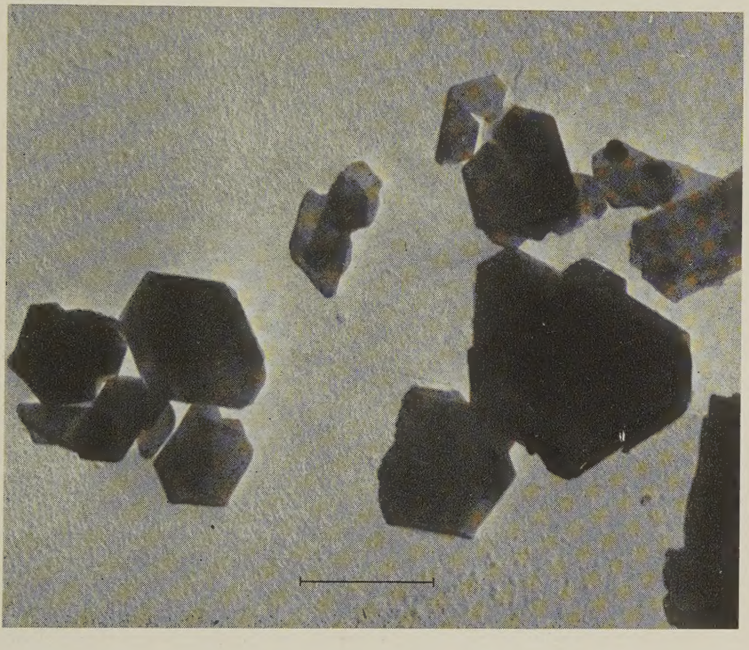

FIG. 1. Kaolinite from Banda, India, showing pseudohexagonal flakes. (The scale on all micrographs represents one micron.)

(3) subhedral to anhedral particles of small to medium size;
(4) pseudohexagonal plates with ragged edges and perforations suggestive of solution.

Two other facts may be noted about the morphology of kaolinite which have an important bearing on the relation of this mineral to endellite (halloysite) and halloysite (metahalloysite).

(1) There is no tendency for euhedral kaolinite particles to curl or roll up even though they may be appreciably elongated in one direction;
(2) there is no apparent morphological transition between kaolinite and halloysite (metahalloysite) crystals.

Halloysite (metahalloysite) and endellite (halloysite)

The present study shows that halloysite (metahalloysite) exists in the form of hollow tubes many of which are split longitudinally or have collapsed to form laths or ribbons. Structural considerations lead to the hypothesis that endellite (halloysite) crystals take the form of well-developed tubes and that strain produced by dehydration to halloysite (metahalloysite) causes the tubes to collapse, split, and commonly unroll. The large variation in morphology of different specimens of halloysite (metahalloysite) results from initial differences in particle size and from the degree of splitting and unrolling produced by dehydration.

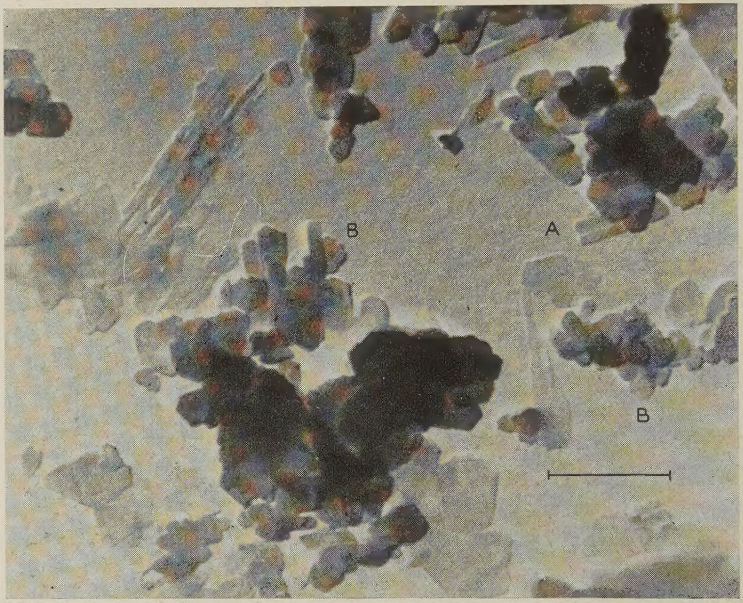

FIG. 2. Kaolinite from Zettlitz, Austria, showing (*A*) elongated, euhedral crystals, and (*B*) overlapping, oriented plates.

Tubes which on dehydration have apparently been modified only slightly or not at all are shown in halloysite (metahalloysite) from Leaky, Real County (formerly Edwards County), Texas, Fig. 3. Tubes at positions marked (*A*) show an oblique view of an end section. Double tubes, which are not uncommon, are seen at two positions marked (*B*). In such particles there is commonly an "empty" space between the inner and outer tubes, and if the particles are sufficiently translucent, the inner tube can be seen running the length of the outer one and in some cases projecting at both ends.

Splitting and unrolling may result in departure from the tubular shape. In Fig. 3 at (*C*) is a tube which has split and partly unrolled at one end. Such unrolling may produce a spatula-like form (Fig. 4*A*).

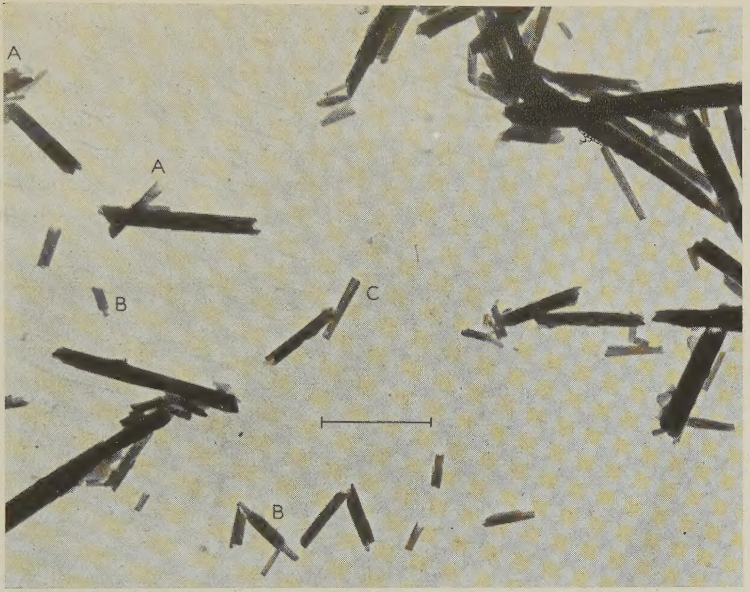

Fig. 3. Halloysite (metahalloysite) from Real County, Texas. (A) Oblique view of end section; (B) double tubes (tube in tube); (C) split and partially unrolled tube.

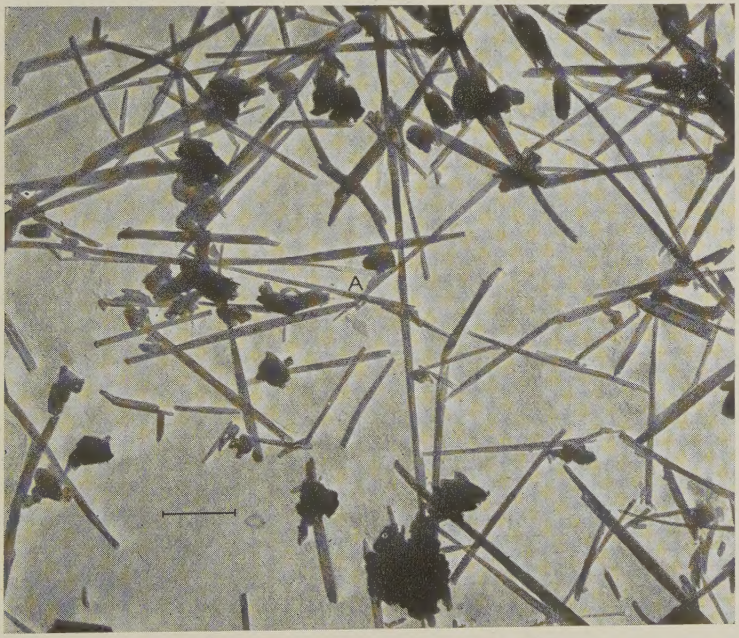

Fig. 4. Halloysite (metahalloysite) from Webster, Jackson County, North Carolina, showing long hollow tubes, some of which have collapsed. (A) Spatula produced by splitting and unrolling.

The width of the spatula "blade" in relation to the circumference of the "handle" affords a measure of the degree of unrolling. The diameter of the tube is 440 Å and therefore its circumference or the width of the resulting spatula blade should be 1382 Å. The measured width of the blade is 1000 Å. The discrepancy indicates that complete unrolling has not been achieved.

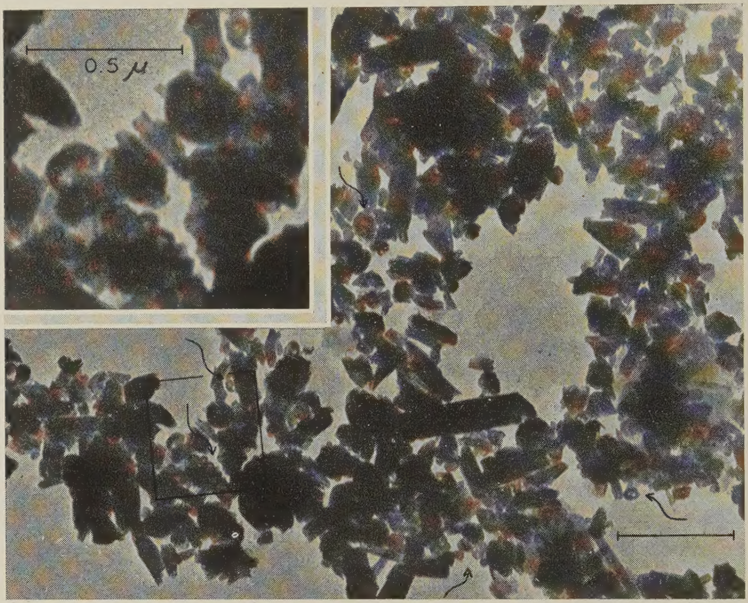

Fig. 5. Halloysite (metahalloysite) from Beuthen, Silesia. Arrows indicate some of the tubular cross-sections.

Figure 5 of halloysite (metahalloysite) from Beuthen, Silesia, shows many tubes in cross section. The latter are observed most frequently in halloysite consisting of short, poorly developed crystals since these have a better chance of standing "on end" when they settle on the collodion film than do the more elongated tubes.

A number of other features in the micrographs are of interest. In some samples the surfaces of the tubes show semicircular concavities or indentations (Fig. 6). Since many of these indentations are of similar radius of curvature to that of other tubes, it is believed that each concavity represents the place where an intergrown tube, crossing at an angle, has been broken out. If such is the case the shape of the indentation is further evidence that the particles are cylindrical. A few of the larger tubes have a cottony appearance possibly resulting from shredding at the surface.

Although splitting and unrolling may result in the formation of well-defined rectangular laths, no example has been found of a hexagonal-shaped flake which was the consequence of such a process. Furthermore, the tubes do not show terminations of a uniform character. The ends are jagged and commonly frayed as if the tubes had been broken. Even in those particles in which the ends are smooth and possibly not the result of fracturing, the angle of termination of the tube with its axis is not constant.

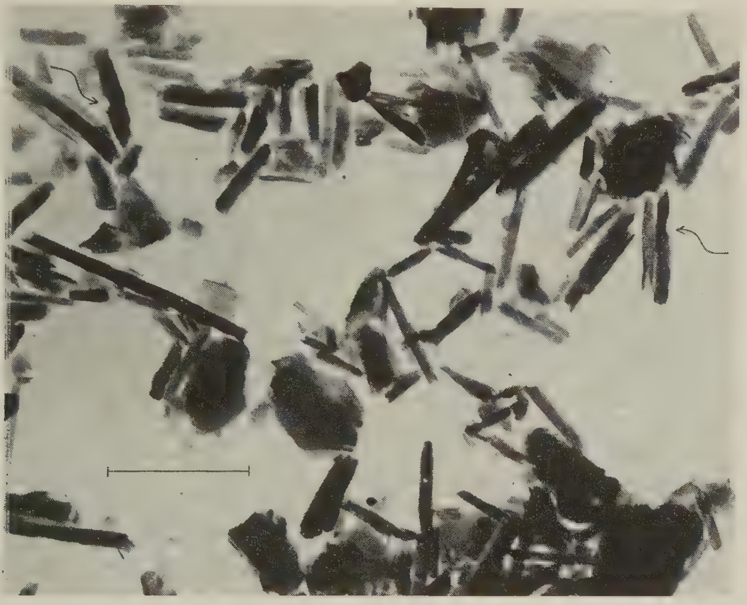

FIG. 6. Halloysite (metahalloysite) from Chatham County, North Carolina. Arrows point to semicircular concavities in some tube surfaces suggesting former presence of intergrown tubes.

Table 2 presents data on diameter and wall thickness of 26 tubes selected from 7 micrographs and of necessity chosen for their clarity and ease of measurement. The outside diameters of the tubes measured range from 400 to 1900 Å, with a median value of 700 Å. The diameters of the holes range from 200 to 1000 Å and average 400 Å. The thickness of the walls has a narrower range of 100 to 700 Å and averages 200 Å.

Measurement of the widths of 1120 halloysite (metahalloysite) particles in 26 electron micrographs, regardless of the degree of collapse or unrolling, shows a range of from 100 to 6700 Å, and a median width of 860 Å. The frequency distribution tends to be log normal.

The morphological variations in halloysite (metahalloysite) resulting from initial differences in particle size and degree of splitting and unrolling are shown in Figs. 4, 7, and 8. Figure 4 of halloysite (metahalloysite) from Webster, North Carolina, illustrates long, thin, well-defined tubes, whereas halloysite (metahalloysite) from Lookout, Alabama, Fig. 8, consists of irregularly shaped flaky particles many of which appear to tbe the result of the splitting and unrolling of short tubes. Most halloysites have crystals which, from the standpoint of morphology, fall between these two extremes.

TABLE 2. MEASUREMENTS OF OUTSIDE DIAMETER, INSIDE DIAMETER, AND WALL THICKNESS OF 26 HALLOYSITE (METAHALLOYSITE) TUBES

Locality	Outside Diam. (Angstroms)	Inside Diam. (Angstroms)	Wall Thickness	
			(Angstroms)	No. of 1:1* Units
Beuthen, Silesia	1000	600	200	28
Beuthen, Silesia	1600	600	500	69
Beuthen, Silesia	600	200	200	28
Beuthen, Silesia	600	200	200	28
Beuthen, Silesia	1700	700	500	69
Beuthen, Silesia	1700	300	700	99
Beuthen, Silesia	600	400	100	14
Beuthen, Silesia	1900	500	700	99
Beuthen, Silesia	400	200	100	14
Beuthen, Silesia	500	300	100	14
Beuthen, Silesia	600	400	100	14
Beuthen, Silesia	600	400	100	14
Beuthen, Silesia	500	300	100	14
Beuthen, Silesia	1400	600	400	56
Beuthen, Silesia	700	300	200	28
Beuthen, Silesia	600	300	200	28
Beuthen, Silesia	800	400	200	28
Beuthen, Silesia	800	400	200	28
Beuthen, Silesia	1700	300	700	99
Beuthen, Silesia	400	200	100	14
Real County, Texas	800	400	200	28
Real County, Texas	1200	1000	100	14
Hickory, North Carolina	700	500	100	14
Ely, Nevada	400	200	100	14
Nelson County, Virginia	900	600	200	28
Maiden, North Carolina	400	200	100	14

* Based on (001) spacing of kaolinite.

Because of the ease with which endellite (halloysite) changes to hal-

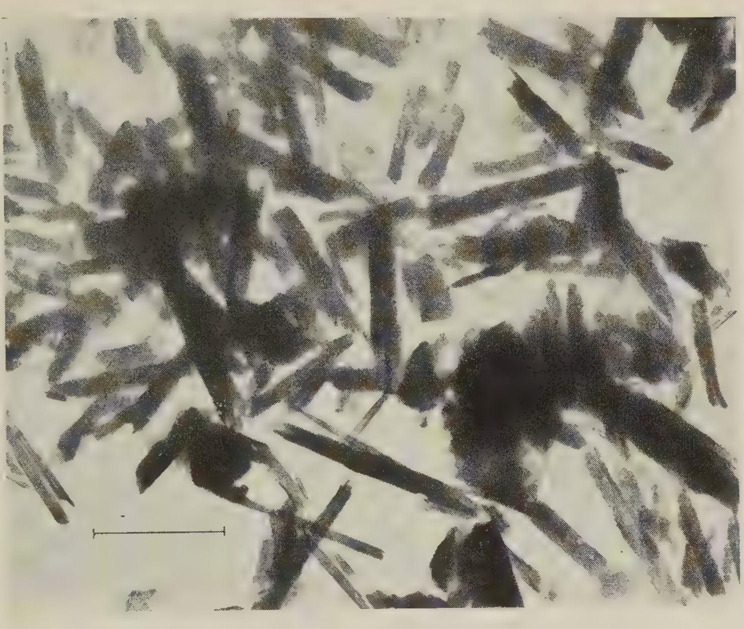

FIG. 7. Halloysite (metahalloysite) from Real County, Texas.

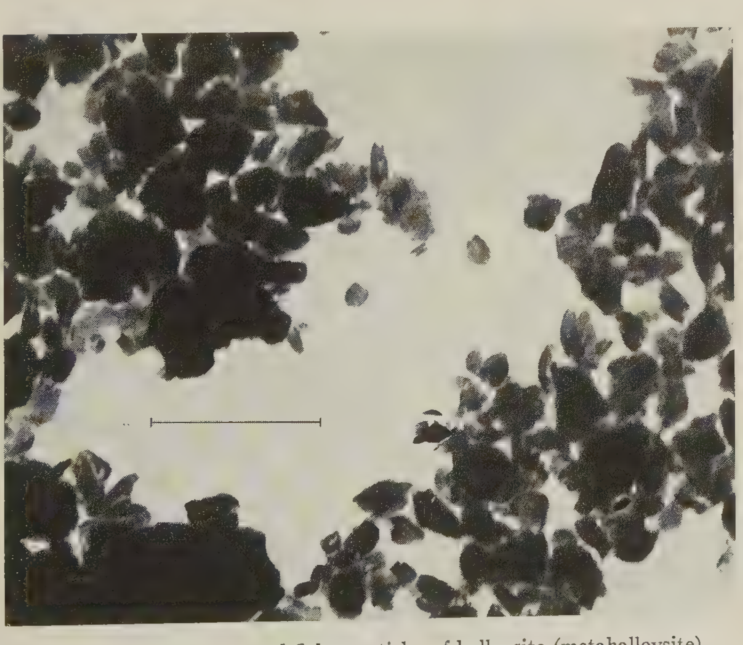

FIG. 8. Irregularly shaped flaky particles of halloysite (metahalloysite) from Lookout, Alabama, formed by splitting and unrolling of short tubes.

loysite (metahalloysite) it has been assumed by previous workers (Alexander, et al., 1943; Callaghan, 1948) that the heat of the electron beam and the vacuum of the electron microscope effect immediate dehydration of endellite (halloysite) when the mineral is placed in the instrument for observation, and further that, in spite of the loss of water, the morphology of the particles does not change. The present writers agree that dehydration probably occurs, but, as a result of structural relationships to be discussed later in this paper, do not concur in the belief that the morphology of the particles remains unchanged. It is hoped that in subsequent electron microscope work using replica techniques the morphology of endellite (halloysite) may be observed and studied.

Correlation of Experimental Data with Morphology

X-ray, optical, and crystal growth data suggest the following relationships between the tubular form of the crystals and the sheet structure which has been assigned to endellite (halloysite) and halloysite (metahalloysite) (Mehmel, 1935; Hendricks, 1938; Edelman and Favejee, 1940). These relationships are represented diagrammatically in Fig. 9.

1. The wall of the tube consists of curved sheets which in the micas and kaolinite are planar.
2. The *c* axis for any section of the tube is nearly perpendicular to a plane tangent to the tube at that point.

X-Ray

The differences in the *x*-ray patterns of kaolinite, halloysite (metahalloysite), and endellite (halloysite) have been studied recently by Brindley and Robinson (1948). Diffraction peaks from the (001) planes are symmetrical but more diffuse in halloysite (metahalloysite) than in kaolinite. Other peaks in halloysite (metahalloysite) take the form of asymmetric bands formed by diffraction from two-dimensional gratings as a result of random structure in the *a* and *b* directions.

The diffuse character of the (00*l*) diffractions may be explained by the curvature of the (001) planes, as brought out in exaggerated form in Fig. 9. The ratio of height to breadth of the (001) peak at 7.5 to 7.1Å from *x*-ray spectrometer patterns of dickite, kaolinite, and halloysite (metahalloysite) is shown in Table 3. Variation in particle size affects this ratio and is probably responsible for part of the difference between kaolinite and dickite. However, electron micrographs of kaolinite and halloysite (metahalloysite) indicate that here the particle size difference is too small to account for the entire variation in peak height to breadth ratios. The (001) diffractions from badly split and unrolled halloysites (metahalloysites) are similar to those from nearly tubular particles,

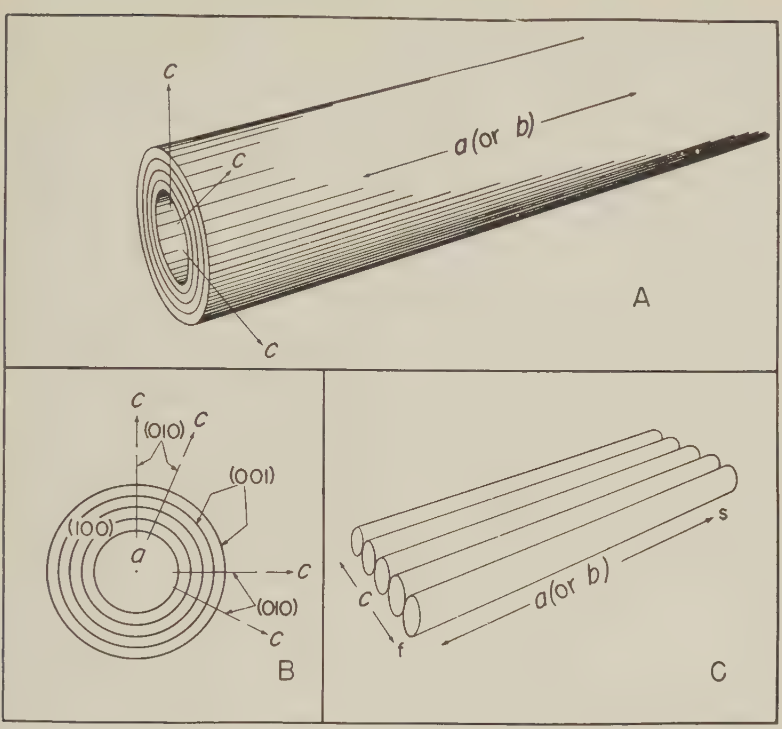

FIG. 9. Proposed relation of morphology to structure in endellite (halloysite).

A. Tube in perspective.

B. Cross section showing crystallographic axes and major planes. $c=n\alpha$, $a=n\beta$, $b=n\gamma$ (assuming optical similarity to kaolinite).

C. Character of optical elongation in oriented aggregate. f = fast vibration direction, s = slow vibration direction.

TABLE 3. RATIOS OF HEIGHT TO BREADTH OF THE (001) PEAK IN x-RAY SPECTROMETER PATTERNS OF DICKITE, KAOLINITE AND HALLOYSITE (METAHALLOYSITE)

Mineral	Number of Specimens	$\frac{\text{Height}}{\text{Breadth}}$ (001) peak		
		Maximum	Minimum	Average
Dickite	6	35.6	20.0	27.6
Kaolinite	13	32.4	9.0	17.9
Halloysite (Metahalloysite)	34	13.0	0.8	5.1

suggesting that some curvature of the sheet remains even though the tube has split or collapsed.

It is doubtful if the arrangement of sheets in concentric cylinders would, of itself, produce the asymmetric bands found in x-ray patterns of halloysite (metahalloysite) and endellite (halloysite) for all reflections except those from (001). Without additional randomness of structure, reflections from planes (100) perpendicular to the tube axis (see Figure 9*B*) would be sharp and symmetrical while those from (010) would probably be diffuse but would show no asymmetry.

Petrographic Microscope

Grim (1942, p. 248) wrote that "careful optical work with halloysite shows certain peculiarities difficult to explain on the basis of suggested structures." In the present study, petrographic microscope work on oriented aggregates indicates that the tubes have positive elongation, and the measured birefringence is 0.002 ± .001. If it is assumed that the indices of halloysite (metahalloysite) bear the same relationship to each other and to the structure as do those of kaolinite, this elongation and a similar birefringence are to be expected from a sheet structure developed in tubular form. The probable relationships are shown in Fig. 9*C* and are discussed in more detail later in this report.

Crystal Growth

It is well established that growth in the micas and in kaolinite, nacrite, and dickite takes place most rapidly at the edges of the sheets, extending them outward. Since the tubes of endellite (halloysite) apparently grow most rapidly in length, it is logical that the ends of the tubes represent the edges of the sheets.

STRUCTURE

Present Concept and Proposed Structure of Endellite (Halloysite)

Figure 10 gives a diagrammatic picture of the structure of endellite (halloysite) proposed by Hendricks (1938). As in the other kaolin minerals there is a 1:1 structure in which a modified gibbsite sheet is bonded to a silicon-oxygen sheet. The height of the resulting unit in the c direction is 4.51 Å in each of the minerals. In the mineral gibbsite the six hydroxyl ions on one side of the unit cell occupy a distance of 8.62 Å, while in the silicon-oxygen sheet in kaolinite the corresponding six oxygen ions occupy a distance of 8.93 Å. Thus, as Pauling (1930) pointed out, the two sheets which make up the structure are not a perfect fit. A hypothetical single 1:1 unit of kaolinite, free of neighboring ions, might have a b_0 dimension of 8.93 Å compatible with the spacing of the oxygen ions on one side and a similar dimension of 8.62 Å typical of the hydroxyl ions on the other. In actual fact, however, since adjoining units are less than 3 Å away the six oxygen ions of one unit apparently "stretch" the opposing hydroxyl ions to fit the cell dimension of 8.93 Å.

It is here proposed that in endellite (halloysite) (Fig. 11*B*) as a result of the greater distance of 5.74 Å and the presence of water molecules between the 1:1 units, the hydroxyl ions are only slightly, if at all, subject to "stretching" forces from opposing oxygen layers of neighboring units. The six hydroxyl ions are, therefore, free to approach their normal spacing of 8.62 Å while the six oxygen ions on the opposite side of the same unit occupy a distance of 8.93 Å. If it is assumed that the "vertical" bonds within the unit remain of equal length relative to each other, a curvature must result such as that shown in exaggerated form in Fig. 11*C*. A simple calculation shows that the inner diameter of the resulting

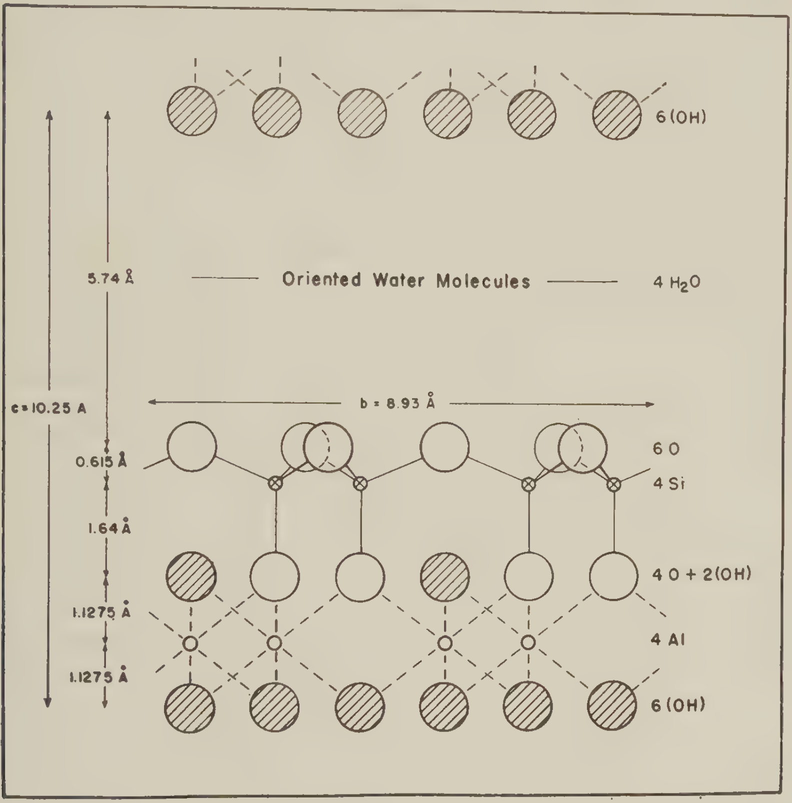

FIG. 10. Structure of endellite (halloysite) according to Hendricks.

cylinder would be 250.8 Å. This is of the same order of magnitude as the inner diameter of the smallest tubes as shown in Table 2.

These structural relationships are to be expected in a tube with a wall of unit cell thickness.* If the diameter is smaller or larger the lattice

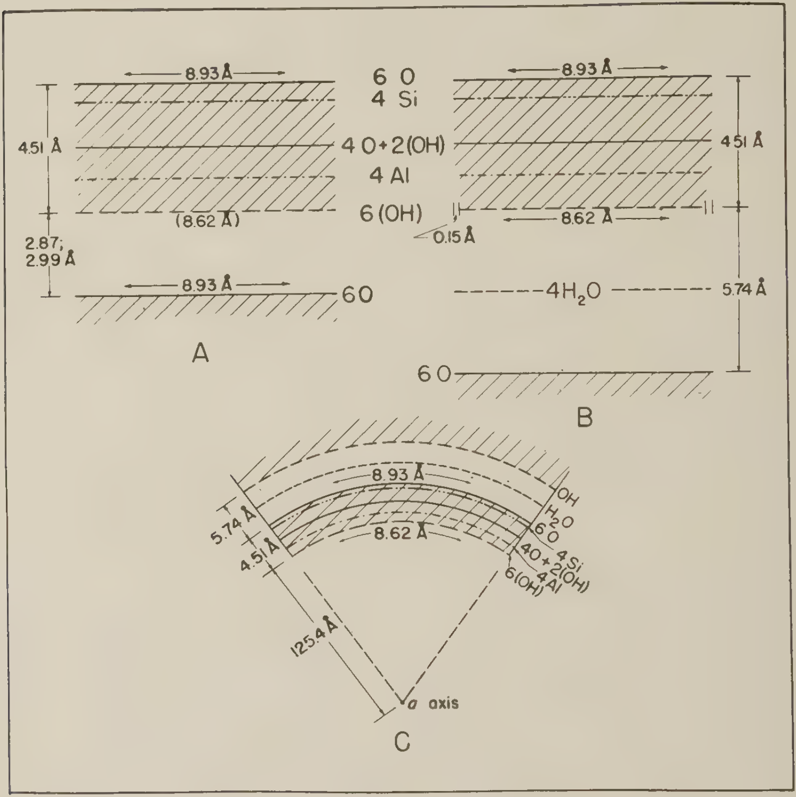

FIG. 11. Diagrammatic representation of the structure of kaolinite and endellite (halloysite).

A. Arrangement of layers in kaolinite.

B. Arrangement of layers in endellite (halloysite) according to Hendricks.

C. Proposed arrangement of endellite (halloysite) layers.

would be strained as a result of the departure from the ideal relationship of oxygen to hydroxyl spacings. If the inner diameter is smaller, the six hydroxyl ions would have to be compressed to occupy a distance less than 8.62 Å relative to the 8.93 Å spacing of the oxygen ions. Because of this limiting condition, a hollow structure would be expected. On the other hand, for tubes with a larger radius of curvature, the hydroxyl ions must occupy a distance greater than 8.62 Å. The resulting strain makes the addition of subsequent layers more difficult. The fuzzy appearance of the edges of some of the largest tubes possibly indicates that the limiting radius of curvature has been reached and that additional units tend to shred off because they are under too great a tensional strain.

---

* On the basis of the unit cell of kaolinite established by Brindley and Robinson (1946).

The foregoing analysis explains curvature about the *a* axis and the units apply to the length of the unit cell in the *b* direction. If the a_0 values are used, the oxygen ions extend 5.14 Å, the corresponding hydroxyl ions 5.06 Å (as in gibbsite) and the resulting tube diameter would be 570 Å. Perhaps the differences in radius of curvature about *a* and about *b* have some bearing upon the existence of double tubes (Fig. 3*B*).

Significance of the Tubular Structure

Relation of endellite (halloysite) to halloysite (metahalloysite). –This concept of the structure of endellite (halloysite) readily accounts for the longitudinal splitting of the tubes when the material dehydrates to halloysite (metahalloysite). Upon loss of the oriented water molecules between the layers, adjoining units come together from a distance of 5.4 Å to approximately 3 Å. The hydroxyl ions, which in the tubular form occupied approximately their normal spacing along b_0 of 8.62 Å and were presumably under little strain in this direction, now become subject to the forces of the closer oxygen ions and are "stretched" to a distance approaching 8.93 Å. As a result the curved sheets tend to become planar and must either split or collapse. Once started, a split would continue along the length of the tube. Unrolling presumably further relieves the strained condition.

The incomplete reversibility of the change from endellite (halloysite) to halloysite (metahalloysite) has never been adequately explained. The picture presented here suggests that the splitting or collapse of the tubes not only relieves the strain set up on dehydration but also tends to prevent return to the hydrated state. It is conceivable that in some crystals the tubular structure might be sufficiently strong to prevent opposing oxygen and hydroxyl layers of adjacent units from coming together when the intervening layer of oriented water molecules is removed. Such tubes would be pseudomorphs of halloysite (metahalloysite) after endellite (halloysite) and could presumably be completely rehydrated. Whether or not they might be abundant in a particular sample or could indeed exist at all would depend upon the structural rigidity of the tubes, but no data are available on this point. Bradley (1945, p. 706) and MacEwan (1948, pp. 356, 357) have shown that when the interlayer water of endellite is replaced with various organic complexes the strong diffraction effect from the (001) planes is displaced from 10.1 Å to values as high as 11.6 Å. This indicates that the tubes may be flexible enough to "absorb" a thirteen per cent increase in radius, and Hendricks (personal communication) has suggested that the crystals may actually be made up of many overlapping curved sheets which can shift slightly over one another. In any case, the well-defined nature of the longitudinal splitting indicates that upon dehydration all the concentric cylindrical sheets of the tube act as a unit.

Random structure in endellite (halloysite) and halloysite (metahalloysite). —It has been shown that if the tubes are developed parallel to the a axis the minimum inner diameter is theoretically 250 Å; if parallel to b, 570 Å. Conceivably the tube axis might be parallel to some intermediate direction in the plane of the sheet in which case the theoretical minimum inner diameter would be between these two extremes. In any of these cases, however, it is likely that in any single crystal the tube axis is parallel to the same crystallographic direction in each of the successive cylindrical sheets which form the tube. This means that the orientation of one unit with respect to others above and below it along the c axis is not completely random but must be partially ordered. Thus, in a tube developed parallel to the a axis, disorder produced by shifting of successive cylindrical sheets parallel to the tube axis (translation parallel to a) or produced by revolution about the tube axis (translation parallel to b), would be permissible. On the other hand, if complete disorder were produced by random rotation about the normal to the sheet (with or without random translation) the tube axis could not have the same crystallographic direction in successive 1:1 units.

As brought out indirectly by Warren (1941, p. 693), in discussing x-ray diffraction effects in random layer lattices, there is no difference in the powder pattern from layers related by random translation and the pattern from those related by random translation plus random rotation. Therefore, this picture of partial rather than complete disorder in the orientation of units stacked parallel to the c axis supplements interpretations of the x-ray data (Hendricks, 1942; Brindley and Robinson, 1948, p. 399).

The case for partial rather than complete disorder in the stacking of 1:1 units is strengthened by birefringence measurements on oriented aggregates. If randomness of successive units were complete, compensation would take place, and no interference color would be visible. Many workers have measured birefringence on oriented aggregates of halloysite (metahalloysites) and, as mentioned previously, present work yielded a value for n_γ (or n_β) $- n_\alpha$ equal to $0.002 \pm .001$.

Effect of tubular structure on optical properties.—Optical data on halloysite (metahalloysite) and endellite (halloysite) are conflicting. Published values for the indices of refraction vary from 1.528 to 1.648 (Correns and Mehmel, 1936, p. 337; Ross and Kerr, 1934, p. 138; Alexander, et al., 1943, p. 12). The birefringence is usually described as less than 0.001, although measurements of the double refraction of endellite suspensions oriented by an electric field (Whiteside and Marshall, 1944, p. 33) gave values of 0.0050 ± for hydrogen saturated halloysite (metahalloysite) and 0.0112 for the same material when sodium saturated. Because of conflicting results obtained from studies of aggregates of halloysite (metahalloysite) crystals, Grim (1942, p. 249) points out that " . . . it would seem . . . that halloysite is composed of units that may easily vary from definite alignment to a random orientation."

It is not unlikely that the birefringence of halloysite (metahalloysite) is similar to that of kaolinite (0.006) and that the observed variation is the result of the tubular structure and of the degree of splitting and unrolling which has taken place in different specimens. In a complete tube, because of the variable direction of the c axis in a plane approximately perpendicular to the tube axis (Fig. 9*B*), the birefringence would change from a minimum value of $n_\gamma - n_\beta$ (0.001 in kaolinite) along the crest of the tube to a maximum value of n_γ (or n_β) $- n_\alpha$ along each edge. In an aggregate of oriented tubes (Fig. 9*C*) the resultant value would probably lie between these extremes. A tube that had completely unrolled or collapsed would have a birefringence of only $n_\gamma - n_\beta$ so that even in oriented aggregates the material would appear nearly isotropic.

Dehydration characteristics.—The role of adsorbed and interlayer water has been carefully evaluated by Brindley and Robinson (1948). The tubular structure suggests that in future dehydration studies the possible effect of capillary water should also be considered.

Applicability of Proposed Concept to Other Minerals

The two fundamental structural conditions which exist in endellite (halloysite) and cause the crystals to be tubular are: (1) a sheet structure of the 1:1 type in which the sheets have slightly different dimensions in the a_0 and b_0 directions; and (2) bonds between the 1:1 units which are not sufficiently strong to overcome this discrepancy by "stretching" the ions on the "bottom" of one unit to fit the dimensions of the ions on the "top" of the opposing unit. Similar conditions may well exist in other 1:1 sheet structure minerals and a number of possibilities are being investigated. Serpentine appears to be the most promising, for Warren and Hering (1941) and Aruja (1945) have shown that both antigorite and chrysotile possess layer structures. It would seem likely that a morphological and structural analogy to the kaolin minerals may exist, in which case chrysotile fibers would actually be hollow cylindrical crystals similar to those discussed in this paper.

CONCLUSION

Electron microscope studies show that halloysite (metahalloysite) occurs as modified hollow tubes. Because of the vacuum and the heat of the electron beam endellite (halloysite) has not been observed directly in the electron microscope but structural evidence combined with these studies of halloysite (metahalloysite) suggests that endellite (halloysite) consists of well-developed tubes which collapse, spilt, and unroll upon dehydration. Although it is possible that some crystals do not change form upon dehydration because of the structural strength of the cylindrical 1:1 units which form the tube, true pseudomorphs of halloysite (metahalloysite) after endellite (halloysite) are probably rare. In general, the presence of split or collapsed rather than complete tubes is judged to be one of the major differences between the two minerals. The present work not only supports the conclusion of others that halloysite (metahalloysite) is formed by dehydration of endellite (halloysite) but indicates that this is the only way in which it is produced.

Data on the minerals lead to the belief that (1) the wall of the tube consists of curved (001) sheets, and (2) the *c* axis for any point on the tube is nearly perpendicular to a plane tangent to the tube at that point. The axis of the tube may be parallel to either the *a* or *b* axis, or possibly to any intermediate crystallographic direction in the plane of the sheets.

The proposed explanation of the tubular structure takes account of (1) the discrepancy of dimensions of the silicon-oxygen sheets as opposed to the modified gibbsite sheets, (2) the larger intervening distance between the 1:1 units in endellite (halloysite) as compared to kaolinite. Removal of the water layers on dehydration of endellite (halloysite) brings the hydroxyl layer of one unit closer to the oxygen layer of the next and causes readjustment of the spacing of the hydroxyl ions. The resulting strain manifests itself in the form of collapsed or split and partially unrolled tubes of halloysite (metahalloysite).

It has been shown that the inner diameters of halloysite (metahalloysite) tubes measured from electron micrographs range from 200 to 1000 Å and are of the same order of magnitude as the values obtained by calculations based on the proposed structure, namely 250 to 570 Å. As would be expected from the structural picture, the spread of the outside diameters is somewhat greater—400 to 1900 Å.

As a result of the tubular form and the optical birefringence of oriented aggregates, it is proposed that the orientation of successive cylindrical 1:1 units in a given tube is not, as hitherto believed, completely random.

Rather, there is partial randomness produced by translation along and rotation about the tube axis.

The varied indices of refraction and birefringence assigned to halloysite (metahalloysite) by previous workers are explained on the basis of the difference in optical orientation produced by tubes in various states of splitting and unrolling.

Finally, in clays of natural occurrence no morphological transition has been observed between the typical pseudohexagonal plates of kaolinite and the hollow tubes of endellite (halloysite) and halloysite (metahalloysite).

ACKNOWLEDGMENT

This research was made possible by Penrose funds granted by the Geological Society of America. We wish to thank the officers of the Society and the members of the Committee on Projects for their cooperation.

Inasmuch as the project was limited in scope to an electron microscope investigation supplemented by *x*-ray study, it was important to obtain samples which had been previously studied with respect to chemical composition, optical characteristics, and origin. We wish particularly to thank Dr. Clarence S. Ross who supplied a large number of samples from his excellent collection, and Dr. William Foshag who gave us full use of the extensive collection of the United States National Museum. Specimens were kindly furnished by Samuel G. Gordon formerly of the Philadelphia Academy of Sciences and Dr. Jasper L. Stuckey, State Geologist of North Carolina, and we are indebted to many other contributors for their help.

The theoretical aspects of the research have been discussed with many workers in the field of clay mineralogy and their pertinent suggestions have been most helpful. We particularly wish to thank Drs. Sterling B. Hendricks, G. W. Brindley, Ralph E. Grim, Paul F. Kerr, and Wilhelm Eitel for the careful consideration they have given to the data and interpretations.

The consistent help of colleagues at the Pennsylvania State College, particularly Drs. J. C. Griffiths, P. D. Krynine, and E. F. Osborn, is gratefully acknowledged.

The electron micrographs were taken by Mary V. Black who handled this part of the work with much patience and skill.

REFERENCES

ALEXANDER, L. T., FAUST, G. T., HENDRICKS, S. B., INSLEY, H., AND MCMURDIE, H. F. (1943), Relationship of the clay minerals halloysite and endellite: *Am. Mineral.*, **28,** 1–18.

ARUJA, ENDEL (1945), An *x*-ray study on the crystal structure of antigorite: *Mineral. Mag.*, **27,** 65–74.

Bates, T. F., Hildebrand, F. A., and Swineford, A. (1949), Electron microscopy of the kaolin minerals: *Am. Mineral.*, **34,** 274.

Berthier, P. (1826), Analyse de l'halloysite: *Ann. Chim. Phys.*, **32,** 332–335.

Bradley, W. F. (1945), Diagnostic criteria for clay minerals: *Am. Mineral.*, **30,** 704–713.

Brindley, G. W., and Robinson, K. (1946), The structure of kaolinite: *Mineral. Mag.*, **27,** 242–253.

——— (1948), *X*-ray studies of halloysite and metahalloysite. Part I, The Structure of metahalloysite, an example of a random layer lattice: *Mineral. Mag.*, **28,** 393–406.

Callaghan, Eugene (1948), Endellite deposits in Gardner Mine Ridge, Lawrence County, Indiana: *Indiana Dept. of Conservation, Division of Geol., Bull.* **1,** p. 1–47.

Correns, C. W., and Mehmel, M. (1936), Über den optischen und röntgenographischen Nachweis von Kaolinit, Halloysit und Montmorillonit: *Zeits. Krist.*, **94,** 337–348.

Dittler, E. (1941), More recent knowledge of the nature of clay: *Tonind.-Ztg.*, **65,** p. 515, 528.

Edelman, C. H., and Favejee, J. Ch. L. (1938), On the crystal structure of montmorillonite and halloysite: *Zeits. Krist.*, **102,** 417–431.

Eitel, W. (1943), Das Elektronmikroskop und seine Anwendung auf keramische Probleme: *Berichte der Deutschen Keramischen Gesellschaft*, **24,** 37–53.

Eitel, W., and Radczewski, O. E. (1943), Zur Kenntnis des Metahalloysite: *Abhandl. Preuss. Akad. Wiss. Jahrgang. Math.-naturw. Klasse. Nr.* **5,**

Grim, R. E. (1942), Modern concepts of clay materials: *Jour. Geol.*, **50,** 225–275.

Hendricks, S. B. (1938), On the crystal structure of the clay minerals: Dickite, halloysite, and hydrated halloysite: *Am. Mineral.* **23,** 295–301.

——— (1942), Lattice structure of clay minerals and some properties of clays: *Jour. Geol.*, **50,** 276–290.

Hofmann, U., Endell, K., and Wilm, D. (1934), Röntgenographische und kolloidchemische Untersuchungen über Ton: *Angew. Chem.*, **47,** 539–547.

Kelley, O. J., and Shaw, B. T. (1942), Studies of clay particles with the electron microscope. III, Hydrodynamic considerations in relation to shape of particles: *Soil Sci. Soc. Am., Proc.*, **7,** 58–68.

Kelley, W. P., and Page, J. B., (1942) Criteria for the identification of the constituents of soil colloids: *Soil Sci. Soc. Am., Proc.*, **7,** 175–181.

MacEwan, D. M. C. (1948), Complexes of clays with organic compounds. I. Complex formation between montmorillonite and halloysite and certain organic liquids: *Faraday Soc. Trans.*, **44,** 349–368.

Marshall, C. E. (1941), Studies in the degree of dispersion of the clays. IV. The shapes of clay particles: *Jour. Phys. Chem.*, **45,** 81–93.

Mehmel, M. (1935), Über die Struktur von Halloysit und Metahalloysit: *Zeits. Krist.*, **90,** 35–42.

Mellor, J. W. (1908), A note on the nomenclature of clays: *Trans. Eng. Cer. Soc.*, **8,** 23–30.

Pauling, L. C. (1930) The structure of micas and related minerals: *Nat. Acad. Sci. Proc.*, **16,** 123–129.

Rogers, A. F. (1917), A review of the amorphous minerals; *Jour. Geol.*, **25,** 515–541.

Ross, C. S., and Kerr, P. F. (1934), Halloysite and allophane: *U. S. Geol. Survey, Prof. Paper* **185-G,** 135–148.

Shaw, B. T., and Humbert, R. P. (1941), Electron micrographs of clay minerals: *Soil Sci. Soc. Am. Proc.*, **6,** 146–149.

Warren, B. E., and Hering, K. W., (1941), The random structure of chrysotile asbestos: *Phys. Rev.*, **59,** 925.

——— (1941), *X*-ray diffraction in random layer lattices: *Phys. Rev.*, **59,** 693–698.

Whiteside, E. P., and Marshall, C. E. (1944), Mineralogical and chemical studies of the Putnam silt loam soil: *Univ. of Missouri Agricultural Exp. Station Res. Bull.* **386,** 1–48.

SYNTHESIS OF SOME HYDRATED MANGANESE MINERALS

A. D. Wadsley, *Commonwealth Scientific & Industrial Research Organisation, Melbourne, Australia.*

Abstract

Attempts have been made to synthesize the minerals psilomelane, cesarolite, ranciéite, chalcophanite, lithiophorite, and lampadite by hydrothermal alteration of the metallic derivatives of a hydrous manganese oxide. The compounds prepared are compared by chemical, x-ray, and electron microscopic methods with mineral specimens, and the conclusions which are drawn offer some evidence for the paragenesis of these minerals.

The term "psilomelane type" has been suggested as a general name for those manganese oxide minerals which are hard, dense, and which generally lack distinctive features (6). Those which are soft and of low apparent specific gravity retain the name "wad" which has been used in a wider sense to describe any manganese material containing much water. It has been realized for many years that these massive materials may contain considerable quantities of other metals, and until x-ray diffraction methods had been applied to their study, it was doubtful whether the metals were present as discrete impurities or as lattice constituents.

Within these groups, several hydrated manganese minerals are regarded as distinct species. These are listed in Table 1 with the formulae and crystalline habits proposed in the literature. It must be emphasized, however, that these formulae, apart from that for psilomelane, are by no means fully established.

Table 1. Hydrated Manganese Oxide Minerals Containing Other Metals

Mineral	Formula	Crystal System
Chalcophanite	$(Mn, Zn)Mn_2O_5 \cdot 2H_2O$	Hexagonal (?)
Lithiophorite	$LiMn_3Al_2O_9 \cdot 3H_2O$	Hexagonal (?)
Ranciéite	$(Mn, Ca)Mn_4O_9 \cdot 3H_2O$	
Cesarolite	$PbMn_3O_7 \cdot H_2O$	
Psilomelane	$MnBaMn_8O_{18} \cdot 2H_2O$	Orthorhombic

The metals other than manganese are major constituents which may be partly replaced by small amounts of other metals. Cobalt is often present in lithiophorite and psilomelane, copper and trivalent iron are common replacement elements, but no acceptable evidence has been produced to show that these metals are major constituents of hydrated manganese minerals.

Very little is known of these minerals. Psilomelane occurrences are common (6) and x-ray work on single crystals has been described (21).

Cesarolite has been reported only from one locality (1) but no *x*-ray examination is recorded; ranciéite is accredited as a mineral species (18) but no chemical analyses are given; lithiophorite, identified during an examination of psilomelane-type minerals (17) has since been found as well developed crystals (22); while chalcophanite, may be recognized from optical evidence (16).

Although none of these minerals has been synthesized, a group of "metal permanganites" is reported by Mellor (11). The derivatives of calcium, zinc, copper, aluminium and other metals, similar to those prepared originally as chemical precipitates by Sarkar and Dhar (20), have been examined by *x*-ray powder photographs (4), but little resemblance is borne by these to the appropriate mineral. Gorgeu prepared many hydrated manganese derivatives (8) and noted a chemical similarity to asbolite and lampadite in the cobalt and copper "permanganites," but these two minerals have yet to be accredited.

The writer has recently described a hydrous manganese oxide with the formula $(Na,Mn)Mn_3O_7 \cdot nH_2O$ (23). The powder diffraction data indicated a hexagonal cell with the dimensions $a = 8.41$, $c = 10.1$ Å, and with four molecules in the unit cell. The sodium ions are irreversibly exchanged for those of other metals from solutions of their salts, and this change is usually accompanied by a small decrease in the *c* axis dimension.

There is a strong chemical resemblance of each of these metal derivatives to the corresponding hydrated mineral listed in Table 1. Recrystallization of the derivatives in some instances may occur, accompanied by structural and minor chemical changes. These experiments will be described in some detail, and compared with mineral specimens on chemical and *x*-ray evidence.

EXPERIMENTAL

The preparation of the hydrous oxide $(Na,Mn)Mn_3O_7 \cdot nH_2O$ by the oxidation with oxygen of a suspension of manganous hydroxide has been described (23). Metal derivatives are readily formed by agitation with an excess of a 10% solution of the metal salt for 24 hours at room temperature, washing till free from soluble salts, and drying by the aspiration of air. On heating to 200° C. the sodium oxyhydrate and its derivatives lost some water, and the powder pattern of manganous magnanite ($MnO_{1.7-1.8}$) is found. Sarkar and Dhar's (4) preparations also give this pattern.

Recrystallization of some of the derivatives may, however, be readily induced by simple hydrothermal treatment. Sealed glass tubes were found suitable for temperatures up to 200° C. For alkaline solutions or higher temperatures, small stoppered stainless steel cylinders were employed.

X-ray patterns were taken on a General Electric XRD unit with a 14.3 cm. camera using Fe radiation filtered with Mn ($\lambda = 1.937$). Because preparations such as these may contain amorphous oxides which would not be revealed by the powder patterns, electron micrographs where necessary were taken by Mr. J. L. Farrant, Division of Industrial Chemistry, C.S.I.R.O. on an R.C.A. type E.M.U. microscope, to confirm homogeneity. Electron diffraction patterns of the recrystallized barium and lead derivatives were obtained by Mr. J. Spink, Division of Tribophysics, C.S.I.R.O.

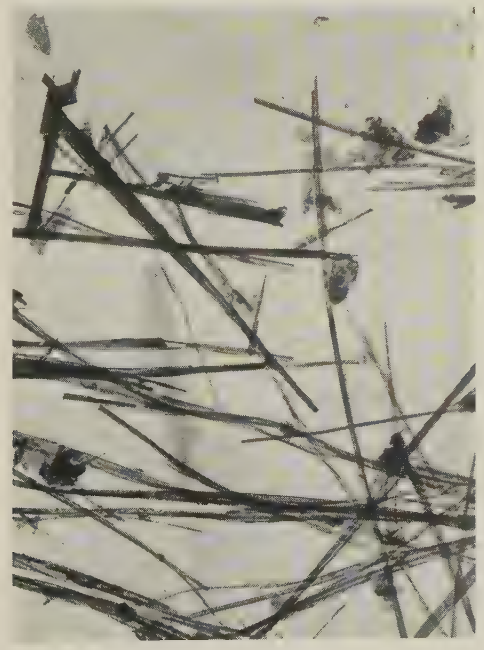

FIG. 1. Electron micrograph of synthetic psilomelane (×20,000).

BARIUM DERIVATIVE AND PSILOMELANE

Psilomelane is readily synthesized by heating the barium derivative at 160° C. for several weeks with a solution containing 1% of barium and manganese chlorides. Electron micrographs show that the synthetic mineral is mainly composed of needles, occasionally twinned, which although attaining a length of several microns, are not resolved by the ore microscope.

The weak x-ray powder photograph was identical with that of the mineral published by Fleischer and Richmond (6), but the electron diffraction pattern was much sharper. This was measured accurately on a recording photometer, and the ring diameters could all be indexed using Vaux's figures for the cell dimensions of orthorhombic psilomelane (21).

$$a=9.1,\ b=13.7,\ c=2.86\ \text{Å}.$$

There was insufficient material for a complete chemical analysis of the synthetic mineral. The determinations made are given in Table 2 together with those for the barium manganate from which it was derived, and a massive psilomelane specimen from Pilbara, Western Australia. The latter was examined optically and found to be homogeneous and fibrous in structure.

TABLE 2. ANALYSIS OF PSILOMELANE

	1	2	3
MnO_2	61.8	62.9	74.36
MnO	11.8	7.6	6.10
BaO	19.6	14.4	13.49
$H_2O_{+120°}$	7.6	N.D.	5.14
K_2O	—		0.81
$(Fe, Al)_2O_3$			0.59
Total	100.8	84.9	100.49
Specific Gravity	4.1	4.4	4.61

1. Barium derivative of $(Na, Mn)Mn_3O_7 \cdot nH_2O$.
2. Recrystallized barium derivative. Contains much loosely held water.
3. Psilomelane, Pilbara, Western Australia.

The atomic ratios $Mn^{4+}:Mn^{2+}:Ba:O$ are 7.90:1.16:1.02:18 for the synthetic mineral (analysis 2), and 8.14:0.82:1.00:18 for the Pilbara specimen (analysis 3) assuming that potassium substitutes for barium. These agree reasonably well with the formula $MnBaMn_8O_{18} \cdot 2H_2O$ which has previously been ascribed to this mineral, although the water in analysis 3 is high. The density calculated from this formula and Vaux's dimensions is 4.42, somewhat lower than that measured for this and other mineral specimens. Recrystallization of the barium derivative (analysis 1) is accompanied by the loss of some barium.

When heated to 550°, the synthetic mineral gives a substance with the powder pattern of hollandite. This agrees with Fleischer and Richmond's observation that hollandite ($BaMn_8O_{16}$) is formed as the dehydration product of psilomelane (6).

LEAD DERIVATIVE

The lead derivative was readily recrystallized by heating at 160° C. for six weeks in a 1% solution of lead and manganese nitrates. The chemical composition resembled that of cesarolite.

TABLE 3. ANALYSIS OF CESAROLITE AND SYNTHETIC CORONADITE

	1	2	3	4
MnO_2	53.3	53.11	60.80	51.40
MnO	9.3	5.23	7.12	0.62
PbO	33.3	37.30	28.66	39.09
$H_2O_{+120°}$	3.7	3.56	1.11	3.30
Remainder			2.31	3.66
Total	99.6	99.20	100.00	98.07
Density	5.5	5.94	5.25	5.29

1. Lead derivative of $(Na,Mn)Mn_3O_7 \cdot nH_2O$.
2. Recrystallized lead derivative (synthetic coronadite).
3. Coronadite, Arizona. W. F. Hillebrand analysis (recalc.) in Lindgren and Hillebrand (10). Remainder = Cu, Al, Fe, Zn.
4. Cesarolite, Tunisia. Recalculated from the data of Buttgenbach and Gillet (1). Remainder = Al, Fe, Na, other metals, insoluble.

X-ray powder photographs were very weak, but the electron diffraction pattern of the recrystallized derivative was similar to that of coronadite given by Frondel and Heinrich (7). Although most coronadite specimens contain water, it is considered to be non-essential (6, 7), and a discussion of this preparation is therefore outside the scope of this account.

ZINC DERIVATIVE AND CHALCOPHANITE

Chalcophanite could not be prepared by autoclaving the zinc derivative of $(Mn,Na)\ Mn_3O_7 \cdot nH_2O$ at 160° with a 1% solution of zinc and manganese chlorides. With this treatment the pattern of hetaerolite with some additional lines (hydrohetaerolite?) is observed. This decomposes to pale brown hetaerolite if the temperature is raised to 300° C. Crystalline chalcophanite loses water readily at 100° C., and is completely dehydrated on heating to 200° C (15); it is thus certain that this recrystallization was attempted at too high a temperature.

A further quantity, autoclaved at 80° with the same solution, showed after six months some additional lines in the diffraction pattern common to the strongest chalcophanite lines. It is considered that complete recrystallization would take a much longer period to complete, probably accompanied by further oxidation.

Table 4 gives the analysis of the zinc derivative. An analysis of a crystalline chalcophanite from Buchan, Victoria, which agrees well with the formula $ZnMn_3O_7 \cdot 3H_2O$ is also included. The tentative new formulation of chalcophanite will be discussed in more detail at some future date, when this specimen will be more fully described.

TABLE 4. ANALYSIS OF ZINC DERIVATIVE AND CHALCOPHANITE

	1	2
MnO_2	65.9	65.39
MnO	12.3	0.22
ZnO	14.8	18.19
$H_2O_{\pm 120°}$	6.0	13.09
Fe_2O_3		0.32
Al_2O_3		0.39
SiO_2		1.88
Total	99.0	99.48
Specific Gravity	4.0	3.70

1. Zinc derivative of $(Mn, Na)Mn_3O_7 \cdot 2H_2O$.
2. Chalcophanite crystals, Buchan, Victoria.

COPPER DERIVATIVE AND LAMPADITE

Lampadite is the name given in a general sense to the cuprian wads (3) but no evidence for the existence of a hydrated copper manganese mineral based on x-ray identification has been recorded.

A cuprian wad of unknown origin, loaned from the University of Adelaide, was found by H. R. Samson on optical examination to consist of a very close intergrowth of two minerals, one black and opaque (manganiferous), the other consisting of transparent green crystals. Separation could not be effected by physical means, but a powder pattern identified the consitutents as dioptase and poorly crystallized lithiophorite. Chemical analysis (Table 5, column 3) gave the $CuO:SiO_2$ ratio as 0.361:0.356 (very nearly 1:1), and it seems evident that no significant quantity of copper is present in the manganese mineral. The composition of the lithiophorite (Table 5, column 4) was found by subtracting $CuO \cdot SiO_2 \cdot H_2O$ from the total analysis.

Attempts to synthesize lampadite met with no success. The copper derivative of $(Mn,Na)Mn_3O_7 \cdot nH_2O$ was readily formed, the analysis of which, given in Table 5, is very similar to that of a cuprian wad recorded in Dana (3, p. 567). The powder pattern resembled that of manganous manganite. Autoclaving at 160° C. with a mixed solution of copper and manganous sulfates gave copper-free manganite (MnOOH) in close association with small green crystals of a basic copper sulfate. The similarity in appearance of this preparation to that of the dioptase-lithiophorite specimen was most striking, and suggested that the two materials were formed under similar circumstances.

TABLE 5. ANALYSIS OF COPPER DERIVATIVE AND LAMPADITE

	1	2	3	4
MnO_2	65.4	58.77	15.14	34.9
MnO	7.5	9.59	2.65	6.1
CuO	18.8	11.48	28.74	
CoO			1.32	3.0
Fe_2O_3			1.89	4.4
Al_2O_3			8.06	18.6
SiO_2			21.38	
K_2O*			0.37	0.9
$H_2O_{+120°}$	N.D.	21.05	8.19	3.9
$H_2O_{-120°}$	N.D.		11.90	27.4
Total	91.7	100.89	99.64	99.2

* The mixed alkalis in this analysis reported as K_2O–Li present.

1. Copper derivative of $(Na,Mn)Mn_3O_7 \cdot nH_2O$.
2. Lampadite. Dana p. 567 Analysis 6.
3. Dioptase-lithiophorite specimen, South Australia.
4. Analysis 3 corrected for dioptase ($CuO \cdot SiO_2 \cdot H_2O$).

ALUMINIUM DERIVATIVE AND LITHIOPHORITE

The aluminium-lithium derivative was readily recrystallized by heating at 160° for three weeks in a solution containing 1% each of lithium chloride and aluminium sulfate.

Electron micrographs of the derivative were similar to those of the parent hydrous oxide. They consist of series of very thin overlapping films of oxide (Fig. 2), which is characteristic of materials showing a marked *c* axis development. The recrystallized derivative was made up of large hexagonal prisms with well developed facial angles of approximately 120° (Fig. 3). Figure 4 shows a flake of lithiophorite (Postmasburg, South Africa) from a specimen originally described by deVilliers and van der Walt (22), who generously made some of their material available.

The chemical compositions of these derivatives, the Postmasburg

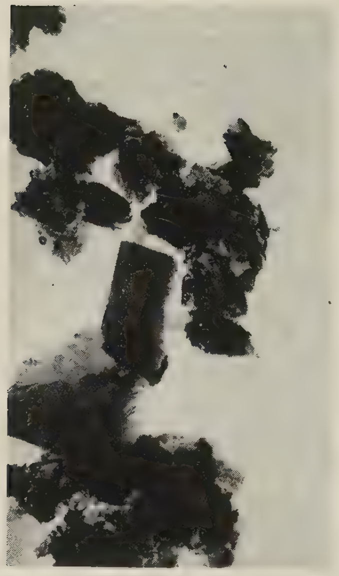

FIG. 2.

FIG. 3.

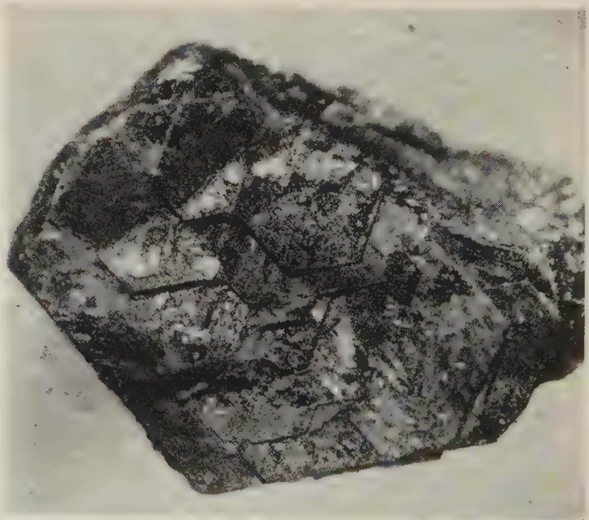

FIG. 4.

FIG. 2. Electron micrograph of the aluminium-lithium derivative of $(Mn,Na)Mn_3O_7 \cdot nH_2O \cdot$ (×20,000).

FIG. 3. Electron micrograph of the aluminium-lithium derivative recrystallized under hydrothermal conditions (×12,000).

FIG. 4. Lithiophorite, Postmasburg, South Africa. (×50). (Photograph J. Weymouth.)

specimen, and a new analysis of a cobaltian lithiophorite from New Caledonia containing some free goethite as impurity are given in Table 6.

TABLE 6. ANALYSIS OF ALUMINIUM/LITHIUM DERIVATIVES AND LITHIOPHORITE

	1	2	3	4
MnO_2	57.9	68.18	48.96	35.71
MnO	14.0	7.14	8.20	2.92
Al_2O_3	17.9	15.42	23.84	19.22
Fe_2O_3		—	0.96	15.95
Li_2O	0.22	Present	3.30	0.51
CoO		—	—	6.99
$H_2O_{+120°}$	9.9	8.32	13.15	11.97
$H_2O_{-120°}$		0.73	1.45	4.72
SiO_2		—	0.30	1.63
Total	99.9	99.79	100.16	99.62
Density	3.6	3.95	3.37	N.D.

1. Aluminium/lithium derivative of $(Na,Mn)Mn_3O_7 \cdot nH_2O$. Corrected for $H_2O_{-120°}$.
2. Recrystallized derivative. Insufficient for accurate Li_2O determination.
3. Lithiophorite, Gloucester, South Africa. Analyst C. F. J. van der Walt (22).
4. Lithiophorite, New Caledonia (with some goethite).

The differences in composition between the mineral specimens (including the one associated with dioptase and recorded in Table 5) and the recrystallized derivative is reflected in the *x*-ray evidence. The powder diffraction patterns of the synthetic materials and the South African specimen are given in Table 7, together with tentative indices, unit cell dimensions and densities calculated from formulae developed from the chemical data.

Laue patterns of the Postmasburg specimen confirmed the hexagonal symmetry suggested by deVilliers and van der Walt, and the powder pattern resembled that of lithiophorite reported by Fleischer and Richmond (6).

It is uncertain whether the *c* dimension is 9.39 Å or twice this value. The unit cell contents will be either $(Li,Mn,Al)_2O_3 \cdot H_2O$ or $(Li,Mn,Al)_4O_6 \cdot 2H_2O$ with the possibility that lithium substitutes for aluminium as it may do in the micas.

The axes given for this mineral will not fit the other lithiophorite specimens which have been examined. A complete index of the lines of the New Caledonia and of the dioptase-associated specimens is not possible because of confusion due to the lines of the other minerals present, but the well developed (0001) lines permit the *c* dimensions to

TABLE 7. *X*-RAY POWDER DATA FOR ALUMINIUM DERIVATIVE AND LITHIOPHORITE

	1			2			3			4		
	I	*d*	*hkīl*	*I*	*d*	*hkīl*	*I*	*d*	*hkīl*	*I*	*d*	*hkīl*
	S	10.0	(0001)	S	9.78	(0001)	M	9.66	(0001)	M	9.45	(0001)
	W	7.28	$(10\bar{1}0)$	VW	7.46	$(10\bar{1}0)$	M	4.97	$(10\bar{1}1)$	S	4.70	(0002)
	M	5.06	(0002)	MW	4.85	(0002)	MS	4.76	(0002)	MW	3.123	(0003)
	VW(d)	4.76		VW(d)	3.26	(0003)	W	3.51	$(10\bar{1}2)$	MW	2.385	(0004)
	W(d)	3.47	$(20\bar{2}1)$	M	2.458	(0004)	MS	2.988	$(11\bar{2}1)$	M	1.882	(0005)
	W	3.372	(0003)	MW	2.071	$(31\bar{4}0)$	M	2.385	(0004)	W	1.508	$(10\bar{1}5)$
	W(d)	2.500	$\left\{\begin{matrix}(0004)\\(20\bar{2}3)\end{matrix}\right\}$	MW	2.031	$(31\bar{4}1)$	W	2.255	$(11\bar{2}3)$	VW	1.459	$(11\bar{2}0)$
	W	2.429	$(30\bar{3}0)$	W(d)	1.79	$(22\bar{4}3)$	M	1.903	(0005)	VW	1.445	$(11\bar{2}1)$
	W(d)	2.38	(1014)	VW(d)	1.63	(0006)	M	1.887	$(30\bar{3}0)$	VW	1.396	$(11\bar{2}2)$
	VW(d)	2.14	$(21\bar{3}3)$	S	1.421	$(31\bar{4}5)$	MW	1.752	$(30\bar{3}2)$	W	1.229	$\left\{\begin{matrix}(20\bar{2}2)\\(11\bar{2}4)\end{matrix}\right\}$
	VW(d)	1.85	$(21\bar{3}4)$				VW	1.648	$(11\bar{2}5)$	VW	1.171	(0008)
	MW	1.472	$(40\bar{4}4)$				VW	1.582	$(20\bar{2}5)$	VW	1.154	$(11\bar{2}5)$
	W	1.420	(0007)				VW	1.489	$(31\bar{4}2)$			
							VW	1.480	$(30\bar{3}5)$			
							W	1.457	$(22\bar{4}3)$			
							VW	1.393	$(40\bar{4}1)$			
							VW	1.373	(0007)			
							VW	1.286	$(32\bar{5}1)$			
							VW	1.241	$(22\bar{4}5)$			
							VW	1.199	(0008)			
Crystal System	Hexagonal			Hexagonal			Hexagonal			Hexagonal		
Axial Dimensions (Å)	$a = 8.41$ $c = 10.1$			$a = 8.59$ $c = 9.7$			$a = 6.52$ $c = 9.56$			$a = 2.92$ $c = 9.39$ or 18.78		
Unit cell volume (Å)³	620			624			351			69 or 138		
Density (Obs)	3.8			3.6			3.95			3.37		
Density (Calc)	3.77			3.86			3.96			3.42		
Unit cell contents	$(Na,Mn)_4Mn_{12}O_{28} \cdot 8H_2O$			$Al_5Mn_{13}O_{28} \cdot 8H_2O$			$(Li,Al,Mn)_4Mn_6O_{18} \cdot 4H_2O$			$(Li,Al)MnO_3 \cdot H_2O$ or $(Li,Al)_2Mn_2O_6 \cdot 2H_2O$		

S = Strong, MS = Med. strong, M = Medium, MW = Med. weak, W = weak, VW = Very weak, (d) = diffuse.

1. Manganese oxyhydrate. 3. Recrystallized derivative

be calculated. The values 9.50±0.04 and 9.68±0.04 Å, respectively, which are found suggest that the structure may be variable, which, in view of the wide variety of composition suggested to the writer by Dr. M. Fleischer (5) is not surprising.

The chemical composition of the recrystallized derivative differs considerably from that of the minerals examined, and consequently both *a* and *c* dimensions differ from those of the South African specimen. The unit cell volume is almost exactly five times that of the mineral specimen, and this together with the general similarity of the empirical formulae, suggest that they are members of series capable of considerable variation.

CALCIUM DERIVATIVE AND RANCIÉITE

Although many naturally occurring psilomelane-type and wad minerals have been examined, no ranciéite has been found. The calcium derivative of the parent manganese oxyhydrate may however be given the formula $(Ca,Mn)Mn_4O_9 \cdot 5H_2O$ as can be seen from Table 8.

TABLE 8. ANALYSIS OF CALCIUM DERIVATIVE

	1	2
MnO_2	70.0	69.8
MnO	3.6	3.9
CaO	7.7	8.2
$H_2O_{+120°}$	17.7	18.1
Total	99.0	100.0
Density	3.7	

1. Calcium derivative of $(Na,Mn)Mn_3O_7 \cdot nH_2O$.
2. Calculated from $(Ca,Mn)Mn_4O_9 \cdot 5H_2O$ with $Ca:Mn^{++}=8:3$.

No recrystallization of this material could be effected. When autoclaved with calcium and manganous chlorides at 160° C., a phase change to a calcian manganite identical in most respects with the mineral MnOOH was observed, while heating at a low temperature in air or in a closed tube without additional water resulted in the development of the bixbyite structure. Autoclaving at 80° C. for six months produced very little change in the *x*-ray data.

The powder pattern differs appreciably from that of the parent oxyhydrate, but most of the lines can be indexed as belonging to a hexagonal cell with the dimensions $a=8.44$, $c=9.87$ Å.

The scarcity of $(hk\bar{i}l)$ reflections is characteristic of a very disordered structure, and it may well be that the formula which has been given assigns too many molecules of water to the material. A lesser degree of hydration would lead to better agreement between the calculated and observed density values.

This pattern differs in many respects from the published data for ranciéite (6). While it would be speculative to say that the powder patterns appear to be derived from similar structures, the similarities in composition between the calcium derivative and corresponding values in the brief reports which have appeared on ranciéite (18) suggest they are closely related.

TABLE 9. *X*-RAY POWDER DIFFRACTION DATA FOR CALCIUM DERIVATIVE OF (Na,Mn)$Mn_3O_7 \cdot 2H_2O$

Observed		Calculated	
Intensity	*d* (Å)	*d* (Å)	*hkīl*
S	7.17	7.17	(1000)
VW(d)	4.8		
W(d)	3.57	3.59	(2000)
VW	2.57	2.576	$(11\bar{2}3)$
W	2.468	2.468	(0004)
W	2.414	2.426	$(20\bar{2}3)$
VW(d)	2.3		
M	2.069	2.071	$(22\bar{4}0)$
MW	2.029	2.034	$(20\bar{2}4)$
VW	1.804	1.794	(4000)
VW	1.461	1.451	$(40\bar{4}4)$
VW	1.410	1.411	(0007)
VW(d)	1.26		

S=strong, M=medium, MW=Med. weak, W=weak, VW=very weak, (d)=diffuse.

System	Hexagonal
Unit cell dimensions (Å)	$a=8.44$
	$c=9.87$
Unit cell volume (Å³)	609
Density (Calc.)	4.06
Density (Obs.)	3.7
Unit cell contents	$(Mn,Ca)_3Mn_{12}O_{27} \cdot 15H_2O$

THE DERIVATION OF THE HYDRATED MANGANESE MINERALS

From comparisons of the chemistry and mineralogy of the higher manganese oxyhydrates it is possible to deduce how these minerals may have been formed.

The oxyhydrate $(Mn,Na)Mn_3O_7 \cdot nH_2O$ is metastable, losing some water at a low temperature to form the more stable "manganous manganite" (23). The similarity between this substance and a mineral specimen has recently been demonstrated (19).

On the other hand it will readily form loose hydrous complexes with metals which, while not giving close fitting formulae, may in most cases be represented as $(R,Mn)Mn_3O_7 \cdot nH_2O$, where R is the added metal (23).

Earthy manganese material commonly known as wad may contain considerable amounts of other metals. It is most likely that these substances were formed either by substitution of the "foreign" ion in a hydrous oxide formed naturally by the oxidation of $Mn(OH)_2$ or else by the oxidation with air of mixed sols of $Mn(OH)_2$ with other hydroxides. Although single ionic species in our experiments have been exchanged for sodium in the parent oxide, there is no reason why two or more metals should not be substituted, and the presence of barium, cobalt, tungsten, vanadium, etc., which are common constituents of the wads and other manganese minerals, would be due to this ready substitution.

If the wad so formed is not subjected to further change by heat, pressure, or any violent means of oxidation, then its structure will bear some resemblance to that of the parent hydrous oxide. Although some very soft wads have been examined in this laboratory, *x*-ray powder patterns show mainly the mineral impurities present, although some additional very diffuse lines similar to those reported by Smitheringale (24) and more recently by McMurdie and Golovato (13) may be observed *if they are sought.* These lines are characteristic of delta-MnO_2 (12), the relationship of which to manganous manganite has been discussed previously (2).

Autoclaving the derivatives at a low temperature in some instances induces rearrangement of the disordered lattice to that of the more stable and sharply defined mineral species, accompanied in some instances by slight changes in composition. Psilomelane can certainly be formed in this way; coronadite and a compound closely resembling lithiophorite may similarly be synthesized; chalcophanite andranciéite will probably be formed by recrystallization after prolonged autoclaving at a low temperature. The failure of synthesize lampadite does not necessarily mean that this mineral may not exist.

These minerals, seldom found except as massive specimens (i.e. microcrystalline) could well be formed from the hydrous wad with which they are often associated, by hydrothermal alteration, pressure, or perhaps simply by ageing under oxidizing conditions. The rarer crystalline deposits were presumably formed only under conditions where the mangenese and other metals were slowly precipitated from solutions which were saturated with oxygen, perhaps at elevated temperatures.

This theory, derived from chemical experiments, has some support from geological evidence. The crystalline lithiophorite from the Postmasburg deposits was considered by deVillers to be formed directly from solutions of magmatic origin and not by the weathering of an anhydrous mineral. Chalcophanite which may be formed as an alteration product of hetaerolite and franklinite (14) has been reported free of these minerals (9), and has been found by Mr. H. R. Samson and the writer in a manganese deposit in the Buchan District, Victoria, intimately associated with lithiophorite. In this latter case the two minerals undoubtedly crystallized simultaneously, and the conditions for their formation would therefore be identical. The "asbolite" specimen, shown to be an association of dioptase and lithiophorite, most probably was formed by the action of siliceous solutions on a cuprian wad, which removed the copper to form another mineral (dioptase) in much the same way as basic copper sulfate was formed in the laboratory by autoclaving the copper derivative. Psilomelane may be regarded as recrystallized barium wad, and owing to the relative ease with which it is transformed to hollandite, is probably a necessary phase in the paragenesis of this mineral. Little can be said of cesarolite or rancíéite, but their formation as crystalline minerals could occur by the methods which have been suggested.

These minerals are made conspicuous by the presence of metals other than manganese. When there are no substituents, the hydrous oxide $(Mn,Na)Mn_3O_7 \cdot nH_2O$ can be further oxidized at a low temperature only to manganous manganite, or possibly to delta-MnO_2. It is suggested that pyrolusite, cryptomelane, ramsdellite and γ-MnO_2, each of which requires special conditions for its synthesis in the laboratory could be formed on a geological scale at a more elevated temperature, under acid conditions, or perhaps by bacterial oxidation. Consequently the mineral, reported by Samson and Wadsley (19) to resemble manganous manganite may be regarded as a link in the mineralogy of the manganese oxides.

This generic scheme may be represented diagrammatically:

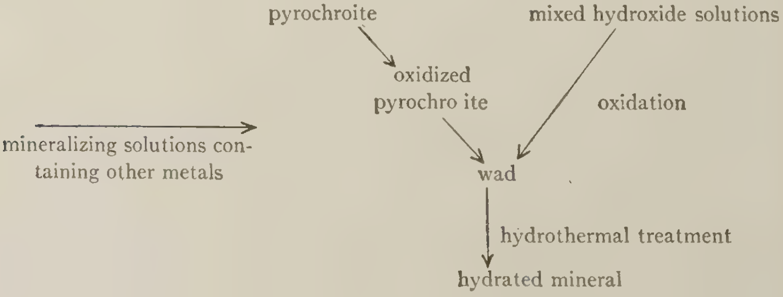

ACKNOWLEDGMENTS

The writer wishes to thank Dr. C Frondel, Harvard University, for supplying a type specimen of cesarolite together with some *x*-ray data; Dr. A. L. G. Rees, for the use of the facilities of his section in which to carry out some of the work described; to J. L. Farrant and J. Spink for taking electron micrographs and electron diffraction patterns; to H. R. Samson for collecting some of the mineral specimens, for their optical examination, and for very helpful discussions; and to Dr. I. W. Wark, for his criticism of the manuscript.

The work described in this report was carried out as part of the research program of the Division of Industrial Chemistry, Commonwealth Scientific and Industrial Research Organisation, Melbourne, Australia.

REFERENCES

1. BUTTGENBACH M., & GILLET, C., *Soc. Géol. Belgique, Ann.*, **43**, 239–241 (1920).
2. COLE, W. F., WADSLEY, A. D., & WALKLEY, A., *Trans. Electrochem. Soc.* Preprint 92–2 (1947).
3. Dana's System of Mineralogy, 7th Ed. Wiley & Sons, N. Y. (**1944**).
4. FEITKNECHT W., & MARTI, W., *Helv. Chim. Acta*, **28**, 128–148; 149–155 (1945).
5. FLEISCHER, M. Private communication.
6. FLEISCHER M., & RICHMOND, W. E., *Econ. Geol.*, **38**, 269–286)1943).
7. FRONDEL, C., & HEINRICH, E. W., *Am. Mineral.*, **27**, 48–56 (1942).
8. GORGEU, A., *Bull. Soc. Chim.*, **4**, 16–30 (1890).
9. KRISHNAN, M. S., & GHOSH, P. K., *Rec. Geol. Survey India* 75, *Prof. Pap.* **8**, (1941).
10. LINDGREN, W., & HILLEBRAND, W. F., *U. S. Geol. Surv., Bull.* **262**, 42–45 (1905).
11. MELLOR, J. W., Comprehensive Treatise. Longmans & Co. London, vol. **XII** (1932) P. 274 et. seq.
12. MCMURDIE, H. F., *Trans. Electrochem Soc.* **86**, 313–326 (1944).
13. MCMURDIE, H. F., & GOLOVATO, E., *J. Res. Nat. Bur. Stand.*, **41**, 589–600 (1948).
14. PALACHE, C., *U. S. Geol. Survey, Prof. Pap.* **180**, (1935).
15. PENFIELD, S. L., & KREIDER, D. A., *Am. J. Sci.*, **48**, 141–143 (1894).
16. RAMDOHR, P., *Zentr. Min. Geol.*, 129–136 (**1938**A).
17. RAMSDELL, L. S., *Am. Mineral.*, **17**, 143–149 (1932).
18. RICHMOND, W. E., & FLEISCHER, M., *Am. Mineral.*, **27**, 231 (1942) abstract.
19. SAMSON, H. R., & WADSLEY, A. D., *Am. Mineral.*, **33**, 695–702 (1948).
20. SARKAR, P. B., & DHAR, N. R., *Zeit. anorg. Chem.*, **121**, 135–155 (1921).
21. VAUX, G., *Min. Mag.*, **24**, 521–526 (1937).
22. DEVILLIERS, J. E., & VAN DER WALT, C. F. J., *Am. Mineral.*, **30**, 629–634 (1945).
23. WADSLEY, A. D., *J.A.C.S.*, **72**, 1781–1784 (1950).
24. SMITHERINGALE, W. V., *Econ. Geol.*, **24**, 481–505 (1929).

AN OCCURRENCE OF NATROLITE, ANDRADITE, AND ALLANITE IN THE FRANKLIN FURNACE QUADRANGLE, NEW JERSEY*

CHARLES MILTON AND NORMAN DAVIDSON,† *U. S. Geological Survey, Washington, D. C.*

ABSTRACT

Masses of natrolite containing small crystals of green andradite and dark-brown allanite occur in the weathered debris of a nepheline syenite dike. Optical, chemical, and spectrographic data are given for these three minerals, with a brief discussion of paragenetic relationships. The nepheline syenite contains abundant brown melanite, but no andradite.

LOCATION AND GEOLOGICAL RELATIONS

Natrolite, andradite, allanite, and a little quartz occur together as a satellitic hydrothermal deposit in the heavily weathered portion of a dike of porphyritic nepheline syenite. They are found in a small area a hundred feet or so across at the western end of the dike, which extends eastward for more than a thousand feet, forming a pronounced topographic ridge. The exact locality, shown on the Franklin Furnace, N. J., Folio geologic map (1), is one mile slightly south of west from Wykertown. It is also shown on the more recent Army Map Service topographic map of the Branchville, N. J., quadrangle (2).

The dike is described briefly by J. E. Wolff (3) as consisting of: phenocrysts of biotite corroded and replaced by aegirite; crystals of augite, red in the center and green on the periphery; and apatite and melanite in a background of orthoclase and nepheline. In some specimens of the rock, collected by Charles Milton, there is also abundant cancrinite. The dike has been further studied as a possible source of feldspar by John M. Parker, III (4).

NATROLITE

The natrolite, with its associated minerals, is found in loose masses in a crumbly dark gravel resulting from the disintegration of the nepheline syenite. Only at the west end of this dike, and nowhere else in dikes of similar petrographic character in this region, was a similar state of disintegration noted; and this is the only locality where natrolite and the accompanying minerals were found. The abrupt ending of the nepheline syenite ridge at this place, with the other features mentioned, suggest that the dike has been faulted off and that here a zone of shearing has

---

* Published by permission of the Director, U. S. Geological Survey.

† Mr. Norman Davidson died on December 31, 1949.

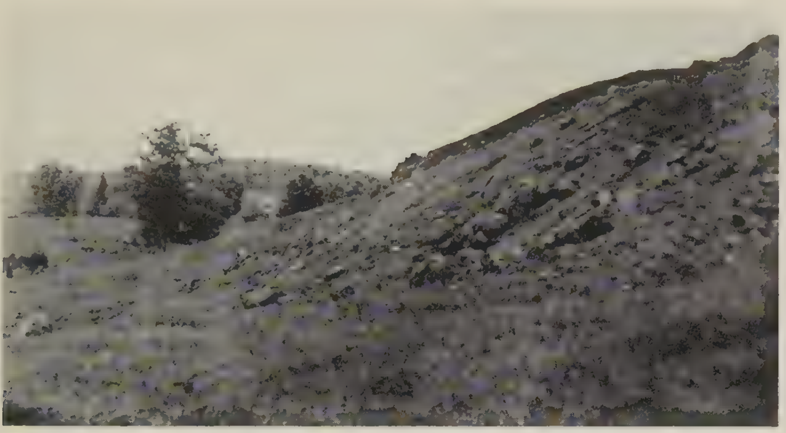

FIG. 1. View of natrolite-andradite-allanite locality, near Wykertown, New Jersey, from the south. This is the west end of the nepheline syenite dike, in an advanced state of disintegration. The natrolite, etc., fragments are strewn in the rubble.

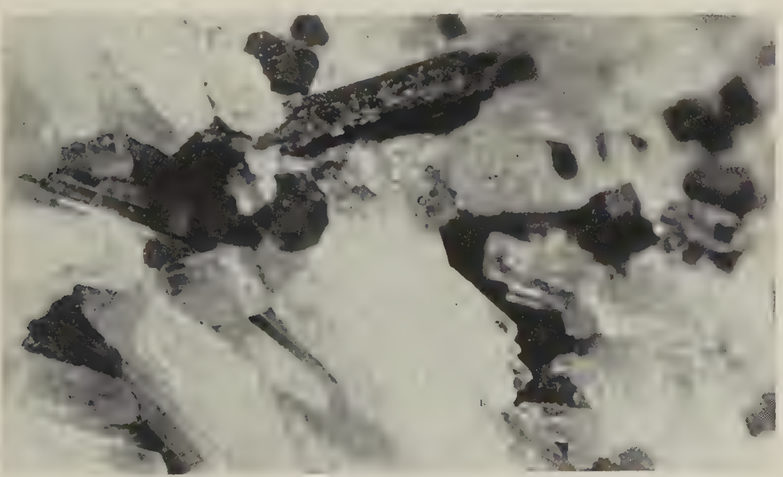

FIG. 2. x25. Glassy crystallized drusy natrolite, with rhombohedral andradite and prismatic allanite (upper center).

crumbled the dike and permitted the entry of the solutions from which these minerals were deposited. Figure 1 shows the appearance of the locality.

In the crumbly nepheline syenite, which looks much like a twenty-foot bank of pea-coal, the natrolite with its associated minerals is readily distinguished by its white color. It varies from almost clear glassy crystallized masses with individual crystals several inches long, to dull, almost opaque shapeless aggregates. Commonly well-crystallized aggregates of small crystals are found on such masses (Fig. 2).

Both the semi-opaque masses and the clear crystallized natrolite were analyzed, without finding any sensible difference in composition. The analyses are given below:

TABLE 1. ANALYSES OF NATROLITE, NEAR WYKERTOWN, N. J.
(Charles Milton, Analyst)

	1.		2.	
		Ratio		*Ratio*
SiO_2	47.64	3.01	47.33	2.97
Al_2O_3	26.90	1.00	27.13	1.00
Fe_2O_3	Trace			
CaO	.07		.10	
MgO	None			
Na_2O	15.51	.95	15.63	.96
K_2O	None			
H_2O-	9.59(ign)	2.02	.13	.03
H_2O+			9.54	1.99
	99.71		99.86	
Cs_2O	None			
Rb_2O	None			
Li_2O	.000x			

NOTES: Analysis 1 was made on white semi-opaque material. Alkalies were determined after removal of SiO_2, R_2O_3, and CaO, and of ammonium salts by volatilization, leaving only alkali chlorides. MgO was determined on separate sample. Rare alkalies were determined spectrographically by A. T. Myers, Spectrographer, U. S. Geological Survey.

Analysis 2. Made on clear crystallized material. Water by Penfield method. Alkalies by J. Lawrence Smith method.

Formula: $Na_2Al_2Si_3O_{10} \cdot 2H_2O$

Indices: $\alpha = 1.477$, $\beta = 1.480$, $\gamma = 1.490$ (on clear material)

Optically positive.

ANDRADITE

The andradite garnet is well crystallized; many crystals show perfect dodecahedra, a few with suppressed faces simulate a rhombohedron (Fig. 3). It is sea green in color; in thin section colorless. This green andradite has been called demantoid. It shows optical anomalies; under crossed nicols each crystal is divided into numerous segments whose sides appear parallel to the dodecahedral planes. Each segment is biaxial with a moderate optic angle, estimated from 55° to 60°, positive character, and

$\alpha = 1.813$, $\gamma = 1.823$. Figure 4 shows the appearance of the segments under crossed nicols. The optics for the andradite were kindly determined by Miss J. J. Glass, mineralogist, of the Geological Survey.

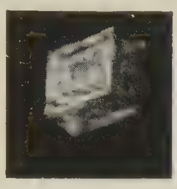

FIG. 3. ×35. Andradite garnet (single crystal). The shape is that of a rhombohedron, produced by suppression of a zone of six dodecahedral planes, parallel to an axis of trigonal symmetry.

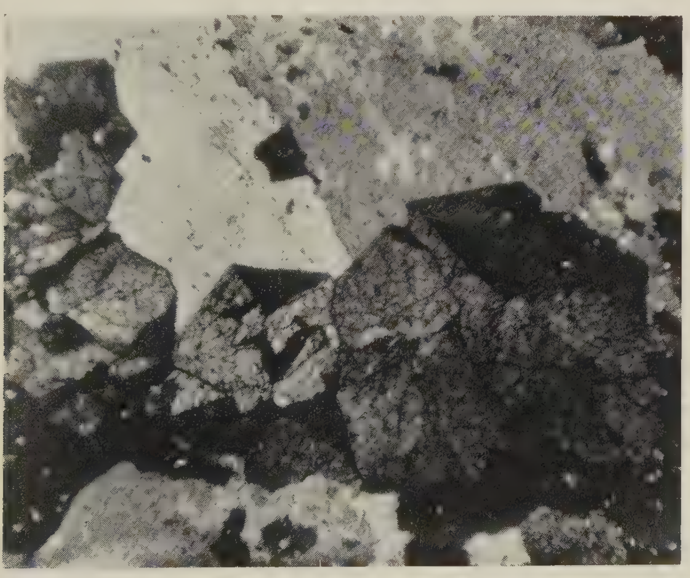

FIG. 4. This section ×100, crossed nicols. Andradite garnet and natrolite. Shows birefracting segments in andradite.

The optical anisotropy of garnets has been recognized for more than a century as anomalous in view of the isometric symmetry, Hintze (5) states, citing numerous instances: "Most macroscopic garnet crystals are not optically isotropic." The microscopic rock-forming garnets, on the other hand, are in general completely isotropic, or at most faintly anisotropic.

The analysis of the andradite garnet is given in Table 2.

Fleischer (6), in a discussion of the chemical composition and related physical properties of the garnet group, points out that deviations from

TABLE 2. ANALYSIS OF ANDRADITE, NEAR WYKERTOWN, N. J.
(Norman Davidson, analyst)

		Ratios
SiO_2	36.04	6.00
Al_2O_3	8.33	.82
Fe_2O_3	15.97	1.00
FeO	.92	.12
TiO_2	2.59 (Ti_2O_3 2.33)	.32 (.16)
CaO	35.20	6.28
MnO	.40	.06
MgO	.75	.19
H_2O-	.05	
	100.25	
Specific Gravity	3.69	

A. T. Myers further examined the andradite spectrographically. He found:

Major (>1%) Si, Al, Ca, Fe, Ti	
Minor (0.X%)	Mg, Mn
(0.0X−0.00X%)	Y, Yb, Be
Trace	Pb, Cu
Not found	Zn, Sr

Calculating titanium as TiO_2, with SiO_2, gives

SiO_2+TiO_2	632	3.47
$Al_2O_3+Fe_2O_3$	182	1.00
FeO+CaO+MnO+MgO	665	3.65

Calculating titanium as Ti_2O_3, with Al_2O_3 and Fe_2O_3 gives:

SiO_2	600	3.03
$Al_2O_3+Fe_2O_3+Ti_2O_3$	198	1.00
FeO+CaO+MnO+MgO	665	3.36

Calculation in terms of constituent molecules gives:

Grossularite	36.0%	with calculated refractive index 1.812
Pyrope	2.7	(as against measured 1.813–1.823)
Almandite	2.3	and density calculated 3.654
Spessartite	1.1	(as against measured 3.69)
Andradite	56.9	

the ideal $3RO \cdot R_2O_3 \cdot 3SiO_2$ formula occur most commonly in garnets with appreciable TiO_2, or much FeO. The deviation of the New Jersey andradite from the ideal formula, namely:

RO_2	R_2O_3	RO	
3.47	1.00	3.65	(Ti as TiO_2)
	or		
3.03	1.00	3.36	(Ti as Ti_2O_3)

is presumably to be referred to the titanium content of the garnet, 2.59% (as TiO_2), as the FeO is quite low (0.92%). Also, titaniferous garnets cited by Fleischer normally show high RO_2 and RO, and low R_2O_3, as does this. Calculating the titanium as Ti_2O_3, as suggested by Zedlitz (7), would give as shown above a more nearly ideal ratio. However, as trivalent titanium is a strong reducing agent, it would immediately reduce ferric iron to ferrous iron, and Ti_2O_3 would become TiO_2. Because there is only 0.92% FeO present, the most Ti_2O_3 that can be present is also 0.92%. Therefore, we cannot assume the titanium to be in the reduced form.

Examination of the literature with reference to andradite indicates that similar doubly refracting garnets have been described by Brögger (8) from Norway with generally similar paragenesis (i.e. in small veins of analcime and calcite, cutting augite porphyry; in calcite-albite veins, associated with a pitch-black or brownish-black isotropic mineral in small grains—(allanite?) and also leek-green garnet associated with natrolite). Weinschenk (9) has described similar garnets from the Alps, and mentions a high ferrous iron content (as opposed to high Fe_2O_3) as characteristic of "true-rock forming garnets" found in granites and schists. Stose and Glass (10) have described andradite crystals from Pennsylvania: deep reddish brown, almost black in color, which occur in cavities formed by solution of limestone pebbles in conglomerate adjacent to Triassic diabase. The garnets are doubly refracting, with refractive indices 1.85–1.87, considerably higher than those of the New Jersey garnets. No analysis is given.

Klein (11), after a study of several hundred thin sections of garnets, concluded that the optical structure is conditioned by the external form, and has no relation to chemical composition. Thus, with Hintze's observation cited above as to macroscopic garnets being characteristically anisotropic, it would appear that the anisotropy is of purely physical character, related to shape and size, and not to the elements composing the garnet.

Garnet having the composition of manganian andradite, called polyadelphite (12), has been found in the pegmatite cutting the ore body at Franklin Furnace, New Jersey. At the old Gooseberry iron mine in the same vicinity garnets essentially free from manganese were found, with magnetite. Both of these occurrences are evidently of altogether different paragenesis from the Wykertown garnet.

ALLANITE

The allanite is by far the least abundant of the minerals constituting the hydrothermal deposit. The ratio of abundance of natrolite-andradite-allanite may be the order of $10^6:10^2:1$.

The crystals were too small, and included too much of the surrounding natrolite to permit chemical analysis. The optical characters, together with an x-ray diffraction pattern obtained by Joseph M. Axelrod, and a spectrographic examination by A. T. Myers, satisfactorily establish its identity. Myers found:

Major (>1%) Si, Al, Ca, Fe, La, Nd, Ce
Minor (0.X%) Mn, Th, Sr
Trace Pb
Not found Be

The allanite is illustrated in Fig. 2.

Miss J. J. Glass has carefully investigated the optics of the allanite, a rather difficult matter in view of the intense absorption and variable indices of refraction of the mineral. No zoning is present. She found:

	Color
$\alpha=1.746$ to 1.765	colorless to pale reddish brown
$\beta=1.760$ to 1.779	reddish brown
$\gamma=1.771$ to 1.791	dark reddish brown, nearly opaque
$\Delta=$ .025 to .026	Large optic angle, distinct dispersion of the optic axes
$c\wedge X=38°$	$v>r$

These values are somewhat higher than those noted by Larsen (13) for allanite from Wyoming, namely $\alpha=1.727$; $\beta=1.739$; $\gamma=1.751$.

Larsen gives data for five allanites, including the one cited above and finds that they consist of "at least two and probably three distinct minerals." One of them is pale, sensibly isotropic, and has an index of refraction of about 1.68 to 1.70; another, possibly related to the one just mentioned, has a somewhat higher index of refraction, a weak birefringence, and is pleochroic in green and yellow; the third is clearly derived from the others and has the following optical properties: 2V rather large (−) sign, $r>v$ rather strong, $\beta=1.71-1.76$, $\Delta=0.01-0.02$, pleochroic in red-brown, with absorption Y and Z>X. Most of the Wykertown, New Jersey, allanite differs from the five studied by Larsen, in being optically a single substance, similar to the third type described by him.

Although nearly all of the allanite appears to be homogeneous, there are occasional crystals which do show a composite character, consisting of a few alternating zones or shells of the usual brown allanite, with others of a pale-yellow substance which may be the first of the three minerals noted by Larsen.

Allanite has been found in a pegmatite from the Franklin Furnace mine, described by Palache (14).

ACKNOWLEDGMENTS

Dr. Earl Ingerson and Dr. Michael Fleischer, of the U. S. Geological Survey, have kindly read and instructively commented on this manuscript.

REFERENCES

1. WOLFF, J. E., in SPENCER, A. C., et. al., *U. S. Geol. Survey Atlas, Franklin Furnace Folio*, No, **161** (1908).
2. BRACHVILLE, N. J. *Sheet* **606611** *N. W. AMS Series V***822**, 2d Ed. (1946).
3. Reference 1, page 13.
4. PARKER, JOHN M. III, New Jersey's potential feldspar resources: *Bull.* **5**, Part 1, Rutgers University (1948), p. 56.
5. HINTZE, CARL, Handbuch der Mineralogie, vol. **2**, 47 et seq. Leipzig (1897).
6. FLEISCHER, MICHAEL, The relation between chemical composition and physical properties in the garnet group: *Am. Mineral.* **22**, 751–759 (1937).
7. ZEDLITZ, O., Ueber titanhaltige Kalkeisengranate: II. *Zentralblatt Min.* **(1935A)**, p. 68.
8. BRÖGGER, W. C., Mineralien der sudnorwegischen Augitsyenit: *Z. Krist.*, **16**, page 160 et seq. (1890).
9. WEINSCHENK, ERNST, Ueber einige neue Mineralvorkommen des bayerischen Waldes; *Z. Krist.*, **25**, 36 (1896).
10. STOSE, G. W., AND GLASS, J. J. Garnet crystals in cavities in metamorphosed Triassic conglomerate in York County, Penn.: *Am. Mineral.*, **23**, 430–435 (1938).
11. KLEIN, C., *N. Jahrb.*, **1**, 87 (1883).
12. PALACHE, C., The minerals of Franklin and Sterling Hill, Sussex County, New Jersey: *U. S. Geol. Surv., Prof. Paper* **180**, 75 (1935).
13. LARSEN, E. S., JR., Microscopic determination of the non-opaque minerals: *U. S. Geol. Surv.* **679**, 37 (1921).
14. PALACHE, C., *loc. cit.*, pages 98–99.

AN AMPLIFIER FOR DIFFERENTIAL THERMAL ANALYSIS*

Carl W. Beck,
Department of Geology, University of New Mexico,
Albuquerque, New Mexico.

Abstract

An amplifier to be used with pen and ink recorders in the differential thermal analysis studies of minerals is described. The fundamentals of the amplifier are: (1) conversion of direct voltage to alternating voltage, (2) amplification of the alternating voltage, and (3) rectification of the amplified alternating voltage to direct voltage.

Curves for 14 analyzed minerals recorded with a pen and ink recorder are compared with photographically recorded curves obtained by Speil (1945) on the same minerals.

Introduction

The method of differential thermal analysis is a recognized and useful technique for the study of certain minerals or mineral groups that undergo either physical or chemical changes, or both, when heated. The theory of differential thermal analysis has been explained and the technique and apparatus described adequately by many workers in the field, such as Berkelhamer (1945), Grim and Bradley (1940), Grim and Rowland (1942), Hendricks et al. (1946), Jourdain (1937), Kerr and Kulp (1948), Norton (1939 and 1940), Orcel and Caillère (1933), and Orcel (1935). The standard recorder for differential thermal analysis curves has been the photographic type well-described by most of the above authors. More recently workers in the field have turned to pen and ink recorders. Kerr and Kulp (1948) describe a multiple differential thermal analysis apparatus in which they use a Leeds and Northrup "speedomax" as the recorder. Commercial recorders do not possess a sensitivity great enough to detect small thermal reactions, so it becomes desirable in the thermal analyses of most minerals to increase the sensitivity. It is the purpose of this paper to describe an amplifier used successfully by the author in differential thermal analysis studies.

Amplifier

It was desired by the author to use a pen and ink recorder in his differential thermal analysis studies. Several types of existing recorders could be adapted to the purpose, but an Esterline-Angus Graphic Ammeter was available and was used. The instrument is not sensitive enough without amplification to record the small potentials developed by thermo-

---

* Abridged from a Ph.D. thesis, "An Improved Method of Differential Thermal Analysis and Its Use in the Study of Natural Carbonates," Harvard University. Contribution from the Department of Mineralogy and Petrography, Harvard University, No. 315.

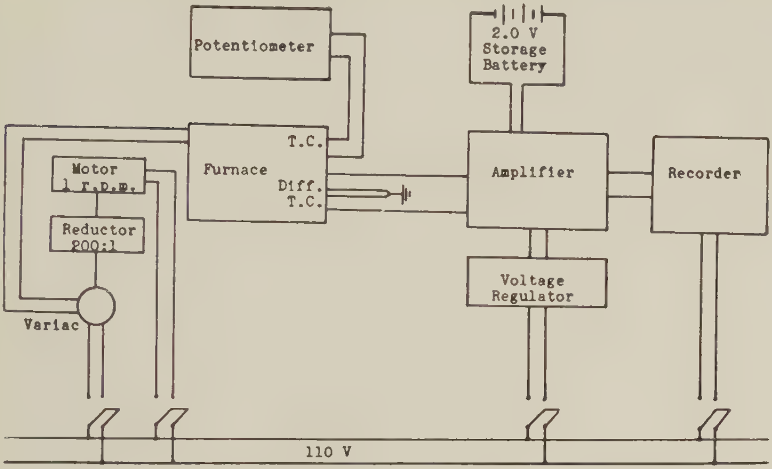

FIG. 1. Wiring diagram for differential thermal analysis apparatus.

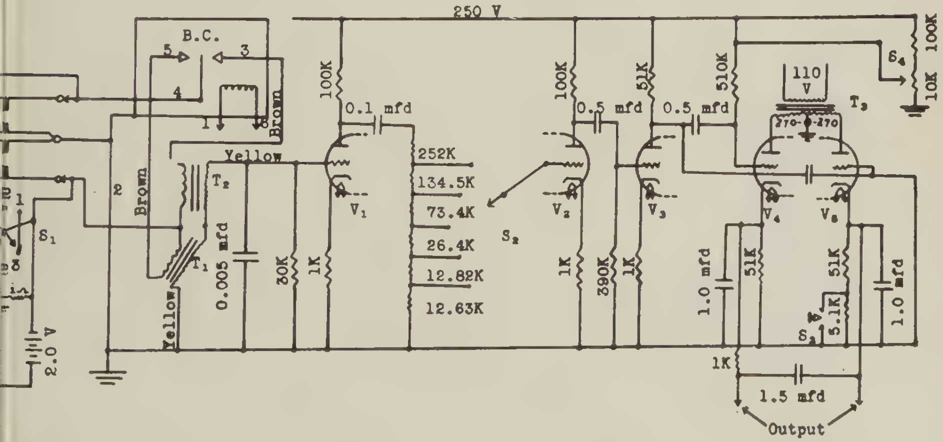

B.C. = Brown Converter
S_1 = Calibration Switch
S_2 = Sensitivity Switch
S_3 = Temperature Indicator Switch

S_4 = Centering Switch

V_1, V_2 = 6SL7
V_3 = ½ 6SN7
V_4, V_5 = 6SN7
T_1, T_2 = Thordarson T-72A59 Transceiver Transformer
T_3 = Acme B-4 Transformer, 110 V to 270-0-270

FIG. 2. Schematic diagram of amplifier.

couples during a thermal reaction in minerals. An Esterline-Angus recorder has an internal resistance of 1400 ohms and 0.5 milliamperes for half-scale deflection. Therefore, it requires 0.7 volts to get half-scale deflection. It was decided that an amplification of 10,000 on the most sensitive scale would give an appreciable peak for such weak reactions as the alpha-beta quartz inversion. Grim and Rowland (1942) say this inversion represents a differential temperature of about 2° C., and this is among the smallest energy changes to be recorded.

The diagram of the amplifier is shown in Fig. 2. Briefly, the basic principle of the amplifier is as follows: the direct voltage generated in the thermocouple by a thermal reaction is changed to alternating voltage; the alternating voltage is then amplified to a desired amount; and, finally, the amplified alternating voltage is rectified to direct voltage in order to operate the Esterline-Angus recorder. There are, therefore, three fundamental functions of this amplifier: (1) conversion, (2) amplification, and (3) rectification.

Conversion

The conversion of the direct voltage generated by the differential thermocouple to alternating current of proportional magnitude is accomplished by a Brown Converter (made by the Brown Instrument Company of Philadelphia) and the input transformers T_1 and T_2 (Fig. 2).

The converter is a flat reed that oscillates between the two contacts that are connected to the opposite ends of the primary winding on the input transformers, T_1 and T_2. Consequently, as the reed moves from one contact to the other, an unbalanced direct voltage generated by a thermal reaction will cause a direct current to move at first in one direction through one half of the primary winding, and then in the opposite direction through the other half of the primary winding. Thus is generated an alternating current in the input transformers. The input transformers then induce an alternating voltage in the secondaries of the transformer. The reed will oscillate synchronously with the alternating supply voltage, so that the direct voltage generated by a thermal reaction becomes a certain number of cycles of alternating voltage in the secondaries, the number of cycles depending on the cycles of the alternating voltage supply. Usually the supply voltage is 60 cycle.

When a thermal reaction takes place in the analyzed sample the thermocouple therein imbedded becomes warmer or colder than the thermocouple in the inert sample, thus generating an unbalanced direct potential to be put across the converter. If the thermal reaction is exothermic the converter will induce in the input transformer secondary an alternating voltage wave whose positive areas correspond with the positive areas of the alternating supply voltage, and the two voltages will be in phase. If the thermal reaction is endothermic the converter will induce in the input transformer secondary an alternating voltage wave whose positive areas correspond with the negative areas of the alternating supply voltage, and the two voltages will be 180° out of phase. This unbalance, following amplification and rectification, provides the means for deflecting the recording pen of the Esterline-Angus from the zero position.

In the apparatus used by the author, the input transformers, T_1 and T_2, were set 20° off parallel to give linearity. The position of the transformer cores must be determined experimentally, and will vary for each pair of transformers. It is necessary to connect the two input transformers in correct phase. The color of the transformer leads in correct phase are given in the schematic diagram, Fig. 2.

The converter and T_1 and T_2 must be shielded and are thus enclosed in a metal box, and the box is grounded. All leads up to the grid of Stage 1 are covered with "spaghetti" and shielding, and the shielding is grounded. This complete grounding serves to minimize any alternating current pickup. In addition, it is desirable to have a non-inductive winding on the furnace used to heat samples during a differential thermal analysis run.

Amplification

The induced alternating voltage from the converter is increased in amplitude and power by the use of thermionic vacuum tubes. The current is passed through three stages of voltage amplification, two triodes of a 6SL7 tube and one triode of a 6SN7 tube. A sensitivity switch, S_2 (Fig. 2), is located between Stages 1 and 2. This adjustment consists of a potential divider by which only a portion of the output voltage from the amplifier Stage 1 is applied to the grid of Stage 2; it thus varies the amount of amplification. This selector switch is designed to pick off five different portions of the Stage 1 output voltage to give sensitivity Scales 1, 2, 3, 4, and 5 in the amplification ratio of 1, 2, 8, 20, and 40; that is, Scale 5 is 40 times as sensitive as Scale 1.

Rectification

The amplified alternating voltage must be rectified to direct voltage in order to operate the Esterline-angus recorder. Two stages of rectification are used in this amplifier. If a negative potential, instead of a positive potential, is applied to the plate, electrons will be forced back to the cathode and no plate current can flow. Thus if an alternating current is applied to the plate, plate current will flow only when the plate is positive. Hence, the current in the tube flows in one direction and is thus rectified to direct current.

List of material used in amplifier

1 Brown Converter, Brown Instrument Company, Philadelphia, Pennsylvania.
2 6SL7 thermionic vacuum tubes.
2 6SN7 thermionic vacuum tubes.
2 Thordarson T-72A59 Transceiver Transformer.
1 Acme B-4 Transformer, 110 V to 270-0-270.
1 Regulated Supply, Type 106 PA, 300 volts, Harvey Radio Laboratories, Inc., Cambridge Massachusetts.
1 Storage battery, 6.0 volts.

The author has tried, unsuccessfully, to amplify the potentials developed by thermal reactions by means of a direct current amplifier. A

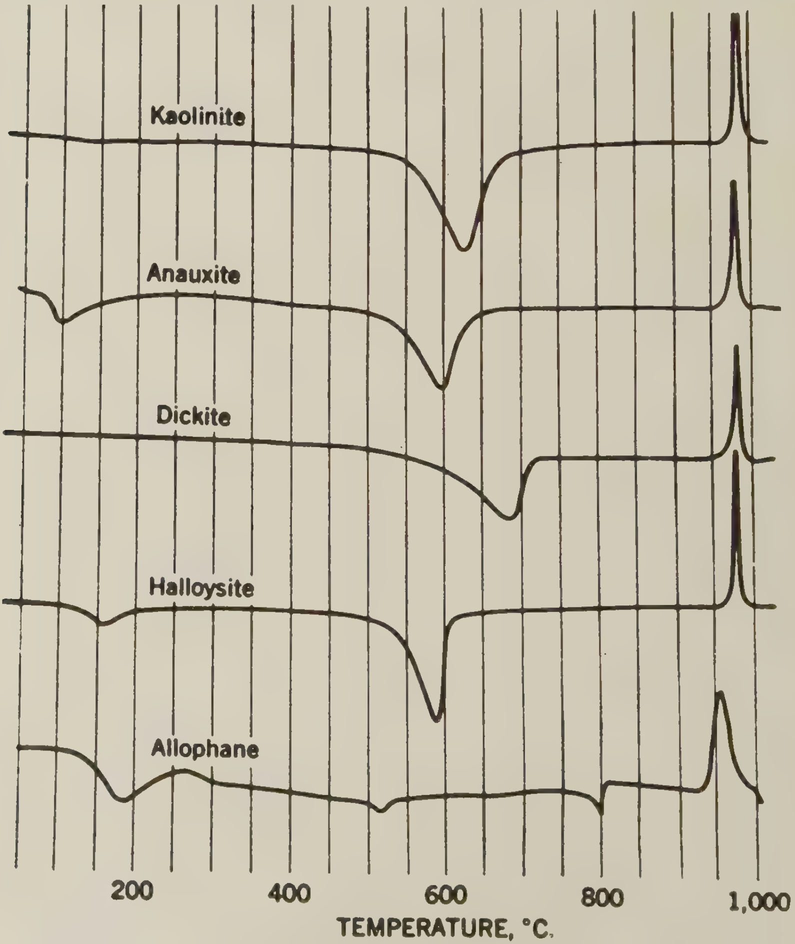

FIG. 3.—Thermal curves of kaolin minerals, scale C. (after Speil)

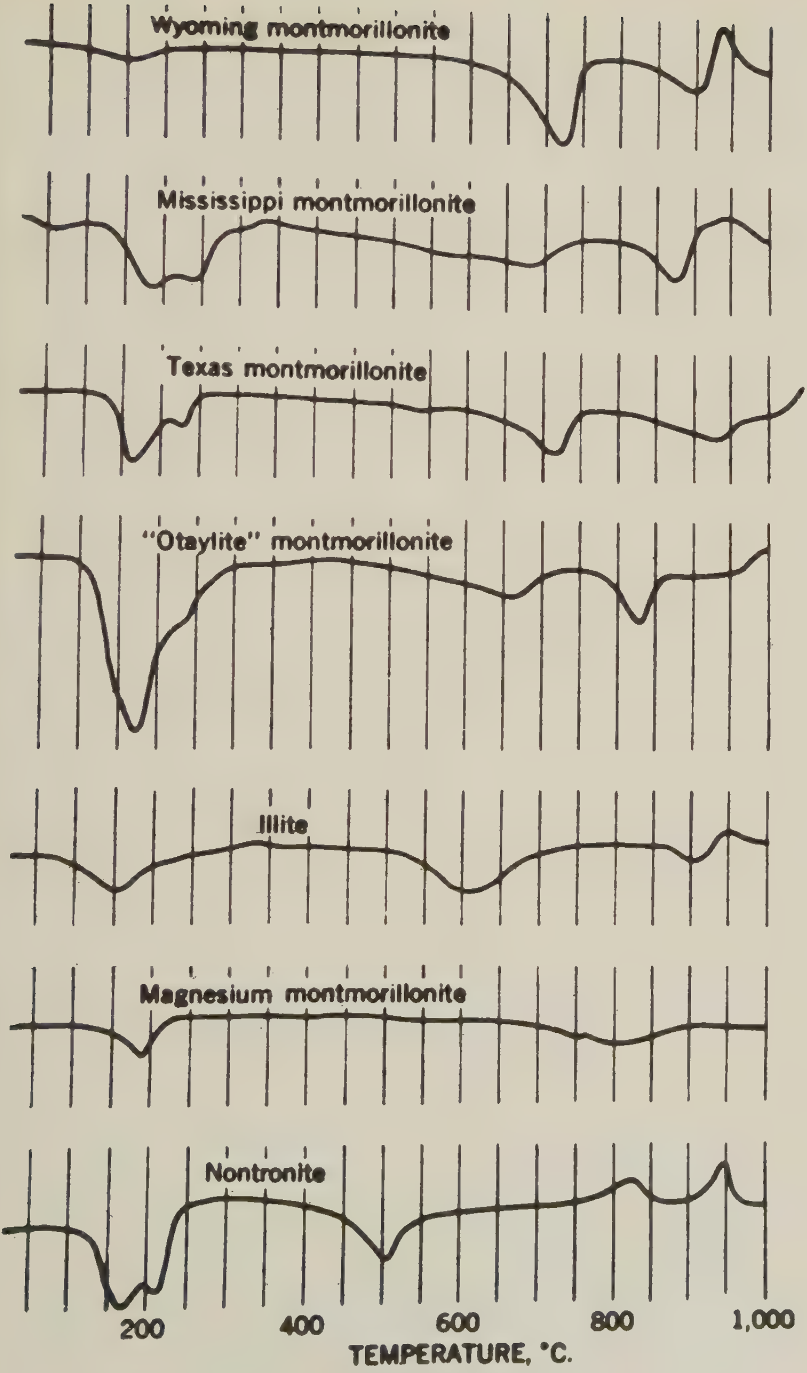

FIG. 4.—Thermal curves of three-layer lattice minerals, scale A. (after Speil)

three-stage amplifier of the ordinary push-pull circuit was constructed using 6SL7 tubes in Stages 1 and 2, and a 6SN7 tube in Stage 3. Stages 2 and 3 were satisfactory, but Stage 1 was unstable, exhibiting wander but no steady drift. 100% alternating current feedback was used on all stages, but no direct current feedback. The direct current amplifier was designed to operate in the linear region of the tube characteristics; that is,

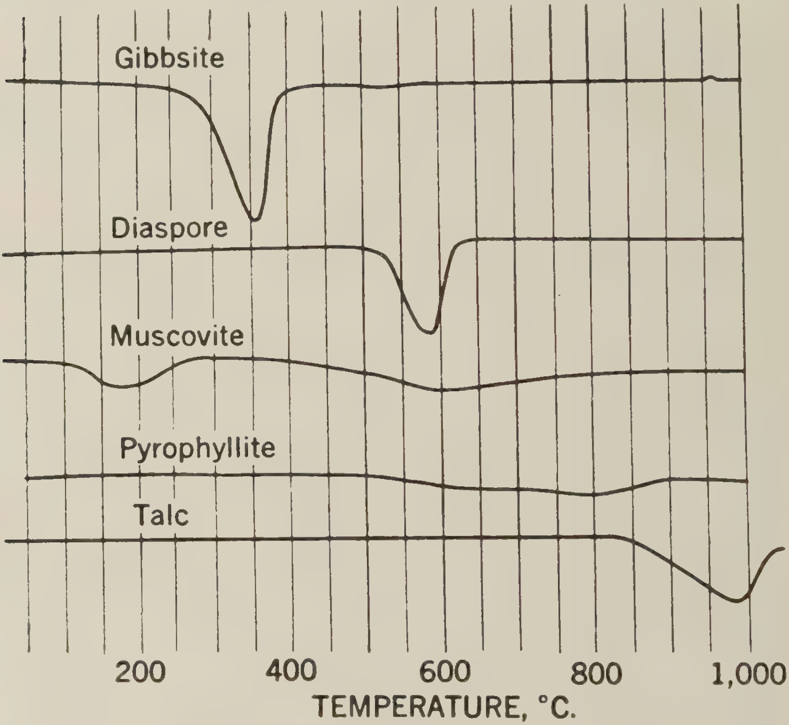

Fig. 5.—Miscellaneous thermal curves: gibbsite and diaspore, scale C; others, scale A. (after Speil)

an attempt was made to design with the plate currents no greater than 0.2 milliamperes per tube and direct coupling was used throughout. The last stage contained a balanced cathode follower for low impedance coupling to the Esterline-Angus recorder because of the high internal resistance of the recorder, namely, 1400 ohms. It is thought that tube leakage and instability of the circuit components of Stage 1 caused the trouble. The author believes it is possible to make a direct current amplifier, and experiments along this line are in progress.

METHOD OF OPERATION

The heating apparatus and sample holder used by the author were modeled after Berkelhamer (1945); the amplifier and recorder are described above. The differential thermal analysis runs were made according to the following scheme. Test samples were ground to minus 100-mesh, plus 200-mesh, and were kept in a desiccator over anhydrous $CaCl_2$ until ready for a run. They were not dried in an oven because it was felt that such drying would destroy adsorbed water on fine-grained minerals, and reduce or destroy the thermal reaction of minerals that lose structural water at a relatively low temperature. The weight of the sample was determined for each run. The material was packed carefully under and around the thermocouple wiring; the rest of the sample was packed above the thermocouple by means of a glass tamp. An attempt was made to pack each sample in the same manner.

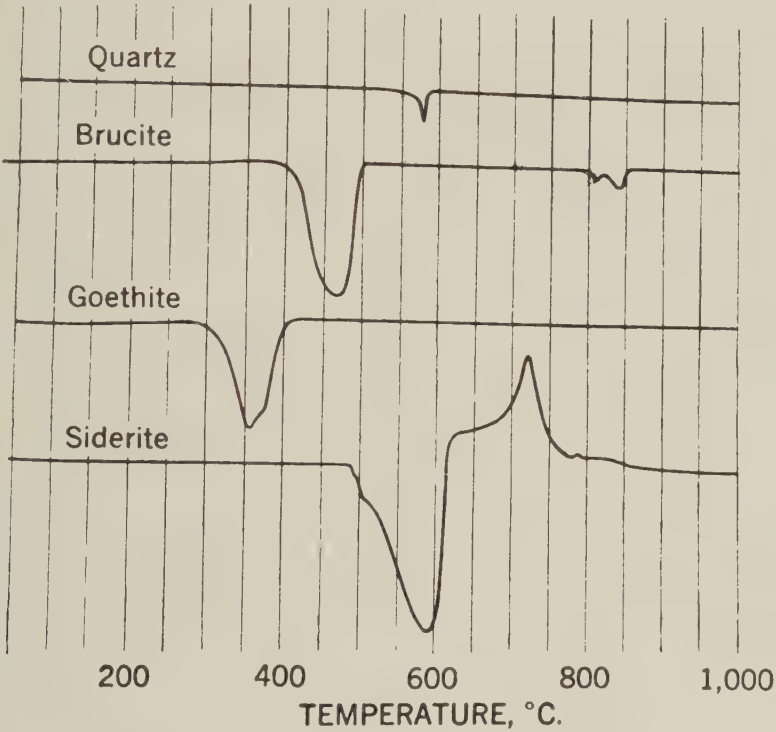

FIG. 6.—Miscellaneous thermal curves: quartz, scale A; others, scale C. (after Speil)

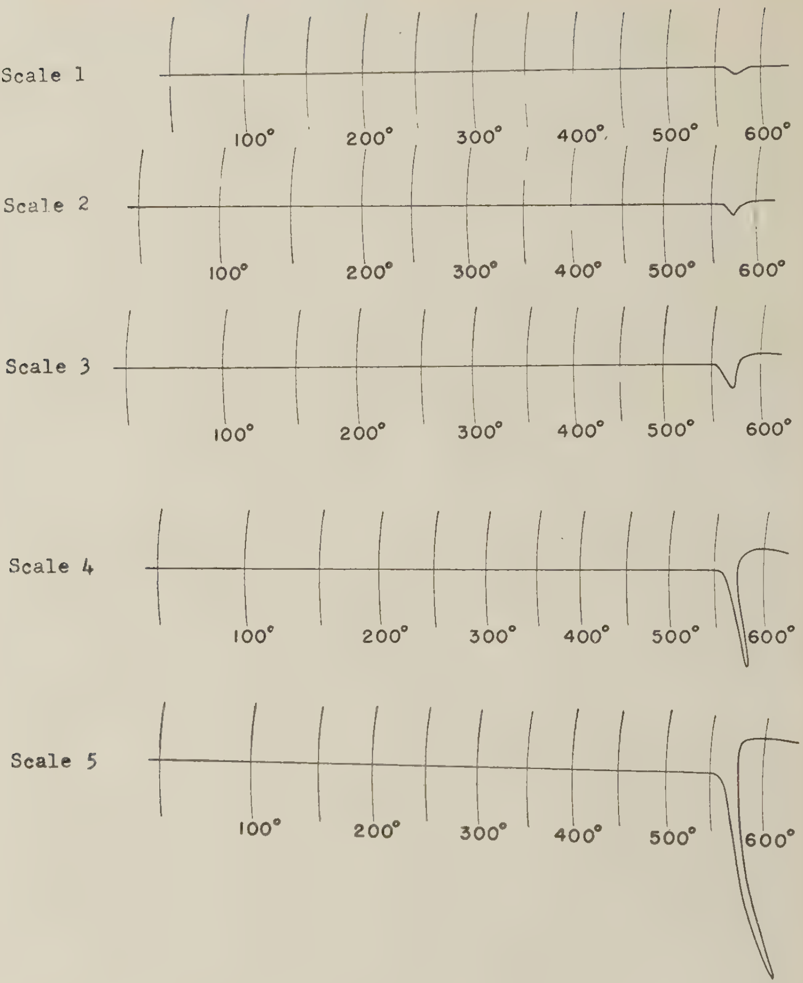

Fig. 7. Thermal curves of quartz showing relationship of scales 1–5.

The specimen holder and samples were covered with a nickel shield to eliminate direct radiation at the top of the samples. Then the furnace was brought forward so that the sample holder was held in the center of the furnace. The Variac was set at 35 volts and the furnace was warmed to 50° C. The sensitivity switch was set on the correct scale; the recorder was set at the zero position with the centering switch, S_4; and the instrument was calibrated by means of the calibration switch, S_1, to be sure it was linear at the start of the run. When the furnace reached 50° C. the Variac drive and the Esterline-Angus recorder were turned on simultaneously. The extra current drawn by the Variac motor drive caused a slight deflection of the recording pen and it was brought back to the zero point by S_4. At 50° C. intervals up to 1000° C., small lines were put onto the thermal curve by the push switch, S_3 (Fig. 2). At 1000° C. the instrument was again calibrated to be sure it was linear at the end of a run. An average run took 83 minutes, and the deviation from average was never more than $1\frac{1}{2}$ minutes.

Comparison of Photographic and Pen and Ink Methods

Eight samples of analyzed clay minerals and six samples of other analyzed minerals were obtained from Mr. Sidney Speil, Bureau of Mines Electrotechnical Laboratory, Norris, Tennessee. These had been used in his 1945 investigation. Reproductions of these curves appear in Figs. 3–6 and a listing of the characteristic thermal peaks and areas of most of these minerals appears in Table 3. A comparison of the deflection scales used by Speil is shown in Table 1.

Table 1. Comparison of Galvanometer Deflection Scales

Scale	Average value of ΔT for 1 cm. deflection, ° C
A	2.2
B	3.05
C	6.1

The differential thermal analysis curves of these same 14 samples recorded by the pen and ink method are shown in Figs. 8–12, and the characteristic thermal peaks and areas of these minerals are listed in Table 4. The comparison of the sensitivity of the different scales of this recorder is shown in Table 2.

Table 2. Comparison of the Sensitivity of the Different Scales of the Pen and Ink Recorder

Scale	Average value of ΔT for 1 cm. deflection, ° C.
1	4.1
2	2.4
3	0.85
4	0.21
5	0.10

In comparing Speil's scales with the scales used in this report, it should be pointed out that Speil used platimum-platinum 10% rhodium for his thermojunctions and the author used chromel-alumel thermojunctions;

the latter develop about 4 times the voltage for the same temperature. Also, it seems to the author that the characteristic areas listed by Speil are too large by a factor of 10.

A graphic illustration of the relation of Scales 1-5 is shown in Fig. 7. These curves show the alpha-beta inversion of quartz.

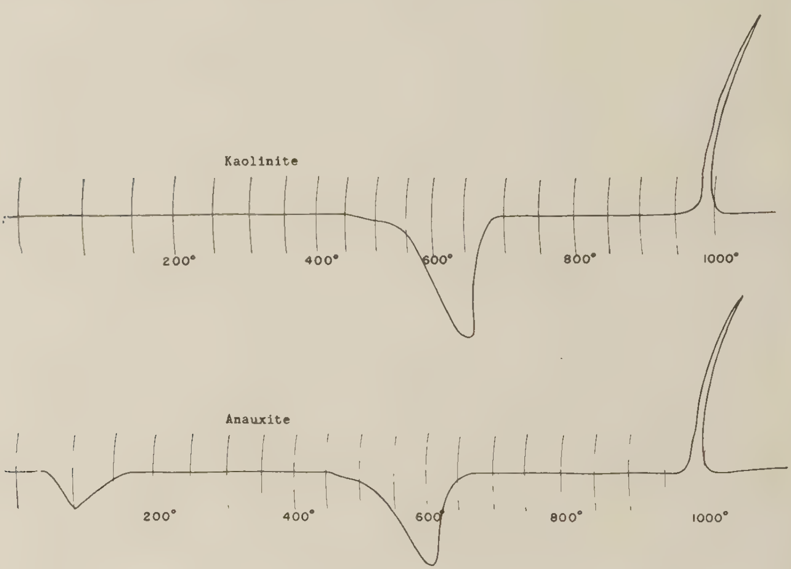

FIG. 8. Differential thermal analysis curves of kaolinite and anauxite, Scale 3.

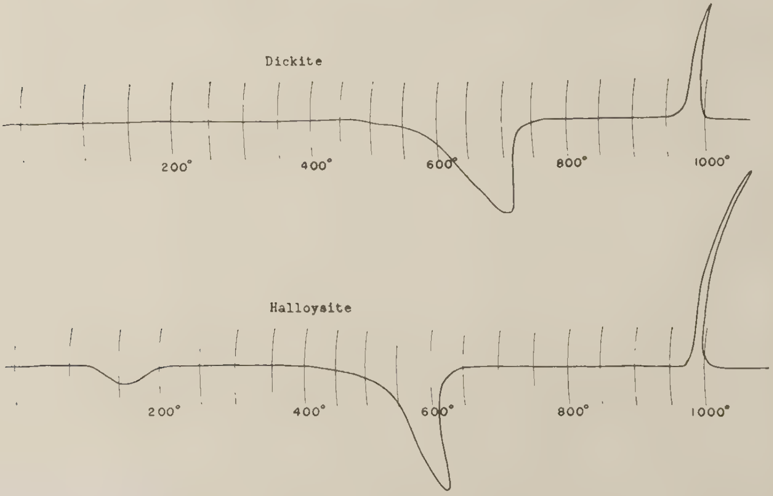

FIG. 9. Differential thermal analysis curves of dickite and halloysite, Scale 3.

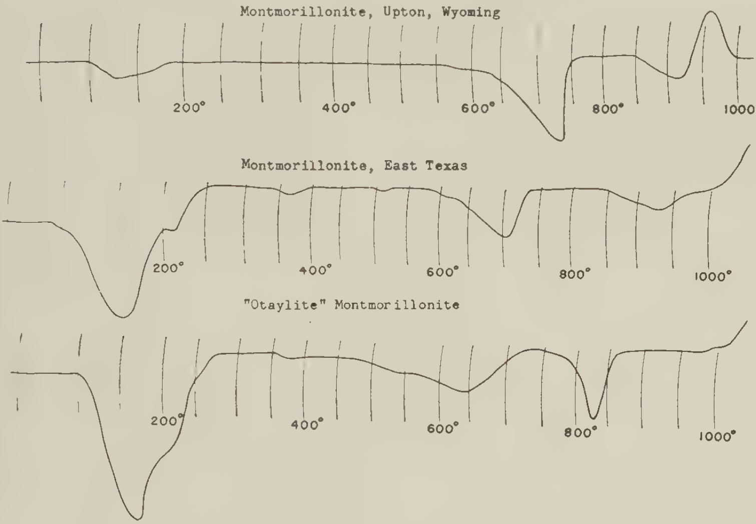

FIG. 10. Differential thermal analysis curves of montmorillonites, Scale 4.

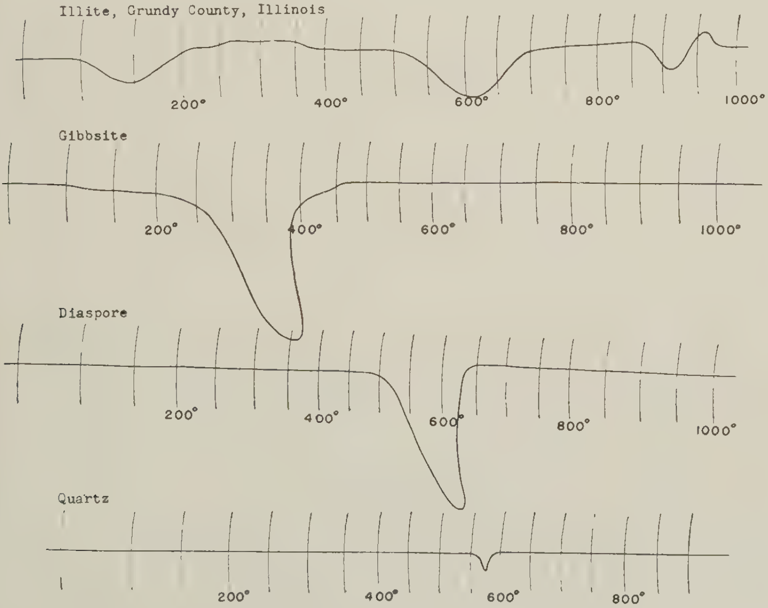

FIG. 11. Differential thermal analysis curves of illite (Scale 4), and gibbsite, diaspore, and quartz (Scale 3).

Examination of the thermal curves recorded by the two methods shows them to be in excellent agreement. Tables 3 and 4 show the thermal peaks to be essentially the same by both methods. There is a tendency for the peaks of the curves obtained on the pen and ink recorder to be at a slightly lower temperature. This is probably due to the fact that the pen and ink recorder reacts within a matter of a small fraction of a second after a thermal reaction takes place in the sample holder, while the Leeds and Northrup Type P galvanometer used in the photographic recorder has a time constant of 10–20 seconds. With the furnace rising at a rate of approximately 12° C. per minute this lag in the response of the galvanometer to the thermal reaction could push the peak temperature up several degrees. Two exceptions to this appear in the list of comparison runs: (1) diaspore has a peak temperature of 595° C. compared with 570° C. obtained by the photographic record, and (2) goethite has a peak temperature of 375° C. compared with 345° C. obtained by the photographic record. The author has no explanation for these two exceptions, but inspection of the curves obtained by Speil leads to the belief that the temperature should be higher for goethite and diaspore than

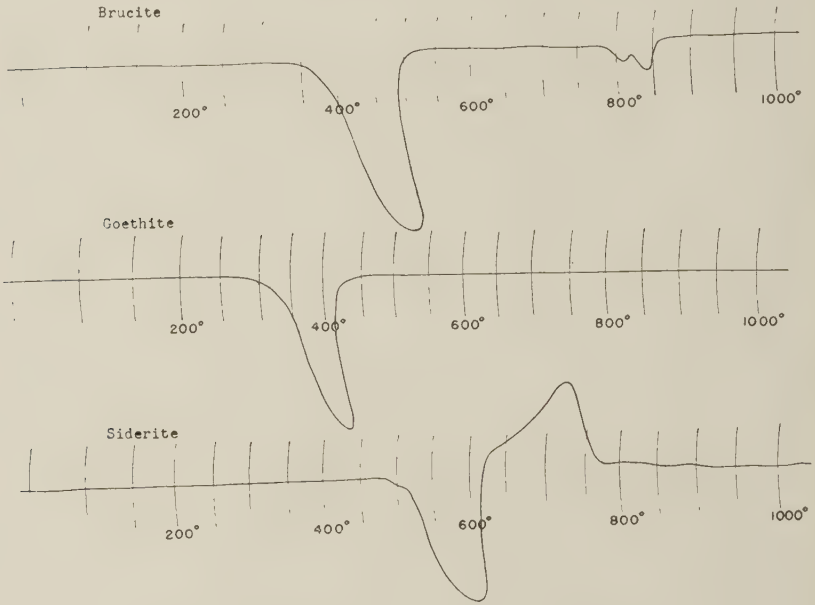

FIG. 12. Differential thermal analysis curves of brucite and goethite (Scale 3) and siderite (Scale 4).

TABLE 3. CHARACTERISTIC THERMAL PEAKS OF MINERALS
(Speil, 1945, p. 21)

Mineral	Temperature, ° C.		Area, mm.² Scale A
	Endothermic	Exothermic	
Kaolinite	620		6,100
		980	1,560
Anauxite	600		4,600
Dickite	690		4,900
Halloysite	175		indefinite
	585		4,250
Montmorillonite (Texas)	165–235		1,350
	725		1,070
	940		480
		1,020	indefinite
Illite	605		1,625
	900		merges
		940	merges
Gibbsite	365		8,400
Diaspore	570		5,200
Quartz	580		170
Brucite	465		7,000
Goethite	345		2,530
Siderite	585		10,300
		735	8,000

reported in Table 3. Re-runs of the diaspore and goethite gave check results for the pen and ink method.

ACKNOWLEDGMENT

This paper represents a portion of a differential thermal analysis doctoral problem. The author wishes to acknowledge the interest and encouragement shown by Professors E. S. Larsen, Jr., C. S. Hurlbut, Jr., and Clifford Frondel of the Department of Mineralogy and Petrography, Harvard University. He is especially indebted to Dr. Lee L. Davenport,

TABLE 4. CHARACTERISTIC THERMAL PEAKS AND AREAS OF COMPARISON MINERALS, PEN AND INK RECORDER

Mineral	Temperature, ° C.		Area, mm.^{2}	Weight, gm.	Scale
	Endothermic	Exothermic			
Kaolinite	620		600	0.325	3
		985	103		
Anauxite	595		406	0.255	3
		985	106		
Dickite	690		470	0.385	3
		985	97		
Halloysite	150		53	0.360	3
	585		403		
		985	107		
Montmorillonite (Texas)	145–220		658	0.265	4
	715		205		
	935		68		
		1050	indefinite		
Montmorillonite (Wyoming)	140		57	0.340	4
	725		370		
	920		merges		
		950	merges		
Montmorillonite "Otaylite"	165–200		920	0.350	4
	650		303		
	825		160		
		1030	indefinite		
Illite	600		140	0.320	4
	910		merges		
		950	merges		
Gibbsite	350		455	0.345	3
Diaspore	595		510	0.430	3
Quartz	573		10	0.395	3
Brucite	460		730	0.360	3
Goethite	375		440	0.585	3
Siderite	585		615	0.540	2
		735	325		

TABLE 5. CHEMICAL ANALYSES OF COMPARISON MINERALS

	1	2	3	4	5	6	7
SiO_2	45.20	64.26	44.91	43.74	64.29	60.26	51.19
Al_2O_3	39.47	18.08	40.64	40.82	16.23	21.50	15.13
Fe_2O_3	0.24	2.63	0.13	0.30	0.43	3.76	0.86
TiO_2	1.53	2.20	0.18	0.00	0.18	0.22	0.16
CaO	0.18	0.65	0.33	0.00	1.15	0.00	1.00
MgO	0.10	0.86	0.17	0.00	2.17	2.50	7.19
Na_2O	—	—	—	—	0.74	2.67	0.73
K_2O	—	—	—	—	5.91	0.43	0.12
H_2O (−)	0.11	2.41	0.03	2.43	8.94	3.53	15.80
Ignition Loss	13.84	7.96	14.61	14.93	5.57	5.34	7.57
Total	100.67	99.05	101.00	102.22	100.25	100.21	99.75

Key to Table 5

1. Kaolinite, Gordon, Georgia.
2. Anauxite, Franklin, North Carolina.
3. Dickite, Chihuahua, Mexico.
4. Halloysite, Eureka, Utah.
5. Montmorillonite, East Texas.
6. Montmorillonite, Upton, Wyoming.
7. Montmorillonite ("otaylite"), Encinatas, California.

H. R. Shell, analyst.

TABLE 5—*Continued*

	8	9	10	11	12	13	14
SiO_2	52.17	3.45	0.5	98.24	1.19	—	$FeCO_3=84.7\%$
Al_2O_3	22.24	60.17	84.8	0.97	—	—	
Fe_2O_3	6.16	2.72	0.1	0.00	0.96	83.63	$MnCO_3=16.8$
TiO_2	0.82	2.46	0.00	—	—	—	
CaO	0.31	—	—	0.00	0.63	—	
MgO	2.42	—	—	0.00	64.78	—	
Na_2O	0.33	—	—	—	0.00	—	
K_2O	0.50	—	—	—	0.19	—	
H_2O (−)	3.08	—	—	0.03	0.08	0.46	
Ignition Loss	6.15	31.20	14.2	0.09	31.20	12.80	
Total	100.13	100.00	99.6	99.33	99.03	96.89	101.5

Key to Table 5—*Continued*

8. Illite, Grundy County, Illinois.
9. Gibbsite, Arkansas (selected nodules).
10. Diaspore, Chester, Massachusetts.
11. Quartz, Potter's Flint.
12. Brucite, Luning, Nevada.
13. Goethite, Oregon Furnace, Maryland.
14. Siderite, Lodenstein, Saxony.

H. R. Shell, analyst.

University of Pittsburgh, and Mr. Robert Rogers, Massachusetts Institute of Technology, for technical advice in the construction of the amplifier. Mr. Sidney Speil of the Bureau of Mines Electrotechnical Laboratory, Norris, Tennessee kindly supplied the analyzed mineral samples.

REFERENCES

BERKELHAMER, L. H. (1945), An apparatus for differential thermal analysis: *Bureau of Mines R. I.* **3762,** 17 pages.

GRIM, R. E., AND BRADLEY, W. F. (1940), Investigation of the effect of heat on the clay minerals illite and montmorillonite: *Jour. Am. Ceram. Soc.*, **23,** 242–248.

GRIM, R. E., AND ROWLAND, R. A. (1942), Differential thermal analysis of clay minerals and other hydrous materials: *Am. Mineral.*, **27,** 746–761; 801–818.

HENDRICKS, S. B., GOLDRICH, S. S., AND NELSON, R. A. (1946), On a portable differential thermal outfit: *Econ. Geol.*, **41,** 41.

JOURDAIN, M. A. (1937), Studies on the constituents of refractory clays by means of thermal analysis: *Ceramique*, **40,** 135–141.

KERR, PUAL F., AND KULP, J. L., (1948) Multiple differential thermal analysis: *Am. Mineral.*, **33,** 387–419.

NORTON, J. H. (1939), Critical study of the differential thermal method for the identification of the clay minerals: *Jour. Am. Ceram. Soc.*, **22,** 54–63.

NORTON, F. H. (1940), Analysis of high-alumina clays by the thermal method: *Jour. Am. Ceram. Soc.*, **23,** 281–282.

ORCEL, J., AND CAILLÈRE, S. (1933), Differential thermal analysis of the montmorillonite clays (bentonite): *Compt. Rend.*, **197,** 174–177.

ORCEL, J. (1935), Differential thermal analysis in the determination of clays, laterites, and bauxites: *Cong. Internat. Mines, Met., Geol. Appl.*, 7th sess., Paris, 359–373.

SPEIL, SIDNEY (1945), Applications of thermal analysis to clays and aluminous minerals: *Bureau of Mines R. I.* **3764,** 36 pages.

STUDIES OF URANIUM MINERALS (III): SALÉEITE FROM SCHNEEBERG, SAXONY*

MARY E. MROSE, *Harvard University, Cambridge, Mass.*

ABSTRACT

Saléeite from Schneeberg, Saxony, has the composition $Mg(UO_2)_2(P,AsO_4)_2 \cdot 10H_2O$, with P:As=84.4:18.8, and is isostructural with fully hydrated artificial autunite, $Ca(UO_2)_2(PO_4)_2 \cdot 10H_2O$. Crystals are flat tablets on {001} with {010} and {012} and are found by *x*-ray and optical study to be tetragonal. Unit cell dimensions: $a_0=6.890$ Å, $c_0=19.813$ ($a_0:c_0=1:2.839$; $a:c=1:2.840$ morphology), with the space group, if holohedral, *I*4/*mmm*. Specific gravity 3.27 (meas.), 3.27 (calc. for two formula-units per cell). Color yellow to lemon-yellow. Perfect cleavage {001}. Optically uniaxial negative with *n*O 1.574 (pale yellow), *n*E 1.559 (nearly colorless). The original saléeite from Katanga has the composition $Mg(UO_2)_2(PO_4)_2 \cdot 8H_2O$ and appears from the available evidence to be a lower hydrate that is isostructural with meta-autunite-I.

INTRODUCTION

In the course of a study of natural and artificial uranospinite, $Ca(UO_2)_2(AsO_4)_2 \cdot 10H_2O$, a specimen from the Weisser Hirsch mine, Schneeberg, Saxony, was examined in some detail in the belief that it was this species, on the basis of apparent similarity in crystallography and optics. Later, on chemical analysis, the mineral was found to be the Mg analogue thereof and hence to be saléeite, $Mg(UO_2)_2(PO_4)_2 \cdot 10 H_2O$. Although the writer was unable to obtain an authentic specimen of saléeite from Katanga for direct comparison, the identity of the Schneeberg mineral therewith appears to be certain.

Saléeite from Katanga, Belgian Congo. The mineral saléeite was originally found at Chinkolobwe, Katanga, in the Belgian Congo, and was first described by J. Thoreau and J. F. Vaes in 1932. The mineral occurred there in a siliceous rock associated with the uranium phosphates torbernite and dewindtite. A chemical analysis (Table 3) on a 400 mg. sample indicated the formula of the mineral to be $Mg(UO_2)_2(PO_4)_2 \cdot 8H_2O$. Saléeite from this locality was described as small, thin, rectangular plates up to 2 mm. on edge, usually grown in parallel position with torbernite. Color lemon-yellow. Cleavages {001} perfect, also {100} and {010}; hardness 2–3; specific gravity a little below 3.3. The optical data are given in Table 1. On the basis of the biaxial optical character Thoreau and Vaes (1932) considered saléeite to be orthorhombic, but possessing pseudo-tetragonal symmetry. On the basis of measurements made under the microscope the crystal forms present were stated to be {001}, {010}, {100}, {120}, and {210}, with {001} as the plane of flattening and perfect cleavage, but an axial ratio was not given. Crystals resting on {001} when viewed in polarized light showed a division into two or four sectors, with the axial planes therein at right angles and parallel to the edges of the square plates, which was interpreted as due to twinning by pseudo-merohedry on [001]. (This feature also may be due to inversion into a lower hydrate isostructural with meta-autunite-I as discussed beyond.) Schoep (1939) later considered the mineral to be monoclinic, with the plane of flattening and perfect cleavage as {010}, and the twinning as on {$\bar{2}01$}, on the basis of etch effects and apparent differences in the ease of cleavage in different directions. This evidence, however, is inconclusive. Autunite thus has been considered to be monoclinic on similar evidence, but the symmetry of the etch figures has been shown to depend on the conditions of etching and the biaxial character to be related to the content of zeolitic water; the *x*-ray structural study of this mineral proves it to be strictly tetragonal.

---

* Contribution from the Department of Mineralogy and Petrography, Harvard University, No. 313.

Table 1. Optical Properties of Saléeite

	Saléeite Schneeberg (Mrose, 1949, on analyzed material)	Saléeite Katanga (Thoreau and Vaes, 1932)
Sign	(−)	(−)
Indices:		
*n*X or E	1.559±0.002	1.559
*n*Y		1.570
*n*Z or O	1.574±0.002	1.574
Opt. Orient.		X=*b*, Y∼*c*, Z∼*a**
Dispersion		*r*>*v*, marked
Pleochroism		
X or E	nearly colorless	
Y		
Z or O	pale greenish yellow	
2V (meas.).	0°	61°00′
2V (calc.)		61°49′

* Orientation of Schoep (1939), who made the crystals monoclinic from a study of etch figures and cleavages.

Saléeite from Schneeberg, Saxony. Saléeite was identified in this study from material on a specimen (Harvard no. 101126) from Schneeberg erroneously labelled uranospinite. This locality is new for the species. The mineral occurs both as small doubly-terminated rectangular crystals and as interlocking rectangular plates, ranging from ½ mm. up to 1 mm. on edge, in a limonite-rich rock associated with uranophane and zeunerite. Most of the crystals are opaque. The color varies from lemon-yellow to yellow with a greenish tint. There is a perfect cleavage on {001}. The hardness is 2–3. The specific gravity was determined for both single crystals and cleavage fragments on the microbalance as 3.27. This value is in exact agreement with the calculated specific gravity for the unit cell contents. The quantitative analysis by F. A. Gonyer on this material, cited in Table 3, proved it to have the composition $Mg(UO_2)_2(P,AsO_4)_2 \cdot 10H_2O$ with P:As = 84.4:18.8. The data cited in Table 1 indicate close optical agreement with material from Katanga. The *x*-ray powder diffraction spacings are cited in Table 4. The mineral fluoresces a bright lemon-yellow in long-wave ultraviolet radiation and pale yellow in short-wave ultraviolet radiation.

CRYSTALLOGRAPHY AND SYMMETRY

The saléeite from Schneeberg occurs as small doubly-terminated crystals most of which are too rough to afford accurate goniometric measurements. Several crystals provided approximate measurements which indicated the forms present to be *c*{001}, *a*{010} and *e*{012}.

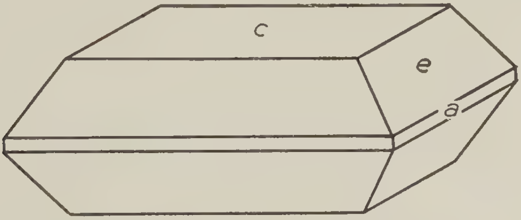

FIG. 1. Saléeite crystal from Schneeberg, Saxony.

An average of the best measurements gave 54° 51′ for {001}∧{010} indicating it to be the form {012}. This is in close agreement with the calculated value based on the *x*-ray elements. An average of the measured angles tabulated below give the ratio *a*:*c* = 1:2.840 which is in agreement with that derived from *x*-ray study.

	ϕ	ρ
c 001	0°00′	—
a 010	0°00′	90°00′
e 012	0°00′	54°51′

An angle table based on the elements derived from *x*-ray study for forms observed on Schneeberg and Katanga crystals is given in Table 2.

The crystals proved suitable for single-crystal *x*-ray work. The following data were obtained by the precession method using molybdenum radiation:

$a_0=6.980$Å. Possible space groups: $I\bar{4}2m$, $I\bar{4}m2$, $I4mm$, $I42$, or $I4/mmm$. $c_0=19.813$; $a_0:c_0=1:2.839$ (*x*-ray cell)

Cell contents: $2[Mg(UO_2)_2(P, AsO_4)_2 \cdot 10H_2O]$

If the crystal class is taken to be ditetragonal dipyramidal, as indicated by the form development and crude goniometric measurements, the space group is established by the diffraction effects as $I4/mmm$. The *x*-ray data conclusively establish the Schneeberg saléeite as tetragonal, in contradiction to the orthorhombic symmetry assigned to the Katanga material by Thoreau and Vaes (1932) and the monoclinic symmetry assigned it by Schoep (1939).

TABLE 2. SALÉEITE: ANGLE TABLE

Tetragonal; ditetragonal-dipyramidal—$4/m\ 2/m\ 2/m$

$a:c=1:2.839$; $p_0:r_0=2.839:1$

	ϕ	ρ	A	$\overline{M}$
c 001	—	0°00′	90°00′	90°00′
a 010	0°00′	90 00	90 00	45 00
d 120	26 34	90 00	63 26	71 34
e 012	0 00	54 50	90 00	54 41

CHEMISTRY

A chemical analysis of the Schneeberg saléeite, cited in column 4 of Table 3, indicates the formula of the mineral to be $Mg(UO_2)_2(P,AsO_4)_2$

TABLE 3. CHEMICAL ANALYSES OF SALÉEITE

	1	2	3	4
MgO	4.49	5.01	4.31	4.31
UO_3	63.67	64.07	61.23	60.32
P_2O_5	15.80	14.44	15.19	11.98
As_2O_5				4.50
H_2O	16.04	16.48	19.27	[18.89]
Total	100.00	100.00	100.00	[100.00]
G		<3.3		3.27

1. $Mg(UO_2)_2(PO_4)_2 \cdot 8H_2O$.
2. Saléeite. Katanga, Belgian Congo. M. Mollet analyst, in Thoreau and Vaes (1932). Recalculated to 100 after deduction of 2.79 per cent insoluble.
3. $Mg(UO_2)_2(PO_4)_2 \cdot 10H_2O$.
4. Saléeite. Schneeberg, Saxony. F. A. Gonyer analyst, June, 1949.

$\cdot 10\ H_2O$ with P:As=84.4:18.8. A spectrographic analysis on the same material in the spectral range between 2200 Å and 4300 Å showed that the minor constituents and traces included *Ca*, *Pb*, *V*, *Bi*, *Cu* and *Ag*.

The saléeite from Katanga differs in formula from the Schneeberg material by the absence of As_2O_5 and by having a water content of $8H_2O$ rather than $10H_2O$. The water content doubtless varies at ordinary temperatures with the humidity as it does with the isostructural minerals torbernite, autunite and zeunerite.

The *x*-ray powder pattern of the Schneeberg saléeite is virtually identical with that of fully hydrated synthetic autunite, $Ca(UO_2)_2(PO_4)_2\cdot 10\ H_2O$, as described by Beintema (1938), and differs from that of the lower hydrates meta-autunite-I with $6\frac{1}{2}$(?)H_2O and meta-autunite-II with 0 to $6H_2O$. The water content of these hydrates is partly zeolitic and the indices of refraction and 2V vary therewith. Meta-autunite-I is structurally tetragonal but optically it is uniaxial or biaxial, with 2V from 0° to 53° depending on the water content. The rectangular plates are divided into four biaxial segments each with its optic plane parallel to the edge of the plate. This mosaic character and optical orientation also are found in the Katanga saléeite and since this mineral has a relatively low water content it may correspond to meta-autunite-I; in such a case, the name meta-saléeite would be appropriate for this material and the name saléeite proper could be restricted to the Schneeberg material here described.

TABLE 4. *X*-RAY POWDER SPACING DATA ON ANALYZED SALÉEITE FROM SCHNEEBERG
Copper radiation, nickel filter (in Å)

No.	*I*	*d* (meas.)	No.	*I*	*d* (meas.)
1	10	9.94	12*	3	3.34
2	5	8.76	13	3	3.12
3	3	7.90	14	2	2.99
4	3	6.61	15	3	2.89
5	1	5.91	16	3	2.49
6	1	5.47	17*	3	2.23
7	8	5.01	18	2	2.00
8*	3	4.42	19	1	1.86
9	1	3.95	20	1	1.77
10	1	3.71	21	1	1.67
11	9	3.52	22	1	1.57

* Diffuse line.

ACKNOWLEDGMENTS

The writer wishes to express her appreciation to Dr. Clifford Frondel of Harvard University for valuable suggestions and advice during the preparation of this paper; to Dr. Howard T. Evans, Jr. of Massachusetts Institute of Technology for his assistance in the taking of the precession photographs; and to Dr. Harold C. Harrison of Harvard University for making the spectrographic analysis.

REFERENCES

BEINTEMA, J., On the composition and the crystallography of autunite and the meta-autunites: *Rec. Trav. Chim. Pays-Bas*, **57**, 155–175 (1938).

SCHOEP, A., Splijtingen, Corrosie-figuren en monokliene Symmetrie van Saléeiet; epitaxie op Metatorberniet: *Meded. Kl. Wetens. Kon Vlaamsche Acad. Wetens Lett.*, 65–70, Gent (1939).

THOREAU, J., AND VAES, J. F., La saléeite, nouveau minéral uranifére: *Bull. soc. belge géol.*, **42**, 96–100 (1932).

STUDIES OF URANIUM MINERALS (IV): JOHANNITE*

Cornelius S. Hurlbut, Jr., *Harvard University, Cambridge, Massachusetts.*

Abstract

X-ray Weissenberg study of johannite gave the following dimensions for the triclinic face-centered cell corresponding to the pseudo-monoclinic morphological cell of Peacock (1935): $a_0=16.51$ kX, $b_0=17.98$, $c_0=6.83$ with $\alpha=90°54'$, $\beta=90°38'$, $\gamma=110°37'$ (from morphology). Cell contents $Cu_4U_8(SO_4)_8(OH)_{40}\cdot 8H_2O$. Specific gravity 3.32 (meas.), 3.27 (calc.). Transformation, face-centered to primitive triclinic cell: $\frac{1}{2}0\bar{\frac{1}{2}}/0\bar{\frac{1}{2}}\bar{\frac{1}{2}}/001$. Elements of the primitive cell: $a_0:b_0:c_0=0.9382:1:0.7143$, $\alpha=108°50'$, $\beta=112°3'$, $\gamma=64°52'$.

Introduction

Johannite, $CuU_2(SO_4)_2(OH)_{10}\cdot 2H_2O$, long known as a mineral species, has been studied by several investigators during the past 120 years. The latest work was by Peacock (1935). Peacock summarizes the previous crystallographic work as follows: "Haidinger (1830) regarded johannite as monoclinic. Ježek (1916) likewise found the crystals he studied to be morphologically monoclinic, although they appeared to be optically triclinic. In order to reconcile the morphology of johannite with its optical behavior Larsen and Berman (1926) proposed a triclinic orientation for the mineral, taking the prismatically developed orthodome zone of Ježek as prism zone and Ježek's $x(011)$ as base." From careful goniometric measurements of crystals of johannite from Joachimsthal, the type locality, Peacock confirmed the triclinic character of the mineral and determined the following morphologic elements:

Johannite: Triclinic—*F* (after Peacock)

$a=0.9182$	$p_0'=0.442$	$p_0=0.4419$
$c=0.3799$	$q_0'=0.406$	$q_0=0.4059$
$\alpha=90°54\frac{1}{2}'$	$x_0'=0.011$	$\lambda=88°48'$
$\beta=90°38'$	$y_0'=0.021$	$\mu=88°59'$
$\gamma=110°37'$		$\nu=69°22'$

From the above elements one can see the pseudo-monoclinic nature of johannite and understand why the early workers considered it monoclinic.

X-Ray Data

The present investigation was undertaken to determine both the constants of the unit cell, and the contents of the unit cell in the light of the available chemical analyses. Using the same material on which Peacock had worked (Harvard specimen no. 89613), a rotation photograph and zero, first and second layer Weissenberg photographs were taken with the *c*-axis as the axis of rotation. It was impossible to find a suitable untwinned crystal, so the photographs were made on a twin composed of two individuals 0.5 mm. long and 0.1 mm. across. Because of this, the first and second layer line photographs showed double diffraction spots, one set from each lattice. These spots on the first layer photograph were so close together that they merged into one large spot; on the second layer line photograph they were resolved and a projection of the photograph gave two interpenetrating nets. An attempt was made to rotate the crystals about another axis, but because of their elongated habit this proved to be impractical.

---

* Contribution from the Department of Mineralogy and Petrography, Harvard University, No. 314.

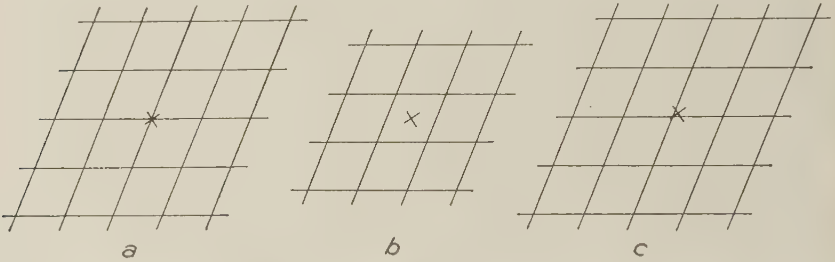

FIG. 1. Projections of Weissenberg photographs of johannite taken with *c* the axis of rotation. (*a*) zero layer. (*b*) first layer. (*c*) second layer.

When the projections of the three Weissenberg photographs about *c* were compared with one another, that of the first layer line showed an apparent exact centering of the zero layer, and the second layer line projection appeared to superimpose on that of the zero layer. These three projections are shown in Fig. 1 with the center of each marked with a cross. Such a centering indicates a multiple cell of an *F*-centered lattice. Careful inspection, however, shows that the second layer projection does not quite superimpose on the zero layer projection but is offset slightly with a small x_0' and y_0' and thus showing the triclinic character. This then is the pseudo-monoclinic cell, the constants of which as determined directly from the Weissenberg and rotation photographs are:

$$c_0 = 6.84 \text{ kX}, \ d(100) = 15.48, \ d(010) = 16.76, \ \nu = 69°30'$$

Reducing Peacock's geometrical values for p_0' and q_0' to $c_0 = 6.84$ we obtain: $c_0/p_0 = 6.84/0.442 = 15.47$ for $d(100)$, $c_0/q_0 = 6.84/0.406 = 16.85$ for d (010). Taking 6.83 as an average value for c_0, we find the following remarkably good agreement between the geometrical and *x*-ray data:

	Peacock	Hurlbut
c	6.83	6.84
$d_{(100)}$	15.46	15.48
$d_{(010)}$	16.82	16.76

For the calculations of the dimensions of the unit cell it seems wise to use the angles determined graphically by Peacock. Since they were the result of the measurement of 12 crystals projected on a 10 centimeter scale, they are no doubt more accurate than those obtained from the graphical solution of one x-ray projection on less than $\frac{1}{4}$ the scale. Using his angles, the dimensions of the F-cell are:

$a_0=16.51$ kX	$\alpha=90°54'$
$b_0=17.98$	$\beta=90°38'$
$c_0=6.83$	$\gamma=110°37'$

Using the above dimensions of the F-cell, the following elements were determined for the triclinic P-cell.

JOHANNITE: TRICLINIC-*P*

$a=0.9382$	$p_0'=0.884$	$p_0=0.7962$
$c=0.7143$	$q_0'=0.812$	$q_0=0.7314$
$\alpha=108°50'$	$x_0'=0.425$	$\lambda=78°\ 9'$
$\beta=112°03'$	$y_0'=0.228$	$\mu=73°22'$
$\gamma=64°52'$		$\nu=110°37'$

The relation of the F-cell and P-cell is shown in Fig. 2. The transformation formula F to P is $\frac{1}{2}0\frac{\bar{1}}{2}/0\frac{\bar{1}}{2}\frac{\bar{1}}{2}/001$. It seems best, however, to retain

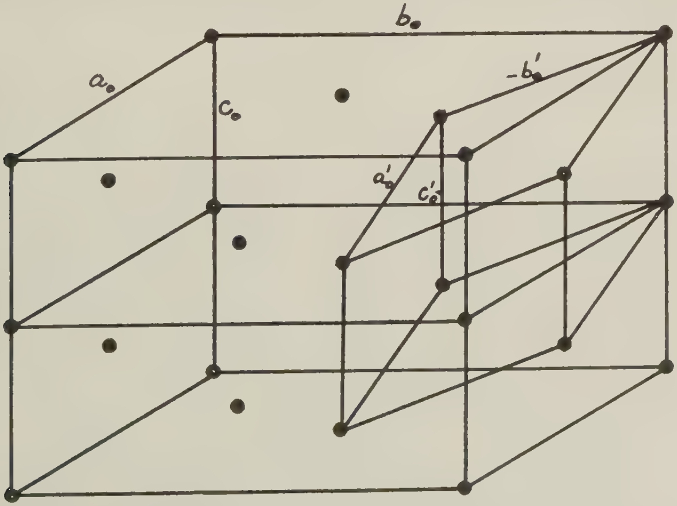

FIG. 2. Relation between the pseudomonoclinic triclinic F-cell and the triclinic P-cell of johannite. Primed letters are on axes of primitive cell.

for johannite the *F* setting of Peacock. In so doing the geometrical crystallography remains unchanged and the pseudo-monoclinic nature of both the morphology and the optics is preserved.

X-RAY POWDER DATA FOR JOHANNITE

Cu radiation, Ni filter

Line No.	*d*	*I*	Line No.	*d*	*I*
1	7.83	6	21	2.09	3
2	6.15	9	22	2.05	1
3	5.57	5	23	2.01	3
4	4.90	1	24	1.929	4
5	4.40	4	25	1.899–1.838	3 (very broad)
6	3.82	10 (broad)	26	1.801	1
7	3.53	2	27	1.765	2
8	3.41	8	28	1.710–1.647	3 (very broad)
9	3.23	1	29	1.595	3
10	3.10	7 (broad)	30	1.563	2
11	2.94	3	31	1.549	2
12	2.80	2 (broad)	32	1.526	3
13	2.67	3	33	1.484	2
14	2.59	4	34	1.459	2
15	2.44	2	35	1.433	1
16	2.38	1	36	1.412	1
17	2.32	1	37	1.375	1
18	2.24	3	38	1.351	1
19	2.19	2	39	1.326	1
20	2.13	3			

UNIT CELL CONTENTS

Three chemical analyses of johannite are available: (1) Johannite from Joachimsthal analyzed by A. Lindacker in 1856, (2) "Gilpinite" from Gilpin County, Colorado, analyzed by G. V. Brown on 0.22 gram (Larsen and Brown, 1917), (3) Johannite from Joachimsthal; the reported data are the results of duplicate microanalyses on 0.035 gram made by R. Nováček (cited in Peacock, 1935). This last analysis is given below:

JOHANNITE: ANALYSIS AND CELL CONTENTS

	1	2	3	4	5	6	7
UO_3	61.34	61.44	.2148	.2148	8.20	8	61.00
CuO	8.07	8.08	.1012	.1012	3.87	4	8.48
SO_3	16.59	16.62	.2075	.2075	7.92	8	17.07
H_2O	13.84	13.86	.7610	1.5220	58.0 (H)	56	13.45
	99.84	100.00		2.1291	81.1 (O)	80	100.00

1. Analysis by R. Nováček.
2. Analysis (1) reduced to 100%.
3. Molecular quotients.
4. Atomic quotient of the metals.
5. Measured cell contents. M = 3,817.
6. Ideal unit cell content.
7. Theoretical composition of $CuU_2(SO_4)_2(OH)_{10}\cdot 2H_2O$.

The specific gravity of johannite is 3.32—an average of five new measurements on the Berman balance. Using this as the density and the volume of the multiple *F*-cell as 1897.1, the molecular weight of the unit cell was found to be 3,817. Assuming the integers given in column 6 above as correct, the formula for johannite can be written $CuU_2(SO_4)_2(OH)_{10}\cdot 2H_2O$. There are four of these formula units in the *F*-cell and one in the *P*-cell. The calculated specific gravity is 3.27.

The writer wishes to acknowledge the help given by Prof. M. A. Peacock in interpreting the meaning of the apparent face-centered triclinic cell.

REFERENCES

1. HAIDINGER, W., *Ann. Phys.*, **20**, 472 (1830).
2. JEŽEK, B., *Bull. Int. Acad. Sci.* (Prague), **70**, 358 (1916).
3. LARSEN, E. S., AND BROWN, G. V., *Am. Mineral.*, **2**, 75 (1917).
4. LARSEN, E. S., AND BERMAN, H., *Am. Mineral.*, **11**, 1 (1926).
5. PEACOCK, M. A., *Zeit. Krist.*, **90**, 112 (1935).

THERMOELECTRIC POWER AND ELECTRICAL RESISTIVITY OF MINERALS*

MARIA TELKES, *Department of Metallurgy, Massachusetts Institute of Technology, Cambridge, Mass.*

ABSTRACT

The thermoelectric power and the electrical resistivity of a relatively extensive group of minerals was determined. These properties were measured on various cut and ground samples of the same specimen to show possible correlation. Different samples of the same mineral were used to establish variations in the magnitude of the electrical properties. The data obtained show considerable variations, probably due to the presence of impurities, but they establish the order of magnitude of the electrical properties. The data should be helpful in the study of pure synthetic semi-conductors and in the understanding of the electronic properties of these materials.

INTRODUCTION

A large group of minerals are semi-conductors, prepared by nature, generally impure, but readily available. Considerable experimental work has been carried out in determining the electrical resistivity of minerals and rather scattered efforts were made in measuring their thermoelectric power. A knowledge of the electrical resistivity and the thermoelectric power of minerals or pure synthetic semi-conductors are necessary adjuncts in the study of the electronic properties of materials.

Rather large variations exist in the resistivity of different specimens of the same mineral, which may be attributed to the presence of heterogeneous or non-stoichiometric impurities. The simultaneous determination of the thermoelectric power and the resistivity on several cut and ground samples of the same mineral specimen, should permit a definite correlation of these properties. Determinations on different specimens of the same mineral should be helpful in establishing order of magnitude correlations.

Comparison of metallic arsenides, sulfides, oxides, etc., should establish further correlations between the chemical nature of these materials and their electrical properties.

The possible use of minerals or their synthetic varieties, as rectifiers, thermocouples, or other electronic devices depends upon a more exact knowledge of their electrical properties.

1. REVIEW OF THE LITERATURE

The electrical resistivity of polished mineral specimens has been determined by Harvey (21). He used the four electrode method (two potential drop leads, between two current supplying leads). His method did not permit the exact determination of the specific electrical resistivity, the values are relative, giving the order of magnitude variations. Harvey used more than 2,000 samples and found that the electrical resistivity of different specimens of the same mineral varied considerably; the previous literature has been summarized by Harvey.

---

* Publication No. 26, M.I.T. Solar Energy Conversion Research Project.

Thermoelectric Power. The various "thermoelectric series" of minerals established by Seebeck (37), Becquerel (5), Hankel (19), Marbach (28), Bunsen (9), Flight (14), Stefan (40), Schrauf and Danna (38), Kundt (26), Iljew (23), and others can be regarded as qualitative indications.

Various specimens of the same mineral differed, often markedly, in the thermoelectric power value. Various specimens sometimes gave positive or negative values and in some cases positive and negative spots could be located on the same specimen. Variations of positive and negative spots have been studied by Groth (18), Hankel (20), and Rose (35). Kundt (26) devised a method to differentiate the thermoelectrically positive and negative regions of a specimen. The mineral was heated slightly and dusted with a mixture of powdered sulfur and minium; the sulfur became attached to the positive regions, while the minium adhered to the negative spots, revealing them in yellow and red colors.

Quantitative data of thermoelectric power determinations on minerals can be found in various Handbooks (Chapters by Laski (27) and Meissner (29), in the International Critical Tables, in Landolt-Bornstein's and other tables). Some of these data give merely an order of magnitude indication. It appeared advisable to collect the data from the literature, which are summarized in Table 1. In this table the thermoelectric power values are shown in microvolt/° C. with copper as the reference metal. Most of the experimental data were obtained with cold junctions at 0° C. (or 20° C.) and the hot junction at 100°. The thermoelectric power varies with the temperature and therefore the range of the measuring temperature should be noted.

The sign of the thermoelectric power is based upon a conventional agreement; material A is positive against a reference material B, if the thermal current flows in the same direction as the conventional electric current does when the circuit is closed. Some of the early papers did not follow this convention and therefore the original papers have been carefully scrutinized and whenever possible the sign convention has been ascertained.

From an examination of Table 1 it is obvious that various specimens of the same mineral show considerable variations in magnitude and may even differ in sign. The existence of positive and negative spots in the same specimen has been established. The reason for the positive and

TABLE 1. THERMOELECTRIC POWER (*e*) OF MINERALS (REVIEW OF THE LITERATURE)

Material	*e* microvolt/° C. ref. Cu	*Temp.* °C	*Reference*
ARGENTITE Ag_2S	−910	20–100	1888 Chaperon (10)
	−285	400	1888 Chaperon (10)
fused	70	20–100	1930 Reinhold (34)
CHALCOCITE Cu_2S	181 to 327	20–100	1866 Becquerel (6)
fused	340	20–100	1866 Becquerel (6)
fused	54	20–100	1932 Waibel (42)
fused	100	20–100	1930 Reinhold (34)
BORNITE Cu_5FeS_4	405	0– 25	1929 Ogawa (31)
GALENA PbS	−290 to 340	20–400	1888 Chaperon (10)
	−250	0–100	1900 Abt (1)
	160	0–100	1913 Streintz (41)
	−248	0– 25	1929 Ogawa (31)
	−490	20–200	1931 Fujii (16)
	−210		1932 Waibel (42)
	150		1933 Rupp (36)
	max. 2100	20–100	1935 Dean (13)
CHALCOPYRITE $CuFeS_2$	−280	0–100	1900 Abt (1)
	−425	0– 25	1929 Ogawa (31)
PYRRHOTITE $Fe_{1-x}S$	14	0–100	1900 Abt (1)
	−20	0–100	1909 Koenigsberger (24)
MILLERITE NiS	0	0–100	1900 Abt (1)
COVELLITE CuS thin film	7	20–100	1905 Baedeker (3)
STIBNITE Sb_2S_3	1600		1913 Planck (33)
BISMUTHINITE Bi_2S_3 fused	−80		1938 Hochberg (22)
PYRITE FeS_2	185	0–100	1900 Abt (1)
	−115	20–200	1931 Fujii (16)
	130 to 210	0–100	1911 Koenigsberger (25)
	−344 to 524	0– 25	1929 Ogawa (31)
	−180		1932 Waibel (42)
MARCASITE FeS_2	280	20–200	1931 Fujii (16)

TABLE 1—*Continued*

Material	e microvolt/° C. ref. Cu	*Temp.* °C	*Reference*
ARSENOPYRITE FeAsS	−265	20–200	1931 Fujii (16)
	−242	0–237	1888 Backstrom (2)
MOLYBDENITE MoS_2			(11)
15 specimens	700 to −1000		1924 Coblentz (12)
	460 to 730	20–100	1914 Gottstein (17)
	560		1921 Miller (30)
8 specimens	175 to −720	0–200	1909 Pierce (32)
	−1400	0– 25	1929 Ogawa (31)
	−750		1932 Waibel (42)
pressed	800		1938 Hochberg (22)
ZINCITE ZnO	−650	0– 25	1929 Ogawa (31)
fused	−720	320–400	1914 Bidwell (7)
sintered in air	839	550–650	1933 Baumbach (4)
sintered in H_2	510	550–650	1933 Baumbach (4)
crystal	400		1935 Fritsch (15)
crystal heated in H_2	200		1935 Fritsch (15)
HEMATITE Fe_2O_3	−660	20–400	1888 Chaperon (10)
	470	20– 50	1909 Koenigsberger (24)
	300	0–237	1888 Backstrom (2)
fused	−700	500–550	1916 Bidwell (7)
oxidized wire	430	20–700	1915 Brown (8)
ILMENITE $FeTiO_3$	−130	20– 50	1909 Koenigsberger (24)
PYROLUSITE MnO_2	−124	0–100	1900 Abt (1)
MANGANITE MnO(OH)	190	20– 50	1909 Koenigsberger (24)
	265	20– 50	1911 Koenigsberger (25)
PSILOMELANE	−3200	0– 25	1929 Ogawa (31)
MAGNETITE Fe_3O_4	55	20– 50	1909 Koenigsberger (24)
fused	−60		1914 Bidwell (7)

negative variations has been attributed to impurities. In molybdenite the difference may have been due to the presence of oxide as impurity, according to Coblentz (12). Ogawa found that argentiferous galena has a positive thermoelectric power (31) as compared to the usual negative value.

The thermoelectric power varies with crystal orientation. There are, however, insufficient data available to permit a quantitative correlation for various materials.

The synthetic materials, or pressed and sintered samples, sometimes show similar results to the minerals, but, depending upon the method of preparation, may differ considerably.

A review of the literature shows that the available data are not sufficient and considerable work is required to collect additional data.

2. EXPERIMENTAL ARRANGEMENT

The mineral specimens were obtained from the collection of the Geology Department of the Massachusetts Institute of Technology, or they were purchased from Ward's Natural Science Establishment. Many of the specimens were polished sections, or they were cut to prismatic shape.

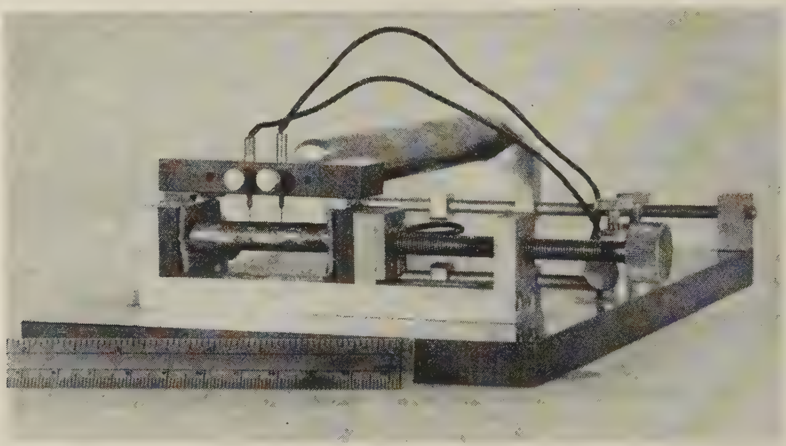

FIG. 1. Convenient resistivity apparatus

The electrical resistivity (specific electric resistance) can be determined only on samples cut to cylindrical or prismatic form. The four electrode method was used, with the specimen clamped between two current supplying blocks. Two needle electrodes were pressed against the surface of the specimen and connected to a potentiometer to measure the voltage drop between them. A convenient apparatus used in these measurements is shown in Fig. 1. The needle electrodes can be moved along the length of the specimen exploring possible variations, which may be present due to cracks, or possible rocky inclusions.

The following data are established:

ρ specific resistance (resistivity), Ohm. cm.
I current flowing through specimen, Amp.
E voltage drop between needle electrodes, Volt.
L distance between needle electrodes, cm.
s cross section of sample, cm^2.

$$\rho = \frac{E.s}{I.L} \text{ (Ohm. cm)}$$

The current was supplied from several large dry cells connected in parallel to minimize fluctuations. The current was measured with an ammeter; for specimens of higher resistivity a milli or microammeter was used. The voltage drop was measured with a potentiometer. The measurements were made at room temperature (around 20-25° C.). It was found that the resistivity of most minerals varied considerably, even on samples cut from the same mineral specimen. Generally the values agreed within 10 per cent when measured on the same specimen. In some cases greater accuracy could be obtained, which is indicated in the results.

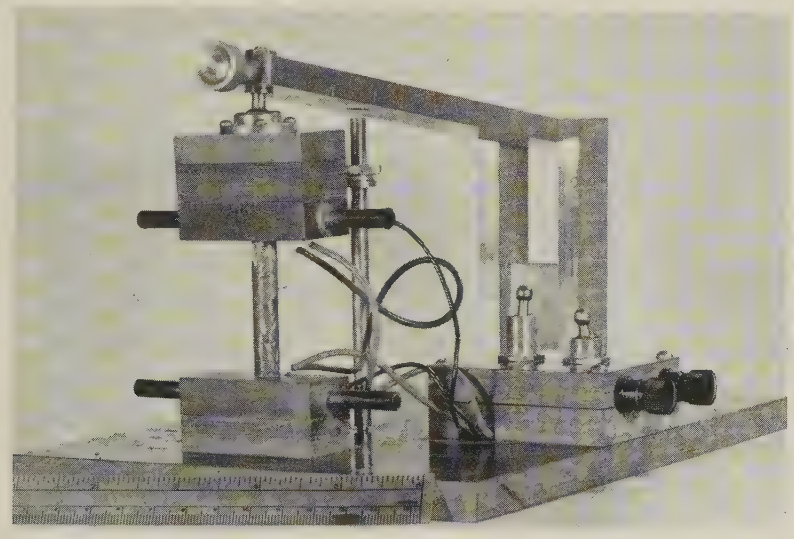

FIG. 2. Apparatus for measuring thermoelectric power

Thermoelectric power. The usual method of determining the thermoelectric power was followed, using the convenient apparatus shown in Fig. 2. The specimen was clamped between two copper blocks, the top one was heated with steam, the lower one cooled with circulating water. A differential thermocouple was attached to the two blocks to permit

TABLE 2

	Mineral	e Thermoelectric power, ref. Cu microvolt/° C.	ρ Specific resistance Ohm. cm.
1113	Huntilite Ag_3As		
	Lake superior, polished	−33	low
2112	Tetradymite Bi_2Te_2S		
	New Mexico	HR	
	Texas	−63	low
212	Nagyagite $Pb_5Au(TeSb)_4S_{5-8}$?		
	Nagyag, Transylvania	−64	low
213	Mohawkite Cu_3As		
	Michigan	−30	low
	Cobalt, Ont.	−33	low
	Polished	−30	low
2131	Algodonite Cu_6As		
	Lake superior, polished	−68	low
2132	Domeykite Cu_3As		
	Portage Lake	−15	low
	Calumet, Mich.	−15	low
2311	Argentite Ag_2S		
	Sonora, Mexico	−1000	high
2321	Chalcocite Cu_2S		
	Butte, Mont.	265	0.06
	Sonora, Mexico	495	0.27
	Cornwall	75	low
	Bristol, Conn.	190	low
	Bristol, Conn.	250	low
	Thuringia	70	low
2322	Stromeyerite AgCuS		
	Ontario	−400	10^5
	Saxony	150	med.
	Arizona	HR	
243	Bornite Cu_5FeS_4		
	Butte, Mont.	260	0.031
	Sangerhausen, Germany	40	0.016
	Silverton, Colo.	100	0.007
	Bisbee, Ariz.	365	0.13

TABLE 2—*Continued*

	Mineral	e Thermoelectric power, ref. Cu microvolt/° C.	ρ Specific resistance Ohm. cm.
	Bornite & Chalcocite		
	Butte, Mont.	320	0.10
	Butte, Mont. (4 specimens)	320	low
	Bornite & Covellite		
	Cornwall	150	low
	Polished	130	low
	Polished	340	low
252	Rickardite Cu_4Te_3	−14	low
	Polished		
2611	Galena PbS		
	Mies, Bohemia	−450	3.0 to −6
	Northport, Wash.	−300	0.08
	Aspen, Colo., Argentiferous	+370 to −450	0.35
	Gregory Mine, Colo.	−150 to −250	0.3 to .22
	Hartz, Germany	−110	0.007 to .0041
	Siebengebirge, Germany	−295 to −320	120
	Wallace, Idaho, Argentiferous	−260	200
	Galena, Ill.	+275 to −220	0.035
	Galena, Kan.	−50 to −260	0.026
	and Chalcopyrite		
	Butte, Mont.	−380	12
	Galena		
	De Soto Mine, Nev.	−295	low
	Franklin, N. J.	−300	low
	New South Wales	−210 to −250	0.02 to .36
	Monte Poni, Sardinia	−220	0.02
	Zeehan, Tasmania	−300	20
	Harvard Collection		
	No. 81742	−370	low
	87947	−345	low
	81749	−385	low
	81731	−360	low
	81718	−120 to +40	+ − spots
	Joplin	−190	+ − spots
	Joplin Roach Mine	−440	+ − spots
	Joplin	−220	+ − spots
	St. Eulalia, Mexico	−370	+ − spots
	Salchendorf, Westfalen	−250	+ − spots
	Leadville, Colo.	−200	+ − spots
	Galena	−200 to −260	+ − spots
	Argentiferous	+85	+ − spots

TABLE 2—*Continued*

	Mineral	*e* Thermoelectric power, ref. Cu microvolt/° C.	ρ Specific resistance Ohm. cm.
2614	Alabandite MnS		
	Nagyag, Hungary	HR	
2621	Sphalerite ZnS		
	Ottawa County, Okla. (excellent heat conductor)	900	high
	Bingham, Utah, 3 samples	180	med.
2622	Metacinnabar HgS, polished	90	low
2623	Tiemannite HgSe		
	Utah, polished	−43	low
2624	Coloradoite HgTe		
	Kalgoorlie, Australia	−27	low
	Kalgoorlie, polished	−30	low
2631	Chalcopyrite & bornite $CuFe_2S_4$		
	South Australia	260 to 210	2.0
2631	Chalcopyrite with quartz		
	Felsöbánya, Rumania	−310 to −410	low
2631	Chalcopyrite $Cu_2Fe_2S_4$		
	Rouyn District	−270 to −320	0.43
	Rouyn District	−365	0.032
	Cornwall, Pa.	−340	0.8
	Chester County, Pa.	−290 to −390	0.24
	Ellenville, N. Y.	−405	0.026
	Butte, Mont.	−60 to −170	0.036
	Cornwall, England	−100 to −170	1.7
	Leadville, Colo.	−350	0.04
	Larimer County, Colo.	−160 to −260	0.8
	Gilpin County, Colo.	−360	low
	Cochise County, Ariz.	−360 to −460	0.7 to .37
	Massive Crystals, pure	−400	0.042
	Polished	−380	low
	Harvard Collection		
	No. 80880	−345	low
	82081	−345	low
	Highly twinned	−80 to −230	low
	Freiberg, polished	−290	low
	Westmoreland, Brit.	−230	low
	Quebec	−170	low
	Single crystal, pure	−250	low

TABLE 2—*Continued*

	Mineral	e Thermoelectric power, ref. Cu microvolt/° C.	ρ Specific resistance Ohm. cm.
2632	Stannite Cu_2FeSnS_4		
	Zinnwald, Bohemia	210	300
	Oruru, Bolivia	370	med.
	Zeehan, Tasmania	60	med.
	Tolwing N.S.W. (2)	60	med.
2641	Wurtzite ZnS, polished	HR	
2642	Greenockite on sphalerite CdS		
	Hanover, Grant County, N. M.	HR	10^6
	5 samples	HR	
2651	Pyrrhotite $Fe_{1-x}S$		
	Frederick County, Maryland	60	0.10
	Standish, Me.	1	low
	Sudbury, Ont.	−14	low
	Cold Springs, N. Y.	0	low
	Troilite $Fe_{1-x}S$		
	Del Norte County, Calif.	−37	low
	Calif., polished	−13	low
	Benholm, Ont.	−11	low
2653	Niccolite NiAs		
	Germany, polished	−34	low
2655	Millerite NiS		
	Lancaster, Pa., 2 samples	−22	low
	Polished	−25	low
2656	Pentlandite $(Fe, Ni)_9S_8$, polished	−25	low
	In pyrrhotite, Worthington, Ontario	11	0.0007
266	Cubanite $CuFe_2S_3$		
	With chalcopyrite, Pinar del Rio, Cuba	−100 to −160	0.035
	Polished	−70 to −10	low
2681	Covellite CuS		
	Butte, Mont., 5 specimens	−10	low
269	Cinnabar HgS		
	Aleknagik, Alaska	HR	
26.10	Realgar AsS		
	Manhattan, Nev.	HR	
	Polished	HR	

TABLE 2—*Continued*

	Mineral	e Thermoelectric power, ref. Cu microvolt/° C.	ρ Specific resistance Ohm. cm.
2711	Linnaeite Co_3S_4		
	Missouri, 2 samples	−10 + spots	low
		−170	low
2714	Violarite Ni_2FeS_4		
	Polished	−240	low
2715	Polydymite Ni_3S_4		
	Algoma, Ont.	−22	low
	Sudbury, Ont., 2 samples	−20	low
	Polished	−20	low
281	Orpiment As_2S_3		
	Saxony	HR	
	Stibnite Sb_2S_3		
	Sevier County, Ark.	HR	
	Iyo, Japan	HR	
	6 samples	HR	
2822	Bismuthinite Bi_2S_3		
	Llallagua, Bolivia	−200	high
2911	Pyrite FeS_2		
	No name	−100 to +300	14
	Yechigo, Japan	−120 to +140	2.6
	Isle of Elba	−35 to −70	0.005
	Leadville, Colo.	+220 to +455	1.5
	Harvard Coll. #82107	−40	low
	92621	−280	low
	82114	−70 to −90	low
	88935	−120 to −290	low
	82097	−96	low
	Single crystals	−10	low
	Distorted crystals	−90	low
	Bingham, U. concretion	70	low
	Bingham, U. concretion	150	low
	Newfoundland concretion	160	low
	Elba crystal	20 to 110	low
	Mineral Point, Wis.	210	low
	Sandy Run, Pa.	50	low
2912	Bravoite (Fe, Ni)S_2 polished	290	low
2915	Hauerite MnS_2		
	Raddusa, Italy	HR	

TABLE 2—*Continued*

	Mineral	*e* Thermoelectric power, ref. Cu microvolt/° C.	*ρ* Specific resistance Ohm. cm.
2921	Cobaltite CoAsS		
	Saxony	−40	low
2922	Gersdorfite, NiAsS		
	Ontario, polished	−20	low
2931	Loellingite $FeAs_2$		
	Sweden, polished	−78	low
	Edenville, N. J.	−77	low
	Paris, Me.	−88	low
2932	Safflorite (Co, Fe)As_2, polished	−70	low
2933	Rammelsbergite $NiAs_2$, polished	−49	low
	Cobalt, Ont. (2 samples)	−37	low
	Brandt, Saxony	−80	low
	Schladnung, Austria (2)	−84	low
294	Marcasite FeS_2		
	Ottawa County, Oklahoma	385 to 770	med.
	Joplin, Mo.	192	low
	Osseg, Bohemia	140	low
	Nagyag, Hungary	170	low
	Polished	120	low
2951	Arsenopyrite FeAsS		
	Jardine, Mont.	−245	0.7
	Anglesea Twp., Ontario	−250	0.7
	Obira, Bungo, Japan	−295	0.08
	Freiburg, Saxony	−140	low
	Nova Scotia	−150	low
	Skykonish, Ash.	−100	low
	Cascade Mountains	−165	low
2952	Glaucodot (Co, Fe)AsS		
	Hakanspoda, Sweden	−55	low
2961	Molybdenite MoS_2		
	Santa Cruz County, Ariz.	−570	10
	Lyndoch, Ontario	460	med.
	Harvard Coll. 81617	80 to 490	med.
	91575	240 to −340	+ − spots
	Haddam County	−480	+ − spots
	Haddam County, polished	−430	+ − spots

TABLE 2—*Continued*

	Mineral	e Thermoelectric power, ref. Cu microvolt/° C.	ρ Specific resistance Ohm. cm.
2962	Tungstenite WS_2		
	Utah, polished	HR	
2973	Sylvanite (Au, Ag) Te_4		
	Cripple Creek, Colo.	−50	low
2.10.11	Skutterudite (Co, Ni)As_3		
	South Lorraine, Ont.	HR	
2.10.12	Smaltite (Co, Ni)As_{3-x}		
	Schwarzenberg	−30	low
2.10.14	Chloanthite (Ni, Co)As_{3-x}		
	Saxony	−51	low
2.10.2	Patronite		
	Minasragra, Peru	−130	high
	Polished	HR	
3112	Pearcite $(AgCu)_{16}As_2S_{11}$, polished	HR	
312	Polyargyrite $12(Ag_2S)Sb_2S_3$	−140	high
	Polished	HR	
	Saxony	HR	
314	Stephanite Ag_5SbS_4		
	Brand, Saxony	HR	
	Polished	HR	
3211	Pyrargyrite Ag_3SbS_3		
	Zacattecas	HR	
	Guanajuato, Mexico	330	high
3212	Proustite Ag_3AsS_3		
	Polished, 2 samples	HR	
3241	Tetrahedrite $(CuFe)_{12}Sb_4S_{13}$		
	Freiberg	HR	
	With pyrite, Bingham, U.	HR	
	With chalcopyrite, Australia	−5	low
	With Ag, Talache, Idaho	80 to 250	low
3241	Tetrahedrite (argentiferous)		
	With siderite, Coeur D'Alene, Idaho	490	37

TABLE 2—*Continued*

	Mineral	e Thermoelectric power, ref. Cu microvolt/° C.	ρ Specific resistance Ohm. cm.
3242	Tennantite $3Cu_2S \cdot As_2S_3$		
	Utah, polished	310	low
	Bingham, Utah	240	low
	Butte, Mont.	240	low
	Cornwall	190	low
	Braden Mine, Chile	270	low
3312	Germanite (Cu, Ge)(S, As)		
	Polished	−80	low
3321	Famantinite $3CuSbS_4$		
	Famatina, Argentina	400 to 560	210
	Famatina, polished	210	med.
3322	Enargite Cu_3AsS_4		
	San Juan Dist., Colo.	465	1.7
	Cerro de Pasco, Peru	325	0.19
	Peru	0 to 100	4.4
	Butte, Mont., polished	410	low
	Butte, Mont.	190	low
	Butte, Mont., Badger vein	300	low
	Butte, Mont., large crystals	420	low
	Tintic, Utah	300	low
	Peru	370	low
335	Geocronite $Pb_5(Sb, As)_2S_8$		
	Polished	−300	med.
336	Gratonite $Pb_9As_4S_{15}$		
	Cerro de Pasco, Peru	HR	
339	Guitermanite $Pb_{10}As_6S_{19}$		
	Colorado	HR	
33.12	Lilliantite $Pb_3Bi_2S_6$		
	Polished	HR	
3411	Bournonite $PbCuSbS_3$		
	Cornwall, polished	85	low
344	Freislebenite $Pb_3Ag_5Sb_5S_{12}$		
	Polished	HR	

TABLE 2—*Continued*

	Mineral	e Thermoelectric power, ref. Cu microvolt/° C.	ρ Specific resistance Ohm. cm.
351	Boulangerite $Pb_5Sb_4S_{11}$		
	Stevens Mine, Wash.	−135	med.
	Deer Lodge, Mont.	−900	high
	two samples	HR	
354	Miargyrite $AgSbS_2$		
	Freiberg, polished	HR	
	Idaho	HR	
356	Matildite $AgBiS_2$		
	Cobalt, Ontario	−150	med.
3592	Emplectite $CuBiS_2$		
	Saxony, polished	HR	
35.11	Teallite $PbSnS_2$		
	Montserrat, Panza, Bolivia	80	high
	Bolivia, 2 samples	HR	
3621	Cosalite $Pb_2Bi_2S_5$		
	Ontario, polished	−330	med.
363	Franckeite $Pb_5Sn_3Sb_2S_{14}$		
	With needle tin, Bolivia	40	420
	Bohemia	HR	
365	Ramdohrite $Pb_3Ag_2Sb_6S_{13}$	HR	
367	Jamesonite $Pb_4FeSb_6S_{14}$		
	Idaho	HR	
388	Zinkenite $Pb_6Sb_{14}S_{27}$	HR	
38.10	Berthierite $FeSb_2S_4$		
	Braunsdorf, Saxony	450	med.
	Braunsdorf, Saxony polished	310	med.
38.11	Cylindrite $Pb_3Sn_4Sb_2S_{14}$		
	Bolivia	180	high
	Bolivia	HR	
391	Livingstonite $Hg_3Sb_4S_7$		
	Mexico, polished	HR	

TABLE 2—*Continued*

	Mineral	e Thermoelectric power, ref. Cu microvolt/° C.	ρ Specific resistance Ohm. cm.
4511	Rutile TiO_2		
	Kragero, Norway	HR	
	var. nigrine, Arkansas	−540	high
4512	Pyrolusite MnO_2		
	Lake Valley, New Mexico	HR	electrolytic cond.
	Polished	−165	electrolytic cond.
6112	Pyrochroite $Mn(OH)_2$		
	Alum Rock, San Jose, Calif.	−400	high
625	Psilomelane $BaMn^{2}Mn^{4}_{8}O_{16}(OH)_4$		
	Woodstock, Va.	−140	10^3
	Polished	−150	med.
7216	Magnetite $FeFe_2O_4$		
	Clifton Mine, N. Y.	−53	low
7221	Hausmannite MnM_2O_4	HR	
	Långban, Sweden		

the measurement of the temperature difference (Δt). The temperature of the hot junction was very nearly 100° C., while the cold junction was generally around 10° C. Copper was used as the reference metal, connecting the apparatus to a potentiometer. A double pole, double throw switch was used to connect the differential temperature measuring thermocouple, or the thermoelectric *EMF* to the potentiometer. Another similar switch was used as required for positive or negative thermoelectric power determinations. The thermoelectric power between 100° C. and the cold junction is the thermoelectric *EMF* and the thermoelectric power (e), expressed in microvolt/° C. is obtained as $e = EMF/\Delta t$.

Several measurements were made on each specimen and the thermoelectric power is given as the average of these measurements. Many specimens showed rather constant values, but some differed considerably, various spots on the same specimen showing considerable differences and even sign reversals. The thermoelectric power could be determined on rather small specimens, measuring about 1 to 2 mm. in length. If necessary, fragments of the mineral could be compressed into a small pellet and used for measurements. Such small fragments were not suitable for the determination of the specific resistance and that is the reason that Table 2 summarizing the results, contains more data of thermoelectric power values.

Minerals of specific resistance in excess of $\rho = 10^6$ Ohm. cm (approximately) could not be measured accurately with the arrangement used and they are marked as *HR* ("high resistance") samples. In some cases the mineral sample was not available for cutting into prismatic shape and the specific resistance could not be measured, although it is indicated as medium resistance (ρ = approximately 1 to 10^3) or low resistance (ρ less than 1 Ohm. cm).

The results of the measurements are summarized in Table 2 listed in the order given in Dana's System of Mineralogy by Palache, Berman and Frondel, vol. I, 1944. The species numbers adopted in the above work have been used.

3. Discussion and Conclusions

A certain correlation between the thermoelectric power and the resistivity is to be expected, because materials of high thermoelectric power generally are of higher resistivity. This correlation is not well established, because impurities may cause great variations in the resistivity without influencing the thermoelectric power (for instance galena, etc.).

The largest groups of minerals examined—the sulfides—are examined for a correlation of the measured electrical properties with the periodic table of the elements.

Sulfides

Group i B (Cu, Ag, Au). *Chalcocite* Cu_2S always shows a rather high positive thermoelectric power, its resistivity being rather low. *Covellite* CuS, on the contrary has a very low negative thermoelectric power and very low resistivity. *Argentite* Ag_2S, has a very high negative thermoelectric power and a high resistivity.

Group ii B (Zn, Cd, Hg). *Sphalerite* ZnS and *metacinnabar* HgS of positive thermoelectric power have a high resistivity, while *greenockite* CdS, *wurtzite* ZnS and *cinnabar* HgS are insulators.

Group iv A (Ge, Sn, Pb). A single sample of *germanite* [(Cu, Ge) (S, As)] had negative thermoelectric power, the large number of samples of *galena* PbS, were mostly negative, in the −200 to −450 microvolt/° C. range. There were a few positive samples of galena (argentiferous?) and occasionally positive and negative spots could be found on the same sample. The resistivity was very low, of the order of 0.01 Ohm. cm, but occasionally much higher values were observed. No simple correlation could be found between the thermoelectric power and resistivity.

GROUP V A (As, Sb, Bi). In this group *realgar* AsS, *orpiment* As_2S_3, and *stibnite* Sb_2S_3 are insulators, while *bismuthinite* Bi_2S_3 shows a negative thermoelectric power with high resistivity.

GROUP VI B (Cr, Mo, W). *Molybdenite* MoS_2 samples show large positive or negative thermoelectric power values and occasionally spots of opposite sign occur on the same sample. The resistivity was of the order of 10 Ohm. cm. *Tungstenite* WS_2 is an insulator.

GROUP VII B (Mn, Ma, Re). Both *alabandite* MnS and *hauerite* MnS_2 are insulators.

GROUP VIII (Fe, Co, Ni, etc.), *Troilite* and *pyrrhotite* $Fe_{1-x}S$ show variable low thermoelectric power values and low resistivity. *Pyrite* FeS_2 can be positive or negative, with great variations in the magnitude of the thermoelectric power and the resistivity. *Marcasite* FeS_2 is always positive. *Linnaeite* Co_3S_4 in two samples showed variable thermoelectric power. *Millerite* NiS and *polydymite* Ni_3S_4 of rather low resistivity had a negative thermoelectric power of the same magnitude as that of pure Ni. *Pentlandite* $(Fe, Ni)_9S_8$ is of low thermoelectric power and low resistivity, while *violarite* Ni_2FeS_4 is negative and *bravoite* $(Fe, Ni)S_2$ is positive.

Bornite Cu_5FeS_4 of positive thermoelectric power and rather low resistivity is similar to Cu_2S, while *chalcopyrite* $CuFeS_2$ of variable resistivity is always highly negative. *Cubanite* $CuFe_2S_3$ is less negative and of rather low resistivity, while *stannite* Cu_2FeSnS_4 is positive and of high resistivity.

COMPLEX SULFIDES

The minerals of this group are mostly combinations of the sulfides of Cu, Ag, Fe, Pb and Sn, with those of As, Sb, Bi. It is possible to note certain regularities in these combinations.

Cu_2S, which has a high positive thermoelectric power and rather low resistivity, in combination with As-sulfides retains its high positive value, although with an increase in resistivity (*tennantite*, *enargite*). In combination with the sulfides of Sb or Bi the high positive thermoelectric power remains unchanged, but the resistivity increases considerably.

Ag_2S of high negative thermoelectric power and high resistivity shows increased resistivity and variable changes in the thermoelectric power.

Galena, PbS, generally shows increased resistivity with negative thermoelectric power predominating, when in combination with other sulfides.

ARSENIDES

The thermoelectric powers of the arsenides of Cu, Ag, Fe, Co, Ni are invariably negative. The resistivity could not be measured exactly, but the quantitative indications show a low resistivity. The sulfoarsenide *arsenopyrite* FeAsS has a considerably higher negative thermoelectric power than the comparable arsenide $FeAs_2$ (*löllingite*). Its resistivity is variable but not high. The other sulfoarsenides show intermediate thermoelectric power values between the corresponding arsenides and sulfides.

OTHER MINERALS

The relatively few tellurides show low negative thermoelectric power values and their resistivity is not high. The oxides of Ti, Mn and Fe are of high negative thermoelectric power and high resistivity.

CONCLUSIONS

The thermoelectric power and the resistivity of the observed minerals indicate that definite order of magnitude values can be established. Variations between different samples of the same mineral are probably due to impurities.

Correlation with the periodic system appears to indicate—in the sulfide group—that low resistivity occurs only in the first horizontal column of group I *B* (Cu) and group VIII (Fe, Co, Ni) and in the third horizontal column of group IV *A* (Pb) and V *A* (Bi). The second horizontal column of group VI *B* (Mo) and I *B* (Ag) show intermediate resistivity.

The thermoelectric power is correlated with the valence and the crystal forms in group I *B* (Cu) and VIII (Fe).

The data obtained should be helpful in the study of semiconductors and in the understanding of the electric properties of these materials.

REFERENCES

1. ABT, A., *Ann. d. Physik*, **2,** 266–279 (1900).
2. BACKSTROM, H., *Kgl., Svenska Akad. Stockholm*, **8,** 553 (1888).
3. BAEDECKER, K., *Ann. d. Physik*, **22,** 749–766 (1907).
   BAEDECKER, K., *Phys. Z.*, **11,** 809–811 (1910). Die elektrische Leitfähigkeit und die Thermoelektrische Kraft eininger Schwermetallverbindungen in *Graetz Handbuch d. Elektrizität*, I, 699–734 (1918).
4. BAUMBACH, v. H. H., AND WAGNER, C., *Z. phys. Chem.*, **22,** 199–211 (1933).
5. BECQUEREL, E., *Ann. d. Chim. et d. Phys.*, (2), **34,** 152– (1827).
6. BECQUEREL, E., *Ann. d. Chim. d. et Phys.*, **8,** 389–436 (1866).
7. BIDWELL, C. C., *Phys. Rev.*, **3,** 204–216 (1914); **8,** 12–19 (1916).
8. BROWN, S., *Phys. Rev.*, **5,** 385–389 (9115).
9. BUNSEN R., *Ann. d. Phys.*, **123,** 505–509 (1864).
10. CHAPERON, M. G., *Lumière electrique*, **20,** 169 (1888).
11. COBLENTZ, W. W., *Bur. Stand. Sci. Papers*, **15,** 121–162 (1919).
12. COBLENTZ, W. W., *Bur. Stand. Sci. Papers*, **19,** 375–418 (1924).
13. DEAN R. S., AND KOSTER, J., *Prog. Rep. Met. Div. Bur. Mines*, No. **3268,** 21–50 (1935).

14. Flight, W., *Phil. Mag.*, **30,** 339–342 (1865).
15. Fritsch, O., *Ann. d. Phys.*, **22,** 375–401 (1935).
16. Fujii, K., U. S. Patent 1,771,887 (1931).
17. Gottstein, G., *Ann. d. Physik,* **43,** 1079–1100 (1914).
18. Groth, P., *Ann. d. Phys.*, **152,** 249–255 (1874).
19. Hankel, W. G., *Ann. d. Physik,* **62,** 197–207 (1844).
20. Hankel, W. G., *Ann. d. Physik,* **6,** 51–58 (1879).
21. Harvey, R. G., *Econ. Geol.*, **23,** 778–803 (1928).
22. Hochberg, B. M., *Physik. Z. Sowjet,* **13,** 198–223 (1938).
23. Iljew, A. M., *J. Russ. Phys. Chem. Soc.*, **40,** 220 (1908).
24. Koenigsberger, J., and Weiss, J., *Physik. Z.*, **10,** 956 (1909).
25. Koenigsberger, J., and Weiss, J., *Ann. d. Physik,* **35,** 1–46 (1911). *Jahrb. d. Radiol. u. Elektronik,* **11,** 84–142 (1914).
26. Kundt, A., *Sitzungsber.*, 421 **(1883).**
27. Laski, G., Thermoelektrizität in Geiger & Scheel's *Handbuch der Physik,* vol. XIII. 182–223 (1928).
28. Marbach, G., *Comp. Rend.*, **45,** 705 (1857).
29. Meissner, W., and Reddemann, H., Thermoelektrizität in W. Wien & F. Harms' *Handbuch der Experimentalphysik,* Vol. **11,** part 2, 395–490 (1935).
30. Miller von O. U., *Proc. Roy. Soc. N.S.W.*, **55,** 220 (1921).
31. Ogawa, W., *Proc. World Eng. Cong. Tokyo,* **31,** 291–304 (1929).
32. Pierce, G. W., *Phys. Rev.*, **28,** 153–187 (1909).
33. Plank, W., Diss. Göttingen **(1913).**
34. Reinhold, H., *Z. Phys. Chem.*, *B,* **11,** 321–341 (1930).
35. Rose, N., *Ann. d. Physik,* **142,** 1 (1871).
36. Rupp, E., *Z. Physik,* **80,** 483–494 (1933).
37. Seebeck, T. J., *Denkschrift d. Kgl. Akad.* **1822, 1823,**
38. Schauf, A., and Dana E., *Am. J. Sci.*, **8,** 255 (1875).
39. Smith, F. G., *Econ. Geol.*, **37,** 519–523 (1942).
    Smith, F. G., *Econ. Geol.*, **42,** 515–523 (1947).
    Smith, F. G., *Am. Mineral.*, **27,** 1–19 (1942).
40. Stefan, J., *Ann. d. Physik,* **124,** 632–635 (1865).
41. Streintz, F., *Jahrb. d. Radioakt. u. Elektr.*, **10,** 221 (1913).
42. Waibel, F. Z., *Z. Physik,* **78,** 423 (1932).

AN OCCURRENCE OF JAROSITE IN ALTERED VOLCANIC ROCKS OF STODDARD MOUNTAIN, SAN BERNARDINO COUNTY, CALIFORNIA

C. Osborne Hutton, *Stanford University, Stanford, California*, and
Oliver E. Bowen, *California State Division of Mines,*
San Francisco, California.

Abstract

The hydrated sulfate of potassium and ferric iron, jarosite, has been identified as a minor constituent of pneumatolytically altered quartz porphyry of Juratrias age that outcrops on the south slope of Stoddard Mountain in the Barstow-Victorville district, San Bernardino County, California. The mineral has been identified on the basis of optical and goniometric measurements, and this diagnosis has been verified by chemical tests.

Field Occurrence

Jarosite-bearing quartz-tourmaline rock outcrops in a lenticular, N–S trending body measuring approximately 100 by 400 feet. Most of this body consists of grayish-white quartzose rock abundantly spotted with radial groups of bluish black tourmaline averaging eight mm. in diameter. In some places tourmalinization has been more complete and discrete crystal groups tend to grade into a reticulated mass of coarsely acicular tourmaline. The tourmalinized zone grades gradually into sericitized quartz porphyry containing little or no tourmaline or jarosite, and finally into relatively unaltered quartz porphyry having a felsitic groundmass. Dikes of greenish gray, deuterically altered hornblende quartz monzonite, have penetrated both the volcanic rocks now tourmalinized and the adjacent relatively unaltered volcanic rocks. The granitic intrusives themselves are tourmalinized and sericitized in some places clearly indicating that these alterations followed the episode of granitic emplacement. Dikelets of granite pegmatite and aplite also occur in the vicinity although none outcrop close to the tourmaline-jarosite zone.

In many places irregular bands of tourmaline can be seen along large and small fractures showing that penetration of replacing vapors or solutions took place along fracture lines as well as by diffusion between the grains. Jarosite is seldom recognizable in hand specimen although the minor accessory rutile is sometimes conspicuous.

The field locality is close to the Keystone Mine on the south slope of Stoddard Mountain in the SE$\frac{1}{4}$ Sec. 18, T7N, R4W, S.B.B. and M. Stoddard Mountain is a 4800-foot landmark lying 14 miles NE of the town of Victorville, San Bernardino County, California. The terrain is typical of the southwestern Mojave Desert.

PETROGRAPHIC OCCURRENCE

For the most part, jarosite occurs as highly irregular, sometimes globular crystals, averaging 0.2 mm. in diameter, that are frequently grouped into clusters or aggregates in which there is no preferred orientation of the individuals (Fig. 1*B*). Here and there sharply euhedral crystals of rhombohedral aspect have formed (Fig. 1*A*) and very occasional narrow veinlets of the mineral were observed. Jarosite appears to be distributed haphazardly throughout the rock, although in some thin slices it is often intimately associated with radiate aggregates or prismatic crystals of tourmaline, and less often with clusters of stumpy prisms of pale yellow rutile.

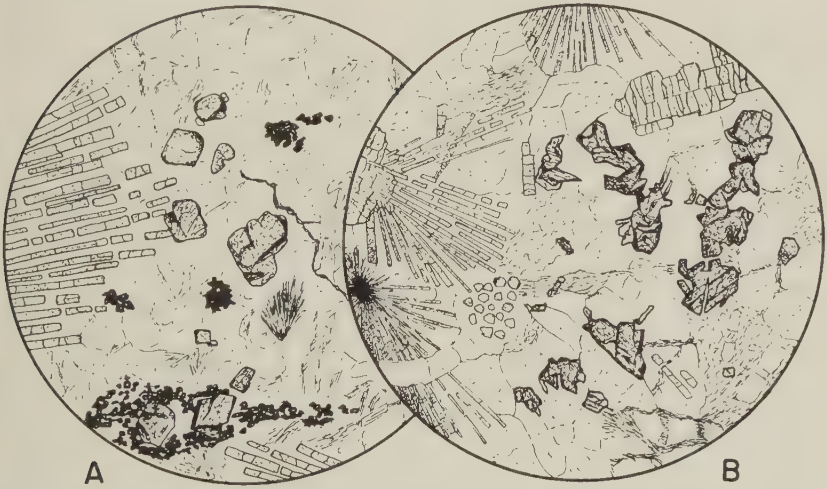

FIG. 1. The usual modes of occurrence of jarosite in tourmalinized quartz porphyry from Stoddard Mountain are illustrated in *A* and *B* above. Note the development of a high degree of idiomorphism in the jarosite in *A* and the absence of it in *B*; also observe the development of rutile in clusters in *A*.

MINERALOGY

The most abundant minerals associated with jarosite are quartz in allotriomorphic and interlocking grains, fine flaky sericite, tourmaline, and kaolinite. Tourmaline occurs in closely radiating aggregates—tourmaline suns—and also as isolated prismatic crystals with characteristic triangular cross-sections. The mineral exhibits a wide range of grain size and composition, and the latter is clearly shown in the variety of absorption tints for the vibration direction of the ordinary ray, *viz.* from deep blue, brownish blue, and greenish blue to palest blue to colorless. Symmetrical and unilateral zoning are both common and frequently peripheral zones of brown tourmaline enclose a blue variety; a reversal of this arrangement is also found.

The more deeply colored varieties were concentrated by a Frantz magnetic separator in a weak field, *viz.* 0.2 and 0.3 amperes, whereas faintly colored or imperceptibly colored crystals were found in those fractions concentrated at 1.2 amperes. For a crystal of intensely colored, and supposedly ferriferous, tourmaline, the following physical properties were determined:

N_o	1.658±0.002
N_e	1.633
N_o–N_e	0.025
$D_{25°}$	3.13±0.01
E	very pale blue to grayish blue
O	deep blue

For a faintly colored crystal concentrated in an intense magnetic field the following properties were found:

N_o	1.638±0.002
N_e	1.618
N_o-N_e	0.020
$D_{25°}$	3.06±0.01
E	colorless
O	very faint blue

The intense blue color of many of the tourmaline rosettes of the Stoddard Mountain locality is rare among tourmalines of the Barstow-Victorville area. Pegmatite and high temperature vein tourmalines are generally pleochroic in shades of brown. Blue or blue-gray shades have not been noted elsewhere in the area.

Among the accessory constituents the presence of the following minerals was verified:

Opaque iron ores, chiefly ilmenite, minute allotriomorphic crystals of barite, kyanite, globular or drop-like particles and stumpy crystals of rutile that are almost universally twinned, colorless zircon, very rare prisms of apatite, and ragged grains of pyrite. Barite is also conspicuously present as fracture filling.

SEPARATION AND PROPERTIES OF JAROSITE

Owing to the scarcity of jarosite, concentration was found to be necessary, and to accomplish this task approximately one pound of the rock containing the mineral was in turn run through a jaw-crusher, rollers, and a pulverizer, thus reducing the material to a grain-size less than 200-mesh (U.S.S. screens). After an appropriate degree of elutriation to get rid of dust, the powder was centrifuged in bromoform of density 2.88. Unfortunately concentration of jarosite was still too low to allow segregation of adequate material for study and, therefore, it was necessary to resort to electromagnetic fractionation. After removal of ferromagnetic material most of the jarosite was concentrated in the more magnetic portion segregated by the Frantz Separator set as follows: slope 10°, tilt 5°, current 0.1 ampere. From this fraction a nearly pure sample was readily prepared by hand-picking.

The following properties were determined for jarosite:

N_o	1.815 ± 0.001
N_ε	1.714 ± 0.003
$N_o - N_\varepsilon$	0.101
$2V$	0°, but angles between 5–10° were observed in individual crystals.
X	very pale yellow
Z	deep golden yellow
$Z\ >$	X

Extinction parallel to distinct basal cleavage.

$D_{24°}$ 3.18 ± 0.03. This figure was found for pure unaltered material but much of the jarosite was decidedly denser than this owing to superficial alteration to limonitic products.

In connection with the biaxial character occasionally found it should be noted that such crystals appeared to be single and homogeneous and there was no indication of twinning or segmentation in this instance, and thus the crystals did not resemble in any respect the features displayed in natrojarosite from Chuquicamata (Bandy, 1938, pp. 755–756), or jarosite from the Tintic District, Utah (Means, 1916, pp. 126–127).

Interfacial angles were measured for several crystals with the universal stage, and angles of approximately 54° and 91° were found; such angles are close to those recorded by Ford (1932, p. 769) for jarosite, *viz.* *cr* $0001 \wedge 10\bar{1}1$, 55° 16′, and *r r′* $10\bar{1}1 \wedge \bar{1}101$, 90° 45′. It should be noted, however, that Gordon (1925) found the interfacial angle *cr* to be 53° 12′.

On a qualitative basis (SO_4), H_2O, Fe''', potash, and a trace of soda were found to be present, but aluminum was absent. Spectrographically no more than a trace of lead was found.

Taken together these properties would seem to compare favorably with those previously recorded for pure jarosite (Winchell, 1933, p. 114; Tyler, 1936, p. 60), and in this instance veritable absence of aluminum, and traces only of sodium and lead exclude the possibility of the presence in solid solution of natrojarosite, alunite, or plumbojarosite.

ORIGIN

Jarosite has been reported to occur under a variety of circumstances, a few of which are as follows: Filling in cavities in Triassic arkoses at

Blanot (Lacroix, 1915, pp. 129–130); as an alteration of sulfides in the Tintic Area of Utah (Butler *et al.*, 1920, p. 116); as an efflorescence on recent lavas at Vesuvius (Zambonini, 1921); in the oxidation zone of lead ores at Leadville, Colorado (Emmons *et al.*, 1927, p. 155); as an oxidation product in altered quartz porphyry, Potosi, Bolivia (Lindgren and Creveling 1928, p. 253); associated with other sulfates in bedded cherts in the Calico Hills, San Bernardino County, California (Foshag, 1931, p. 353); in plant-bearing stratified tuffs, Potosi Mountain, Bolivia (Milton, 1935, pp. 176–178); as a member of the heavy mineral assemblages in the St. Peter Sandstone, Wisconsin (Tyler, 1936, p. 60); in oxidized zones at Chuquicamata and other mines in Northern Chile (Bandy, 1938, pp. 754–755); as a surface alteration to pyrite ornaments that had been buried for a considerable period (Pough, 1941, pp. 563–564); in Eocene clays at Refsnaes, Denmark (Bøgvad, 1942, pp. 108–114); and as an oxidation product of pyrite deposits in the Urals and other localities in Russia (Breshenkov, 1946, pp. 329–332).

In the occurrence described in this note jarosite is a constituent of a highly altered acid volcanic rock type and only the merest trace of sulfides in the form of pyrite has been found therein. It is believed that the association between tourmaline and jarosite is not coincidental but has genetic significance in spite of the occasional presence of jarosite in veinlets. However, it is thought that the time during which the jarosite crystallized probably post-dates the period of introduction of aqueous solutions containing boron that brought about subsequent crystallization of tourmaline, sericite, and possibly rutile and kyanite.[1] It is perfectly clear, however, that the pronounced development of zoning in the tourmaline indicates that the crystallization history in this instance has been a complex one. All occurrences of jarosite familiar to the writers appear to indicate that the mineral has formed from solutions at low temperatures; in fact, it is pertinent to point out that Fairchild (1933, pp. 543–544) was able to prepare pure jarosite in the laboratory at temperatures as low as 110° C. The association of barite and jarosite in this rock is also of interest since a somewhat similar association has been found in Jurassic arkoses by Lacroix (1915), although the genesis of the sulfates in this particular instance is quite distinct. Barite in these Southern Californian rocks possibly owes its origin to the same sulfate-bearing solutions that resulted in crystallization of jarosite, and it is believed that these solutions may represent the very latest or hydrothermal phase of the long and varied sequence of crystallization and metasomatism, the early stages of which, however, did not continue for a sufficient period to allow development of pegmatites comparable to those recognized by Varlamoff (1946, p. B. 122) as Type 9.

---

[1] Grosemans (1948) has shown that kyanite, usually considered to owe its origin to the conditions of dynamothermal metamorphism, may be of hydrothermal or pegmatitic origin.

REFERENCES

BANDY, M. C., (1938), Mineralogy of three sulphate deposits of Northern Chile: *Am. Mineral.*, **23**, no. 11, 669–760.

BØGVAD, R. (1942), Jarosit fra Danmark: *Medd. Dansk, Geol. For.*, **10**, 108–114.

BRESHENKOV, B. K. (1946), On the problem of the genesis of jarosites: *Compt. Rend (Doklady) de l'Acad. des Scieces de l'URSS.*, **52**, no. 4, 329–332.

BUTLER, B. S., LOUGHLIN, G. F., HEIKES, V. C., AND OTHERS (1920), The ore deposits of Utah: *U.S.G.S., Prof. Paper* 111.

EMMONS, S. F., IRVING, J. D., AND LOUGHLIN, G. F. (1927), Geology and ore deposits of the Leadville Mining District, Colorado: *U.S.G.S., Prof. Paper* **148**.

FOSHAG, W. F. (1931), Krausite, a new sulphate from California: *Am. Mineral.*, **16**, 352–360.

FORD, W. E. (1932), A Textbook of Mineralogy (Dana), 4th ed. John Wiley & Sons. Inc., New York.

GORDON, S. G. (1925), Mineralogical notes 1–10: *Proc. Acad. Nat. Sci. Philadelphia*, **77**, 1–13.

GROSEMANS, P. (1948), Le gisement de disthène de la Haute-Kabompo (borne 36/VIII, frontière Katanga-Rhodésie: *Bull. Soc. Belge Géol. Bruxelles*, **57**, 150–155.

LACROIX, A. (1915), Sur un nouveau gisement français de jarosite: *Bull. Soc. Franç. Min.*, **38**, 129–130.

LINDGREN, W., AND CREVELING, J. G. (1928), The ores of Potosi, Bolivia: *Econ. Geol.*, **23**, 233–262.

MEANS, A. H. (1916), Some new mineral occurrences from the Tintic District, Utah: *Am. Jour. Sci.*, ser. 4, **41**, 125–130.

MILTON, CHARLES (1935), Jarosite in tuff from Potosi, Bolivia: *Am. Mineral.*, **20**, no. 3, 176–178.

POUGH, F. H. (1941), The formation of jarosite on pyrite ornaments: *Am. Mineral.*, **26**, no. 9, 562–564.

TYLER, S. A. (1936), Heavy minerals of the St. Peter sandstone in Wisconsin: *Jour. Sed., Petr.*, **6**, no. 2, 55–84.

VARLAMOFF, N. (1946), La repartition de la mineralisation d'apres la clef geochemique de Fersman: *Soc. Geol. de Belgique*, **70**, nos. 1–3, B108–B138.

WINCHELL, A. N. (1933), Elements of Optical Mineralogy, Pt. 2. 3rd. ed., John Wiley & Sons, Inc., New York.

ZAMBONINI, F. (1921), Sur la Palmiérite du Vésuve et les minéraux qui l'accompagnent: *Compt. Rend. Acad. Sci., Paris*, **172**, 1419–1422.

THE CRYSTAL STRUCTURE OF FERROAN ZINCIAN RHODOCHROSITE

Ernesto E. Galloni, *Facultad de Ciencias Exactas Físicas y Naturales Universidad de Buenos Aires, Buenos Aires, Rep. Argentina.*

Abstract

Roentgenographic and thermal analysis of this new variety proved that it is a Mn-Fe and Zn carbonate isomorphous with $MnCO_3$.

Specific gravity and refractive indices have been determined.

We have studied samples of a new variety discovered by and obtained from Eng. Victorio Angelelli. This mineral has been found in Capillitas, Catamarca, Argentine Republic.

Its chemical analysis, checked against the chemical analysis of rhodochrosite found in the same place, is shown in Table 1. The results of

Table 1

	Ferroan zincian rhodochrosite	Rhodochrosite
MnO	29.80%	57.23%
FeO	13.93	trace
ZnO	14.88	—
CaO	3.13	2.41
CO_2	37.45	39.68
MgO	trace	1.23
H_2O	0.20	—
Insol. acid	trace	Insol. H_2SO_4 0.15
Total	99.39	100.70

Table 2. Chemical Analysis Interpreted as Carbonate Molecules

	Mol weight	Ferroan zincian rhodochrosite		Rhodochrosite %
		%	Mol. conc.	
$MnCO_3$	114.94	48.25	0.42	92.8
$FeCO_3$	115.86	22.45	0.194	trace
$ZnCO_3$	125.39	22.96	0.183	—
$CaCO_3$	100.09	5.59	0.056	4.3
$MgCO_3$	84.33	trace		2.6
Total		99.25		99.7

this analysis are significant if we consider the new mineral as being a mixture of carbonates. Table 2 shows that in this mineral two molecules of manganese carbonate appear to be associated with one molecule of zinc carbonate and one of iron carbonate. In other words, in a better accordance with the concept of crystalline molecules, four carbonate groups appear to be associated with two manganese atoms, one zinc atom, and one iron atom.

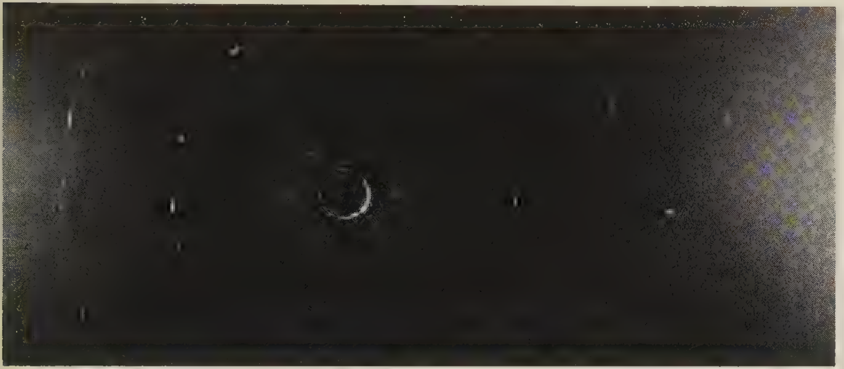

(a) Rhodochrosite

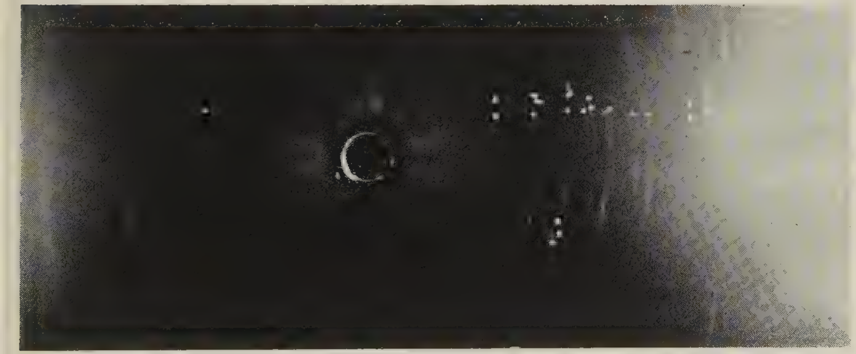

(b) Ferroan zincian rhodochrosite

FIG. 1. ROTATION PHOTOGRAPHS

This simple relation suggests an isomorphous compound of rhodochrosite in which a regular substitution of the metallic ions has taken place. In order to verify this assumption, we have determined its physical constants, x-ray crystalline structure, and differential thermal analysis, and compared the results so obtained with those obtained from the pure and mixed carbonates.

R. G. Wayland (1) has studied the composition, specific gravity, and refractive indices of different samples of rhodochrosite from Butte, Montana, giving variation diagrams of those properties in connection with their composition. But all of them have very small amounts of zinc carbonate. The consequence is that these results do not provide us with any significant information.

Nevertheless, we have tried the Wayland criteria in our study of this new mineral.

CRYSTAL STRUCTURE

Rotation patterns were obtained of rhodochrosite and the new mineral in order to obtain information relating to the manner of growth of the crystals. The results were as follows. Although the rhodochrosite pattern showed very sharp spots, which indicates that this mineral has a definite crystalline orientation (Fig. 1*a*) the new mineral showed discontinuous and almost complete rings which shows an irregular growth of crystals (Fig. 1*b*). We have also tried the Hull-Debye powder method, in order to find any possible difference between the two samples (Fig. 2). The results indicate a complete identity between the crystalline structures of the two minerals.

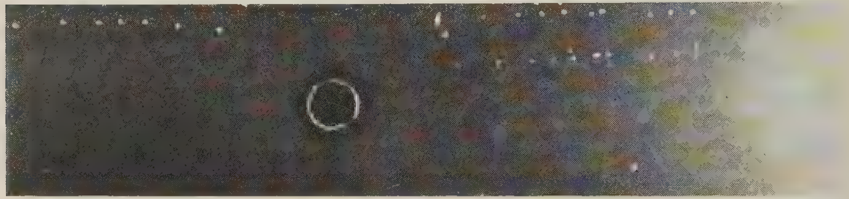

(a) Rhodochrosite

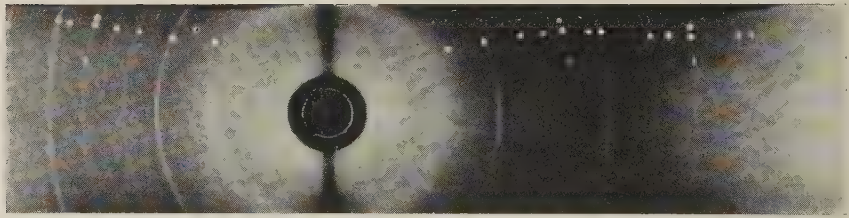

(b) Ferroan zincian rhodochrosite

FIG. 2. POWDER PHOTOGRAPHS

Table 3 shows the results obtained with three samples of ferroan zincian rhodochrosite and one of rhodochrosite, checked against the values calculated from Bragg's data (2) for a rhombohedral lattice with $a=5.84$ Å; $\alpha=47°\ 20'$, space group $D_{3d}^6=R\bar{3}c$.

Patterns were obtained with CoKα radiation in a 50 mm. radius camera. Table 3 shows a very good correspondence of the new mineral and rhodochrosite spacings.

This correspondence of the spacings and the sharpness of the lines in the powder pattern contribute strongly to the hypothesis that the mineral is isomorphous with rhodochrosite. If we take into account the (211) and (322) lines, which are the strongest in the carbonate's patterns, we see that the corresponding spacings for Mn, Fe and Zn carbonates are: 2.81, 2.81 and 2.71 for (211) and 1.75, 1.745 and 1.685 for (322), respectively.

TABLE 3

	d (obs.)					*d* (cal.)
hkl	Ferroan zincian rhodochrosite				Rhodochrosite	
	Sample 1	Sample 2	Sample 3	Average		
110	3.613	3.637	3.594	3.614	3.600	3.598
211	2.820	2.809	2.788	2.806	2.794	2.806
110	2.363	2.357	2.377	2.366	2.341	2.355
210	2.152	2.145	2.139	2.144	2.144	2.135
200	1.979	1.975	1.977	1.977	1.961	1.964
220	1.810	1.802	1.798	1.803	1.804	1.799
332	1.751	1.745	1.737	1.744	1.744	1.751
$\bar{2}10$	1.519	1.515	1.506	1.513	1.512	1.527
$2\bar{1}1$						1.506
310	1.439	1.434	1.430	1.434	1.435	1.450
433						1.427
320	1.366	1.362	1.357	1.365	1.366	1.376
$\bar{2}11$						1.353

So small a difference suggests the possibility of a wider reflection in the case of a mixture of those carbonates with no possible resolution, and, consequently, no possible evidence of the presence of the three carbonates.

Nevertheless, a pattern of a mixture of equal parts of rhodochrosite ($MnCO_3$) and siderite ($FeCO_3$) shows sharp pairs of reflections. Consequently, this new mineral which shows no resolution, appears to be not a mixture of carbonates, but an isomorphous form of rhodochrosite.

The case of dolomite, in which half of the Ca ions of calcium carbonate has been substituted for Mg ions, is well known. This substitution is accompanied by a lowering in the crystal symmetry. In our case, as the atomic numbers of Mn, Fe and Zn ions are not substantially different

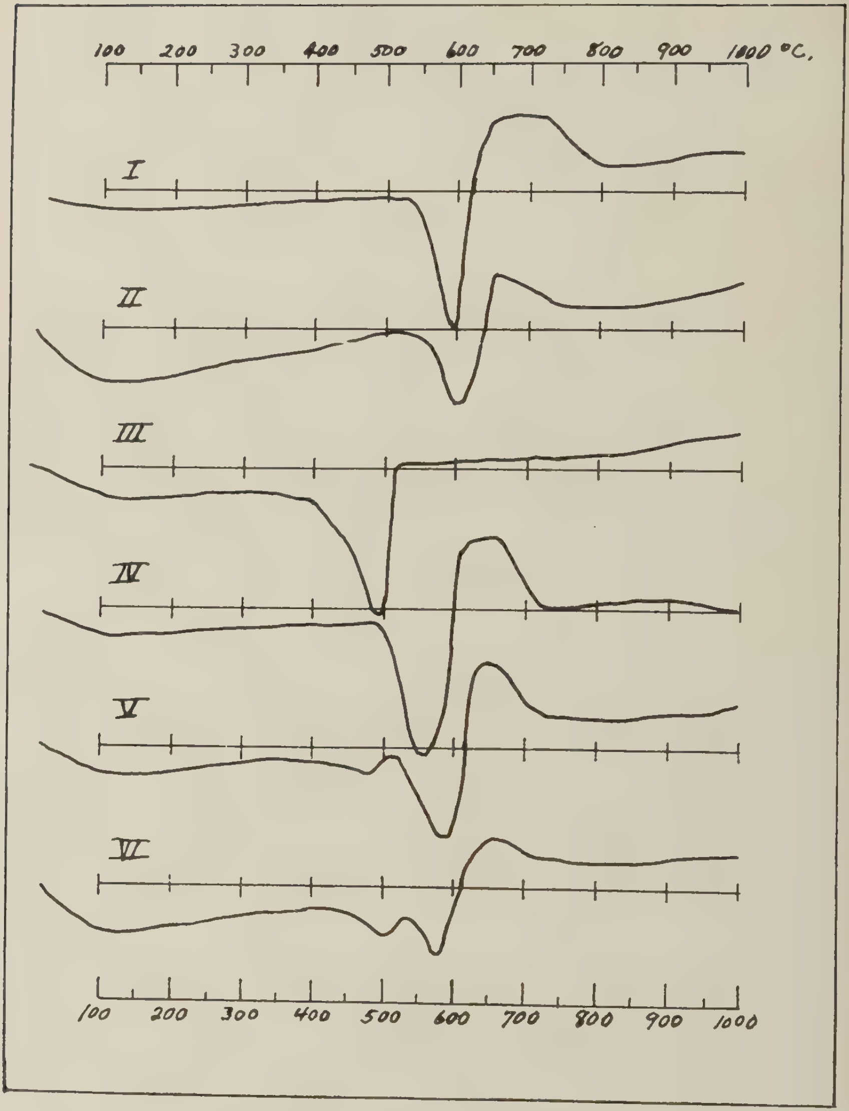

FIG. 3. Thermal differential analyses

Curve I—New Mineral.
Curve II—Rhodochrosite
Curve III—Smithsonite
Curve IV—Siderite
Curve V—50% $MnCO_3$+25%$ZnCO_3$+25%$FeCO_3$
Curve VI—50% curve II+25% curve III+25% curve IV.

(25, 26, and 30), such an effect would be so weak as not to be detectible in the intensity distribution in its pattern reflections.

Differential Thermal Analysis

We have carried out differential thermal analysis following the technique developed by different authors during recent years (3). We made use of an electric furnace with a quartz muffle in which we used, on a refractory support, a nickel disk (37 mm. diameter and 15 mm. height) as a sample holder, with three holes of 7 mm. diameter. The first of them keeps the hot terminal of a chromel-alumel couple in calcined alumina. Its e.m.f. is determined by means of a potentiometer circuit, in order to know the instantaneous temperature of the furnace. The second and third holes contain the terminals of a differential chromel-alumel thermocouple with calcined alumina and sample studied, respectively.

An identical nickel disc covers the first, with three holes through which the thermocouple terminals emerge, in order to avoid the effect of radiant heat on the samples. The e.m.f. on the differential thermocouple was recorded in a Brown Electronic Recorder with 0–10 mV scale which is connected in series with a constant e.m.f. of 4 mV in order to keep the needle in a central position on the scale, and so to record endothermic and exothermic peaks.

The heating rate was about 10° C. per minute. The temperature read on the potentiometer was noted in the record for each 50° approximately. Thermal curves are shown in Fig. 3. The new mineral (curve 1) is characterized by a large endothermic peak ranging from 530° to 620° with a maximum from 590 to 600°, characteristic of all the carbonates, and a large exothermic peak with a maximum ranging from 660 to 730° C.

The rhodochrosite (curve 2) is quite similar, with an endothermic peak with a maximum from 590 to 605 °C. and a sharp exothermic peak with a maximum at 650–660° C. Smithsonite (curve 3) shows the endothermic maximum peak at a lower temperature (490–500° C.) and no maximum in the exothermic one. Siderite (curve 4) shows the endothermic maximum at 560° C and an exothermic peak with a maximum ranging from 625° to 770° C.

These last three curves are in complete agreement with those mentioned in the bibliography (4). We have analyzed, for comparison, a mixture of $MnCO_3$ 50%, $FeCO_3$ 25% and $ZnCO_3$ 25%; which is the composition of the new material. The curve so obtained is shown as curve 5. It shows two endothermic maxima at 460° and 580°, respectively, and one exothermic maximum at 640° C.

It must be noted that the same result is obtained by adding half of the ordinates of curve 2 ($MnCO_3$), with the fourth part of the ordinates of curves 3 and 4 ($ZnCO_3$ and $FeCO_3$). We concluded that the observed reactions in the mixture correspond to the addition of the individual reaction of each component, without any secondary reactions between them.

We may also state that the new variety is a single substance, and not a mixture of carbonates. Half of the Mn ions of the rhodochrosite have been substituted by Fe and Zn ions in equal parts.

REFRACTIVE INDICES

We have determined the refractive index by means of the Pulfrich refractometer, obtaining a value: $n_0 = 1.836$. The computation, according to Wayland's criterion, by adding the products of concentrations and refractive indices of each carbonate, gives a value $n_0 = 1.807$ which differs by 0.029 from the observed value.

This computation has no justification; we have preferred to compute the molar refractions M.R. in accordance with the expression:

$$\text{M.R.} = \frac{(n^2-1)}{(n^2+2)}\ \frac{M}{d} \qquad \text{(Lorentz Lorenz).}$$

M being the molecular weight and *d* the density for each of the carbonates, and then adding the products of these M.R. by concentrations. The value so obtained for the refractive index is: $n_0 = 1.827$ which differs only by 0.009 (0.5%) from the observed value.

Better results are obtained by adding the ionic refractivities, following J. A. Wasastjerna. By means of numerical values tabulated by W. L. Bragg (2), the value $n_0 = 1.838$ has been obtained, which only differs by 0.1% from the observed one.

DENSITY

The theoretical value of rhodochrosite's density as calculated for a rhombohedral lattice of $a = 5.84$ Å, $\alpha = 47° 45'$ (Wyckoff's values (5)) with two molecules per unit cell is: $D_{calc} = 3.819$ g/cm³.

The computation from Bragg's results (2) provides us with a slightly higher value: $D'_{calc} = 3.874$ g/cm³.

These results are much higher than those observed by other authors. R. G. Wayland gives the following references: W. E. Ford: D = 3.70 (1917); Brentano and Adamson: D = 3.47 to 3.67 (1929); T. Anderson (6) in 1934 gives the observed value: D = 3.6333 g/cm³.

We have determined the density of Capillitas rhodochrosite and obtained the value: $D_{obs} = 3.665$ g/cm³.

By applying the values of Wayland and taking into consideration its composition, its density would be: $D_w = 3.627$ g/cm.^{3} the difference being 0.038, which is about 1%.

In the case of the new variety, we have determined the density and calculated its theoretical value, on the basis of the dimensions of the cell. We have also calculated the value corresponding to a mixture of carbonates, according to Wayland, and the value obtained by checking with the observed value for the rhodochrosite, taking into consideration the substitution of metallic ions, which raises the mean molecular weight from 114.94 to 117.78. The results are:

Mean density of new mineral	$D_{obs} = 3.762$ g./cm.^{3}
Unit cell calculated	$D_{theory} = 3.913$ g./cm.^{3}
Calculated according to Wayland	$D_w = 3.832$ g./cm.^{3}
Calculated by ion substitution	$D_{calc} = \frac{3.665 \times 117.78}{114.94} = 3.756$ g./cm.^{3}

It is evident that the last value is in better agreement with the observed one. Nevertheless, we believe that the density value is not especially significant, because we are dealing with minerals, and not with individual crystals.

SUMMARY

We have studied the mineral described by Angelelli as ferroan zincian rhodochrosite, from Capillitas, Catamarca, Argentine Republic.

From the interpretation of chemical analysis, *x*-ray diffraction, and thermal differential analysis, it is a triple Mn, Fe, Zn carbonate, isomorphous with $MnCO_3$ (rhodochrosite). Its formula is: $(Mn, Fe, Zn)CO_3$.

The dimensions of the unit cell differ slightly from those of rhodochrosite, and are: rhombohedral lattice, $a = 5.84$ Å, $\alpha = 47° 45'$.

Its refractive index is $n_0 = 1.836$ and its density $D = 3.762$ g/cm.^{3}

ACKNOWLEDGMENT

We are indebted to Eng. V. Angelelli for having given us the samples and the chemical analyses of the new material and rhodochrosite, as well as to Dr. E. Mórtola for having given us various samples of similar carbonates. We are also indebted to Dr. T. Isnardi, Director of the Institute of Physics, who arranged for the acquisition of necessary materials, to Dr. R. Busch for his helpful suggestions, and to Dr. J. A. McMillan for the translation of this paper into English.

REFERENCES

1. WAYLAND, R. G., *Am. Mineral.*, **27**, 614 (1942).
2. BRAGG, W. L., Atomic Structure of Minerals **(1937)**.
3. GRIM, R. E., AND ROWLAND, R. A., *Am. Mineral.*, **27**, 746 (1942); **27**, 801, (1942).

Cuthbert, F. L., and Rowland, R. A., *Am. Mineral.*, **32,** 11 (1947).
Grim, R. E., *Am. Mineral.*, **32,** 493 (1947).
Kerr, P. F., and Kulp, J. L., *Am. Mineral.*, **32,** 678 (1947).
Faust, G. T., *Am. Mineral.*, **33,** 337 (1948).
4. Kerr, P. F., and Kulp, J. L., *Am. Mineral.*, **33,** 387 (1948).
Kulp, J. L., and Wright, H. D., and Holmes, R. J., *Am. Mineral.*, **34,** 195 (1949).
5. Wyckoff, R. W. G., Crystal Structures **(1948).**
6. Anderson, T., *J. Am. Chem. Soc.*, **56,** 849 (1934).

TIN AND INDIUM IN MICA, AS DETERMINED SPECTROCHEMICALLY

L. H. AHRENS, *Dept. of Geology, M.I.T.* AND W. R. LIEBENBERG,
Government Metallurgical Laboratory, Johannesburg, S. Africa.

ABSTRACT

Spectrochemical analysis has shown that small quantities of tin are invariably detected in mica; the concentration of SnO_2 varies from $<0.0005\%$ to nearly 0.5%. Experimental evidence indicates that in specimens enriched in tin, some is present as included cassiterite and some is evidently located in the mineral structure, probably in octahedral co-ordination; in specimens which contain lower concentrations of tin, it is all held as a structure constituent.

Very small quantities of indium (maximum 0.0006% In_2O_3) could be detected in some mica specimens, in which it is probably present as a structure constituent in octahedral co-ordination. Specimens relatively rich in indium are also enriched in tin. The suggestion of a possible radiogenic origin of indium—by the electron capture decay, $Sn^{115} \rightarrow In^{115}$—is discounted.

A rapid survey of the tin content of pegmatitic micas is suggested as a possible aid for prospecting for tin.

An outline is given of spectrochemical procedure, but one item, namely, that of a correction for interference of Mn 3256.137 with In 3256.090 is covered in detail.

INTRODUCTION

In many specimens of mica which had been investigated spectrochemically, sensitive tin lines could be detected: in a few specimens, indium could also be detected. Because data on the abundance and distribution of these two elements in mica are lacking, an attempt was made to make quantitative determinations of tin and indium, using their emission spectra as a means of analysis.

It may be worth noting here that spectrochemical analysis has one advantage over all other methods of analysis, namely, that once the spectra of a given mineral have been recorded, the photographic plate provides not only a permanent record of the presence of the element(s) sought, but also of other elements. In this example, the quantitative analyses given in this paper are a direct consequence of an investigation of the geochemistry of rubidium, thallium, and lithium in micas. On the plates that had recorded the spectra of these three elements, tin and indium lines were also found, and with very little extra effort the same plates could be used for the analysis of these latter two elements. Had other methods of analysis been employed for rubidium, thallium, and lithium, the presence in mica of tin and indium would not have been observed. There are many examples of such observations.

ANALYTICAL PROCEDURE

(1) *General*

The operating technique is basically the same as has been described by one of us before (Ahrens, 1) for the spectrochemical determination of thallium, rubidium, lithium, and lead in minerals. The reader is referred to the above paper for operating details not given here.

Lines selected for the analysis of tin and indium were, Sn 3262.328 and In 3256.09. (Wavelengths used in this paper are from the M.I.T. Wavelength Tables of G. R. Harrison: published by John Wiley and Sons.)

Fortunately, some specimens of muscovite (Uranoop River area, Namaqualand, Union of South Africa) gave no spectroscopic evidence of the presence of tin and indium, and were consequently used as base material to which were added small quantities of SnO_2 (as cassiterite) and In_2O_3. This gave a series of standards covering the concentration range, 0.000032 to 1.0% SnO_2 and In_2O_3. The use of a base material, the composition of which is both chemically and physically identical with the material to be analyzed is advantageous in spectrochemical analysis.

The use of a relatively low amperage (3 amps) was found satisfactory: a very satisfactory sensitivity (limits of detection, 0.0005% for tin and ~0.00003% for indium) was obtainable. The reproducibility, expressed as standard deviation, was approximately ±12–15% for both elements, when analyses were made in duplicate, and sufficed for the investigation in hand.

(2) *Correction for interference of Mn 3256.14 with In 3256.09*

Two sensitive indium lines, In 3256 and In 3258, are located close to the tin line (Sn 3262) employed, and their use was attempted. In 3258 was found considerably less sensitive than In 3256, and could be detected very faintly in only a very few specimens; In 3256 was therefore used, but with caution, because interference from Mn 3256.14 was encountered in some specimens of lepidolite. Correction from such interference was made as follows.

It was assumed that if Mn 3256.14 were emitted, the measured intensity of In 3256.09 and Mn 3256.14 on the plate could be regarded as a simple summation of the relative intensities of these two lines. Ideally this would hold only if the wavelengths of the two lines are identical: whether one may use a summation will, therefore, depend on the wavelength difference of the two lines and the dispersion of the spectrograph. For the above two lines, the displacement on the plate is very nearly 0.01 mm. for the spectrograph used (large Hilger quartz) and this displacement was regarded as sufficiently small to permit a summation of intensities. If then, the intensity of Mn 3256 can be determined, a subtraction of its intensity from the total (In, Mn 3256) intensity would give the intensity of In 3256 alone.

The relative intensity of Mn 3256 in any specimen was determined as follows.

First, the intensity ratio of Mn 3256 to that of a slightly more intense manganese line in this general spectral region had to be determined in the absence of indium: for this purpose a synthetic standard can be used. Manganese emits several lines of similar wavelength to Mn 3256, one of which, Mn 3248.516, is slightly more intense than Mn 3256 and belongs to the same multiplet. Because Mn 3256 and Mn 3248 have the same multiplet assignment, their intensity ratio is constant and is independent of source fluctuations: once determined, therefore, the intensity ratio value can be safely used for all matrixes and conditions of arcing. Seward (2) has examined the line intensities of the spectrum of manganese, and from his relative intensity values, the ratio I 3248/I 3256 is calculated as 0.61. We also made intensity ratio measurements on this multiplet line pair and obtained a value of 0.57 which accords reasonably well with that calculated from Seward's measurements: for correction purposes the mean of 0.57 and 0.61 was used.

If Mn 3248 is absent in an analysis, no interference of Mn 3256 with In 3256 will occur; if Mn 3248 is present, correction is made by a subtraction of 0.59 of the intensity of Mn 3248 from Mn, In 3256. Before these corrections are made, background is corrected in the usual way. The amount of interference from Mn 3256 was found to vary considerably. No specimen of muscovite showed interference, whereas in some specimens of lepidolite, the line at λ 3256 was evidently due to manganese alone. In three specimens where correction could be applied, the amount of interference varied from 10–50%.

Fortunately for the purpose of correction for interference, manganese and indium volatilize into the arc column very differently. In mica indium is very volatile and its lines are emitted with peak intensity during the early period of arcing, during which period the spectra of the alkali metals are most intense, whereas the manganese lines only reach their peak intensities after a large proportion of the alkali metals have volatilized. Because the peak intensities of manganese and indium lines do not coincide with respect to time, correction is facilitated as interference can be minimized by recording only the relatively early period of each exposure. Further, a low amperage and no admixture of carbon powder help; selective volatilization is accentuated and thereby the intensity of the interfering line is further reduced in the early arcing period.

RESULTS

The results of the analyses of indium and tin in the mica specimens are given in Table 1. Most specimens are from pegmatites.

TABLE 1

Locality	% SnO_2	% In_2O_3
(A) MUSCOVITE		
(1) Mica Siding, N.E. Transvaal	0.007	<0.00003%
(2) S.A. Mica Mines, Selati Riv., N.E. Transvaal	0.0085	<0.00003
(3) near Mica Siding, N.E. Transvaal	0.014	<0.00003
(4) Godwa Mine, Leydsdorp, N.E. Transvaal	0.030	<0.00003
(5) Maori Mine, Olifants Riv., Transvaal	0.0019	<0.00003
(6) Maori Mine, Olifants Riv., Transvaal	0.0088	<0.00003
(7) Port Yelland, Zululand	0.0015	<0.00003
(8) Otjimboyo, South West Africa	0.073	0.00007
(9) near Usakos, South West Africa	0.16	0.00008
(10) Usakos, South West Africa	0.075	0.0002
(11) Erongo Tin Fields, S.W. Africa	0.40	0.0003
(12) Uranoop Riv. area, Namaqualand	0.001	<0.00003
(13) Uranoop Riv. area, Namaqualand	0.0005	<0.00003
(14) Uranoop Riv. area, Namaqualand	0.0005	<0.00003
(15) Uranoop Riv. area, Namaqualand	0.0005	<0.00003
(16) Uranoop Riv. area, Namaqualand	0.001	<0.00003
(17) Uranoop Riv. area, Namaqualand	0.0015	<0.00003
(18) Uranoop Riv. area, Namaqualand	0.009	<0.00003
(19) Uranoop Riv. area, Namaqualand	0.011	<0.00003
(20) Uranoop Riv. area, Namaqualand	0.010	<0.00003
(21) Uranoop Riv. area, Namaqualand	0.0005	<0.00003
(22) Uranoop Riv. area, Namaqualand	0.0017	<0.00003
(23) Uranoop Riv. area, Namaqualand	0.002	<0.00003
(24) Illovo Riv., Mid-Illovo, Natal	0.13	<0.00003
(25) near Johannesburg, Transvaal	0.026	<0.00003
(26) Steinkopf Reserve, Namaqualand	0.20	0.00034
(27) Noemaas, near Steinkopf, Namaqualand	0.0072	<0.00003
(28) Kenhardt, Namaqualand	0.070	<0.00003
(29) George, Cape Province	0.011	0.00003?
(30) Sea Point, Cape Province	0.09	<0.00003
(31) Salisbury, Southern Rhodesia	0.004	<0.00003
(32) Southern Rhodesia	0.013	<0.00003
(33) Bucko, Kenya	0.068	<0.00003
(34) Stoneham, Maine, U.S.A.	0.45	<0.00003
(35) North Carolina, U.S.A.	0.0048	<0.00003
(36) Gabel, Silesia	0.0035	<0.00003
(37) Skutterud, Norway	0.0032	<0.00003
(38) Zillerthaler Alps, Tyrol	0.02	<0.00003

TABLE 1—*Continued*

Locality	% SnO_2	% In_2O_3
(B) BIOTITE		
(39) St. Stephen, Cornwall	0.004	<0.00003
(40) Miask, Urals	0.0062	<0.00003
(41) Erzgebirge, Germany	0.0083	<0.00003
(42) Illovo Riv., Mid-Illovo, Natal	0.013	<0.00003
(C) LEPIDOLITE		
(43) Black Hills, South Dakota	0.08	0.0005
(44) Maine, U.S.A.	0.039	<0.00003
(45) San Diego County, California	0.0085	<0.00003
(46) Pala, California	0.011	<0.00003
(47) Portuguese East Africa	0.0027	<0.00003
(48) Warmbaths, South West Africa	0.0005	<0.00003
(49) Arandis, Omaruru, S. West Africa	0.018	<0.00003
(50) Okongava Ost 72, Karibib, S.W. Africa	0.002	0.00003?
(51) Okongava Ost 72, Karibib, S.W. Africa	0.0015	0.00003?
(52) Albrecht's Höhe, S.W. Africa	0.02	0.00004
(53) Omaruru, S.W. Africa	0.09	0.0006
(54) Jackalswater, Namaqualand	0.0005	<0.00003
(55) Jackalswater, Namaqualand	0.0005	<0.00003
(D) PHLOGOPITE		
(56) Antwerp, New York State	0.0005	<0.00003
(57) Burgess, Ontario, Canada	0.0005	<0.00003
(58) Loole Kop., E. Transvaal	0.002	<0.00003
(E) SUNDRY		
(59) Zinnwaldite: Zinnwald, Saxony, Germany	0.44	<0.00003
(60) Manganophyllite: Långban, Sweden	0.0023	<0.00003
(61) Margarite: Chester, Massachusetts	0.039	<0.00003

DISCUSSION

(a) Tin

The presence of tin in mica has been reported by Borovik (3): he gave no indication of the amount present.

From Table 1 it is readily seen that tin in a small amount is a ubiquitous constituent of mica. The quantities found vary considerably, namely, from less than 0.0005% to 0.4–0.5% SnO_2: the latter concentration appears to be a maximum likely to be present in mica. A large proportion of specimens contain a concentration of tin within the range 0.005–0.05% SnO_2.

The manner in which tin is located in the mica structure is somewhat problematical. Borovik (3) concluded that in a specimen of muscovite he examined, it was located as a structure constituent. He treated his specimen with HF, and after filtration analyzed the evaporated filtrate and also the residue. Most tin was found in the filtrate and on the assumption that cassiterite is resistant to attack by HF, he could conclude that tin was a constituent of the structure of the muscovite specimen he examined.

Some of the specimens richest in tin described in this paper were examined microscopically, and some included cassiterite could be observed. The quantity of included cassiterite appeared, however, to be quite insufficient to account for as high a tin content as about 0.4%. HF treatment, as described above, was made and spectrochemical analysis showed a considerable concentration of tin in both filtrate and residue. It seems, therefore, that in the specimens richest in tin, this element is present partly as included cassiterite and partly as a structure constituent. The specimens relatively poor in tin showed an absence of cassiterite under the microscope and in these tin is probably all present as a structure constituent.

The radius of Sn^{++++}, a relatively stable ion of tin, is 0.68 Å, and Sn^{++++} should be able to enter the mica structure octahedrally (6-fold co-ordination).

(*b*) *Indium*

The geochemistry of indium in Finnish minerals has been investigated by Erämetsä (4) and in one of seven specimens of muscovite he examined, indium could be detected and was determined as 0.0001% In. Of the mica specimens we examined, indium could definitely be detected in five of thirty-eight muscovite specimens and in three of thirteen lepidolite specimens. Doubtful traces (~0.00003% In_2O_3) were observed in a few mica specimens.

The radius of the stable indium ion, In^{+++} is 0.92 Å. Although a little large for large-scale substitution, an ion of this size should be capable of entering mica structures octahedrally and it seems that the traces of indium in mica are present as structure constituents. Erämetsä (4) has observed indium in silicates and has reported what appears to be almost a freak amphibole from Finland, in which as much as 0.1–1.0% indium was found.

The association of tin and indium in mica

Each of the seven specimens of mica which contain a relatively high concentration of indium, namely, >0.00005% In_2O_3, contain an unusually high amount of tin. Relevant data, taken from Table 1, are given in Table 2.

A paper by Eastman (5) has drawn attention to the general geochemical association of tin and indium in minerals, and in this paper

TABLE 2

Specimen No. in Table 1	% SnO_2	% In_2O_3
8	0.073	0.00007
9	0.16	0.00008
10	0.075	0.0002
11	0.40	0.0003
26	0.20	0.00034
43	0.08	0.0005
53	0.09	0.0006

Eastman utilizes the Sn-In association as evidence in support of a prediction he made earlier (Eastman, 6) that Sn^{115} probably decays to In^{115}. It will be recalled that Sn^{115} and In^{115} are neighboring isobars, and, the present existence of such an isobaric pair violates a rule of nuclear stability. Mattauch and Fluegge (7) and Kohman (8) have also indicated that in the pair $Sn^{115}-In^{115}$, the former should be unstable and should decay by orbital electron capture to In^{115}, which would of course be a reasonable explanation for In-Sn association in the micas, each of which is pre-Cambrian and is 750×10^6 years old or more. Direct evidence, however, does not support significant decay of Sn^{115}. Thus activity observations by Rusinov and Igelnitzky (9) have failed to reveal possible electron capture decay in tin specimens and Ahrens (10) has found pegmatitic cassiterite (S. E. Manitoba, Canada) of extreme age, namely, 2100×10^6 years, to contain only a doubtful trace of 0.0001% In or less: consequently the fairly common association of indium with tin can not be due to electron capture decay in Sn^{115}.

As is well known, tin concentrates in later pegmatitic emanations, and likewise it is feasible that indium could be enriched in residual liquors because of the relatively large size (for octahedral co-ordination) of In^{+++}, which would tend to be rejected in favor of the smaller-sized ions—for example, those of iron, magnesium and aluminum—in minerals of earlier crystallization.

The presence of tin in mica as a possible aid for tin prospecting

From two general areas, namely, the Usakos-Karibib-Omaruru area in South West Africa, and the Uranoop River area in Namaqualand, several specimens of mica have been analyzed from various pegmatites. In the former area, many of the muscovite specimens (Nos. 8, 9, 10 and 11 of Table 1) are unusually rich in tin, in particular the specimen from Erongo (No. 11) which contains about 0.4% SnO_2, and which is from a pegmatite near a tin mine. In general, the whole of the Usakos-Karibib-

Omaruru area contains cassiterite deposits associated with granite-pegmatites. The Uranoop River area, Namaqualand, however is barren of cassiterite deposits according to de Villiers (11) and each of the twelve muscovite specimens from this region (Nos. 12–25 in Table 1) carry unusually low concentrations of tin.

Although these data are scant, they indicate that if micas from a pegmatite area show a characteristic enrichment in tin, deposits of cassiterite are likely to have been formed, whereas if the muscovites are low in tin, the area is probably barren of such deposits. In a given pegmatite area, mica specimens can usually be quickly collected from suitably spaced pegmatites: spectrochemical analyses of the samples can be made very rapidly, and the results of the analyses may be a clue to whether the area should be closely prospected as a possible tin-rich area, or disregarded. It may be added that the other common pegmatite minerals, albite, microcline, and quartz, invariably do not contain detectable amounts of tin, and would therefore be useless as possible tin prospecting indicators.

ACKNOWLEDGMENTS

Most experimental work was done at the Government Metallurgical Laboratory, University of Witwatersrand, Johannesburg, and grateful acknowledgment is made to its Director, Prof. L. Taverver, for his permission to use the necessary instrumental facilities for spare time research.

REFERENCES

1. AHRENS, L. H., Geochemical studies on some of the rarer elements in South African minerals and rocks. No. 2. The geochemical relationship between thallium and rubidium in minerals of igneous origin: *Trans. Geol. Soc. S. Africa*, XLVII, 207–231 (1945).
2. SEWARD, R. S., Intensity measurements in the spectrum of manganese: *Phys. Rev.*, **37**, 344–361 (1931).
3. BOROVIK, S. A., On finds of tin in micas: *Compt. Rend. Acad. Sci., U.R.S.S.*, **14**, No. 6, 349 (1937).
4. ERÄMETSÄ, O., On the distribution of indium in Finnish minerals and its association with other metals: *Ann. Acad. Sci. Fennicae, Ser. A.* **51**, No. 1 (1938).
5. EASTMAN, E. D., Indication of a genetic relation between indium and tin: *Phys. Rev.*, **52**, 1226–1227 (1937).
6. EASTMAN, E. D., Energy and stability related to composition of atomic nuclei: *Phys. Rev.*, **46**, 1–16 (1934).
7. MATTAUCH, J., AND FLUEGGE, S., Nuclear physics tables and an introduction to nuclear physics, p. 104. Interscience Publishers, Inc., New York (**1946**).
8. KOHMAN, T. P., Limits of beta-stability: *Phys. Rev.*, **73**, 16–21 (1948).
9. RUSINOV, L. I., AND IGELNITZKY, J. M., Stability of neighbouring isobars: *Compt. Rend. Acad. Sci., U.R.S.S.* (Doklady) **49**, 343 (1945).
10. AHRENS, L. H., Evidence of geological age against decay of Sn^{115} to In^{115} by electron capture: *Nature*, **162**, 313 (1948).
11. DE VILLIERS, JOHN. Private communication (**1949**).

X-RAY DIFFRACTION PATTERNS OF ASBESTOS

SUZANNE VAN DIJKE BEATTY*

ABSTRACT

X-ray diffraction patterns are given for 8 samples of chrysotile, 1 crocidolite and 1 anthophyllite. Samples were studied in powder and fiber form and compared to patterns obtained by other investigators. The salient features of the typical asbestos pattern needed for identification purposes are obtained from both fiber and powder samples. Patterns obtained of the various chrysotiles indicate variations in the number, sharpness, *d* values and hence crystallinity of the samples.

INTRODUCTION

The detection and identification of asbestos in commercial materials are of considerable interest in analytical laboratories. The principal purpose of this paper is thus to provide data for the identification of these minerals by means of x-ray diffraction. However, several points of interest to the mineralogist are also discussed. Special emphasis has been placed on the patterns for chrysotile since this is the principal variety used commercially and 8 samples are included in the study. One sample of crocidolite from South Africa is included since this variety is also widely used and 1 sample of anthophyllite from Georgia.

TABLE 1. DESCRIPTION OF BULK ASBESTOS SAMPLES

			Feel	
	Color	Luster	Bulk	Fibre
Chrysotile				
Zermatt	light brown	dull, earthy	slightly waxy	matted, flexible
Thetford	green	high, pearly	very smooth, waxy	silky, very flexible
Richmond	green	high, pearly	very smooth	silky, very flexible
Nevada	green	slight	smooth	soft to threadlike
Corsica	white	high, silky	very soft	soft, very flexible
Easton	white	high, silky	slightly waxy	soft, threadlike
Labrador	white	high, pearly	granular	very brittle
Anthophyllite				
Georgia	brownish-white	dull to pearly	waxy	short fuzz
Crocidolite				
South Africa	blue-gray	dull	soft	soft, flexible

Diffraction patterns were obtained of both the powders and fibers.

---

* Westinghouse Research Laboratories, East Pittsburgh, Pennsylvania.

TABLE 2. DIFFRACTION PATTERN—CHRYSOTILE—ZERMATT, SWITZERLAND

Spectrometer		Film		Spectrometer		Film	
d	Meas. Int.	d	Est. Int.	d	Meas. Int.	d	Est. Int.
10.0	3			2.98	3		
7.2	41	7.3	st.	2.79	2		
5.0	2			2.53	7	2.55	wk.
4.77	4			2.43 w	2		
4.50	4	4.55	wk.	2.16 w	1.5		
4.31	3			2.10 w	1.5		
3.97 w	2			1.82 w	1.5	1.89	wk.
3.85	2			1.51 w	1.5		
3.62	38	3.65	st.	1.45 w	1.5		
3.35	4						

The powder patterns were obtained with the x-ray spectrometer using filtered Cu radiation. All these patterns were made under identical conditions so that the intensities of the lines can be directly compared from one sample to another. Patterns of the fibers were obtained with a standard diffraction unit using filtered Co radiation.

TABLE 3. DIFFRACTION PATTERN—CHRYSOTILE—THETFORD, CANADA

Spectrometer		Film		Spectrometer		Film	
d	Meas. Int.	d	Est. Int.	d	Meas. Int.	d	Est. Int.
7.8	4			2.45	12	2.45	wk.
7.2	19	7.3	st.	2.14 w	2		
5.7 w	2			2.10 w	3		
4.92 w	1.5			1.82 w	2		
4.45	9	4.52	wk.	1.74 w	3	1.74	wk.
4.31 w	2			1.59 w	2		
4.13	3			1.55 w	2		
3.82	2			1.53 w	8	1.54	wk.
3.63	15	3.66	st.	1.51 w	2		
3.34	2			1.50 w	2		
3.28	2			1.31 w	3		
2.79	2			cf. Index cards II 782			
2.58	6			II 140			
2.52	8						

TABLE 4. DIFFRACTION PATTERN—CHRYSOTILE—RICHMOND, CANADA

Spectrometer		Film		Spectrometer		Film	
d	Meas. Int.	d	Est. Int.	d	Meas. Int.	d	Est. Int.
7.8	3			2.40	3		
7.4	10	7.4	st.	2.08	5		
6.1 w	2					1.84	wk.
5.2 w	2			1.61	2	1.69	wk.
4.5	5	4.5	st.	1.56 w	4		
4.2	2	4.0	st.	1.54 w	3	1.54	st.
3.68	10	3.66	st.	1.48	3	1.45	wk.
3.40 w	2					1.21	wk.
2.98 w	2					1.04	wk.
2.60	6					.986	wk.
2.54	10					.947	wk.
2.47	5	2.43	wk.			.912	wk.

DESCRIPTION OF SAMPLES

The bulk samples of chrysotile and anthophyllite were obtained through the courtesy of Mr. David Seaman of Harvard University, then curator of the Mineralogy Department of the Carnegie Museum of Pittsburgh. These include chrysotile from Zermatt, Switzerland; Thetford, Canada; Richmond, Canada; Nevada, California; Corsica; Easton, Pennsylvania, and Labrador. The anthophyllite and crocidolite were

TABLE 5. DIFFRACTION PATTERN—CHRYSOTILE—NEVADA, CALIF.

Spectrometer		Film		Spectrometer		Film	
d	Meas. Int.	d	Est. Int.	d	Meas. Int.	d	Est. Int.
7.4	6	7.4	v. st.	2.70	2		
5.3	2			2.60	3		
4.6	4	4.5	st.	2.53	4	2.45	wk.
4.1	2			2.35	1		
4.0	2					1.84	v. wk.
3.95	3			1.91	1		
3.68	5	3.67	st.	1.54	3	1.54	st.
3.37	2					1.47	
3.06	3.5			1.31	2		
2.96	4					1.221	wk.
2.76	2					1.044	wk.
						.914	wk.

TABLE 6. DIFFRACTION PATTERN—CHRYSOTILE, CORSICA

Spectrometer		Film		Spectrometer		Film	
d	Meas. Int.	d	Est. Int.	d	Meas. Int.	d	Est. Int.
8.8	6	9.1	st.	1.750	2		
8.4	14	8.4	v. st.	1.714	2		
7.4	2			1.691	3	1.70	v. wk.
5.54	2			1.653	7	1.64	wk.
5.24	1.5			1.623	3	1.62	st.
5.09	2	5.10	wk.	1.583	3	1.59	wk.
4.92	7			1.558	1	1.56	v. wk.
4.77	5	4.75	wk.	1.537	2	1.530	v. wk.
4.55	7	4.55	v. st.	1.512	5	1.507	v. st.
4.21	3	4.23	wk.	1.473	1		
3.90	4					1.461	wk.
3.68	1.5			1.453	2		
3.39	11			1.442	8	1.434	wk.
3.28	7	3.30	v. st.	1.366	3	1.357	wk.
3.13	22	3.14	v. st.	1.339	3.5	1.328	v. wk.
2.94	7			1.310	4		
2.81	5	2.83	wk.	1.299	3	1.298	v. wk.
2.71	19			1.278	2		
2.69	1.5					1.261	v. wk.
2.60	7			1.201	1.5		
2.54	8					1.192	st.
2.41	3	2.40	wk.			1.133	wk.
2.34	9					1.047	v. st.
2.30	3					1.028	v. wk.
2.28	3					1.018	v. wk.
2.169	8					.993	v. wk.
2.047	3					.979	wk.
2.021	7	2.01	wk.			.972	v. wk.
1.970	1.5	1.97	wk.			.952	st.
1.897	2	1.90	wk.			.934	wk.
1.871	2					.903	v. wk.
1.842	1					.902	wk.
1.819	2	1.81	wk.			.900	v. wk.

obtained in loose fibers and the chrysotile from Chester, Pennsylvania, in powder form.

A general description of the samples is given in Table 1. The order of appearance of the chrysotiles was decided from a cursory visual inspection, the first sample appearing the least crystalline. All the chrysotile powders are white excepting that of Zermatt which remains brownish. The crocidolite and anthophyllite powders are the same color as the bulk.

TABLE 7. DIFFRACTION PATTERN—CHRYSOTILE—EASTON, PA.

Spectrometer		Film		Spectrometer		Film	
d	Meas. Int.	d	Est. Int.	d	Meas. Int.	d	Est. Int.
8.9	6	9.1	st.	1.747	2		
8.4	10	8.4	v. st.	1.685	3		
5.04	3	5.01	wk.	1.651	5		
4.84	5	4.77	wk.	1.631	2	1.631	st.
4.51	4	4.51	st.			1.613	st.
4.33	2			1.590	4	1.582	wk.
4.21	2	4.20	wk.	1.546	3	1.559	wk.
3.87	5			1.512	4	1.499	st.
3.69	4					1.451	wk.
3.37	11			1.439	5	1.432	wk.
3.26	8	3.28	v. st.	1.363	3	1.374	v. wk.
3.12	15	3.12	v. st.			1.353	wk.
3.02	7			1.336	2		
2.94	8					1.321	v. wk.
2.81	3	2.80	wk.	1.296	2.5	1.295	wk.
2.70	18	2.69	v. wk.			1.265	v. wk.
2.59	6	2.58	v. wk.			1.237	v. wk.
2.54	8			1.200	3		
2.40	2	2.38	wk.			1.188	wk.
2.34	6					1.122	st.
2.29	4					1.045	v. st.
2.28	4	2.22	v. wk.			1.028	v. wk.
2.169	5	2.14	v. wk.			1.017	wk.
2.043	2					.9776	st.
2.017	4	2.070	v. wk.			.9716	wk.
		1.998	wk.			.9512	wk.
		1.960	wk.			.9326	wk.
		1.889	wk.			.9095	wk.
1.864	3					.9022	wk.
1.812	6	1.807	wk.			.9005	wk.

SAMPLE PREPARATION AND PROCEDURE

Powder patterns were obtained for the front reflection region using the spectrometer with slit settings combining to give maximum resolution and intensity, i.e. 4 mm. high and .5 mm. wide. The samples were ground to pass 325 mesh and packed into a holder having a circular opening of 1.4 cm. in the manner described by the author in a previous paper.[1] Four or five runs were made for each sample and the mean values of the interplanar spacings, *d*, and the intensities tabulated. The intensity

---

[1] Beatty, S., Van Dijke, *Am. Mineral.*, **34,** 74–82 (1949).

Table 8. Diffraction Pattern—Chrysotile—Labrador

Spectrometer		Film		Spectrometer		Film	
d	Meas. Int.	d	Est. Int.	d	Meas. Int.	d	Est. Int.
9.0	6	9.1	st.	1.871	3		
8.4	19	8.3	v. st.	1.850	1.5		
7.2	2			1.815	3	1.80	wk.
6.50	2			1.779	1.5	1.78	v. wk.
5.98	2			1.747	2	1.75	v. wk.
5.60	2			1.715	2		
5.24	2			1.688	4		
5.06	3	5.03	wk.	1.653	8		
4.87	4			1.639	2	1.63	st.
4.77	4			1.618	4	1.62	st.
4.51	4	4.49	st.	1.600	1.5		
4.39	1.5			1.585	5.5	1.58	wk.
4.21	3	4.17	v. wk.	1.558	3		
4.00	2			1.535	3.5		
3.88	3			1.514	4		
3.63	2	3.60	v. wk.	1.505	4	1.50	st.
3.56	2			1.473	2		
3.44	2	3.42	wk.	1.440	10	1.434	v. wk.
3.37	8			1.402	1.5		
3.27	10	3.26	st.	1.366	3	1.352	v. wk.
3.12	32	3.10	v. st.	1.339	2		
3.04	2			1.324	1.5	1.321	v. wk.
2.94	9			1.313	3		
2.80	4	2.78	wk.	1.295	3	1.299	v. wk.
2.71	16			1.272	1.5	1.269	v. wk.
2.67	7					1.243	v. wk.
2.60	6			1.201	2		
2.54	8			1.192	3	1.187	wk.
2.453	2			1.162	1.5	1.155	v. wk.
2.389	3	2.37	wk.			1.124	v. wk.
2.336	10					1.079	v. wk.
2.301	3					1.046	st.
2.279	4					1.019	wk.
2.209	2					.978	v. wk.
2.169	9	2.16	v. wk.			.952	v. wk.
2.136	2					.934	v. wk.
2.043	5	2.08	v. wk.			.9107	wk.
2.017	8	1.99	v. wk.			.9030	wk.
1.966	3	1.96	v. wk.			.9014	wk.
1.943	1.5					.8991	v. wk.
1.897	5	1.89	wk.				

scale is comparable to that obtained in a study of mica powders.[2] In the present case, the quartz line at $d=4.25$ has an intensity of 59.

Fine pencils of fibers were then separated from the bulk samples and inserted into a 114.9 mm. camera; the fiber axis being perpendicular to the beam. The purpose in obtaining this type of diffraction pattern in addition to the spectrometer powder pattern is threefold. A long film exposure may bring out weak lines which disappear into the background noise of an instantaneous electronic recording. It is further interesting to see how similar the film and powder patterns will be for identification purposes since they represent extremes in sample preparation. Last of all, a comparison of these pairs of patterns should give some indication of the randomness in the structure at right angles to the fibers axis. If the orientation about the fiber axis were random, the two patterns would agree closely. Strictly speaking, of course, this is not the conventional "fiber pattern."

TABLE 9. DIFFRACTION PATTERN—CHRYSOTILE—CHESTER, PA.

Spectrometer		Spectrometer		Spectrometer		Spectrometer	
d	Meas. Int.	d	Meas. Int.	d	Meas. Int.	d	Meas. Int.
8.6	7	2.54	9	3.29	5	1.653	3
5.12	1.5	2.40	1.5	3.13	9	1.583	3
4.85	3	2.34	3	2.95	4	1.537	2
4.55	4	2.17	3.5	2.81	2	1.518	4
4.48	4	2.04	2	2.76	4	1.467	1
4.23	2	2.02	3	2.70	10	1.440	4
3.91	1.5	1.867	2	2.60	5	1.340	2
3.39	5	1.688	2			1.302	3

On the whole the patterns are quite diffuse and weak, and in most cases the measurements are accurate at best to 0.1° in 2θ. Lines marked "w" are particularly wide or diffuse and in some cases the assigned value of 2θ is merely the center of a band or hump. All intensities of the spectrometer patterns were measured above the local background. The visual intensity scale for the film patterns is very rough and serves merely for comparison with corresponding spectrometer patterns.

DISCUSSION OF RESULTS

The pattern for Zermatt chrysotile given in Table 2 is sparse and quite

[2] *Ibid.*

TABLE 10. DIFFRACTION PATTERN—CROCIDOLITE, SOUTH AFRICA

Spectrometer		Film		Spectrometer		Film	
d	Meas. Int.	d	Est. Int.	d	Meas. Int.	d	Est. Int.
		9.2	st.			1.613	st.
8.4	13	8.4	v. st.			1.572	wk.
7.19	2			1.52	2	1.533	wk.
4.92	3	4.93	v. wk.			1.499	st.
4.52	4.5	4.51	st.	1.44	3	1.449	wk.
		4.20	v. wk.			1.420	st.
		3.89	v. wk.			1.369	wk.
		3.61	v. wk.			1.345	st.
3.42	2	3.41	wk.			1.310	v. wk.
3.36	4					1.291	st.
3.29	2	3.26	wk.			1.265	st.
3.11	8	3.11	v. st.			1.249	v. wk.
2.98	1.5	2.98	v. wk.			1.186	wk.
2.79	3.5	2.79	wk.			1.119	wk.
2.71	12	2.71	st.			1.100	wk.
2.61	3	2.60	wk.			1.080	wk.
2.54	6	2.53	v. wk.			1.056	wk.
2.48	1.5	2.44	wk.			1.041	st.
2.34	2	2.31	st.			1.027	st.
2.27	2					1.014	st.
2.18	2	2.18	st.			1.000	wk.
2.03	3	2.02	wk.			.9881	wk.
		1.990	v. wk.			.9787	wk.
		1.860	st.			.9704	wk.
		1.799	st.			.9460	wk.
		1.714	v. wk.			.9247	wk.
		1.684	v. wk.			.9167	wk.
		1.649	st.			.9097	wk.

diffuse although the reflections at $d=7.2$, and 3.62 are quite well defined, the very weak spectrometer lines did not appear on the film, and this is undoubtedly due to their very low intensity and diffuseness.

The pattern for Thetford chrysotile given in Table 3 is quite similar to that obtained from the Zermatt sample. Additional reflections appear but the pattern as a whole is still very diffuse.

Tables 4 and 5 give the diffraction data for the chrysotiles from Richmond, Canada, and Nevada, California. These are both extremely diffuse, particularly the latter. It is noted that the values of the interplanar spacings have shifted to larger values compared to the two previous samples.

The diffraction patterns of the chrysotiles from Corsica; Easton,

TABLE 11. DIFFRACTION PATTERNS—ANTHOPHYLLITE, GEORGIA

Spectrometer		Film		Spectrometer		Film	
d	Meas. Int.	d	Est. Int.	d	Meas. Int.	d	Est. Int.
9.3	6	9.4	st.			2.026	v. wk.
8.9	8	9.1	st.	1.991	4	1.982	v. wk.
8.26	14	8.25	v. st.			1.951	v. kw.
7.48	1.5			1.875	2.5		
5.04	3	5.05	v. wk.	1.839	5	1.838	st.
4.90	2			1.734	7	1.768	wk.
4.62	3			1.693	3		
4.50	6	4.51	v. wk.	1.639	2		
4.13	5	4.13	st.	1.618	7	1.610	st.
3.90	3			1.583	5		
3.65	9			1.549	4	1.542	st.
3.36	7	3.36	st.	1.530	2		
3.24	15	3.23	v. st.	1.514	5		
		3.12	wk.	1.503	7	1.498	wk.
3.05	26	3.04	v. st.	1.451	2		
2.87	5					1.443	wk.
2.84	10			1.419	6		
2.74	5	2.75	st.	1.364	3		
2.688	8			1.332	5		
2.590	7					1.319	wk.
2.540	10	2.52	v. wk.	1.308	2		
2.434	3			1.294	2.5		
2.318	5	2.350	v. wk.	1.260	1.5		
2.290	5					1.221	wk.
2.252	3	2.252	v. wk.			1.156	wk.
2.174	2			cf. Index Card		1.107	wk.
2.142	7			II 1320		1.100	wk.
2.074	2					1.028	st.
2.060	2					.926	st.

Pennsylvania; and Labrador given in Tables 6, 7, and 8 are all rich with fairly sharp lines. The values of the interplanar spacings have again shifted to even larger values. Furthermore, several strong lines appear in the powder sample which are absent or very weak in the fiber type pattern e.g. $d=2.71$, 3.37, 2.34. This would seem to indicate that the structures here are not as simple as that of the Thetford chrysotile where the distribution about the c axis is random.

The pattern of the chrysotile sample from Chester, Pennsylvania, given in Table 9 seems to fit in this latter group since it has a rich, fairly sharp pattern and the d values correspond closely. The reflection at $d=8.6$ is probably unresolved since the pattern as a whole is somewhat more diffuse.

TABLE 12. DIFFRACTION PATTERN OF THETFORD CHRYSOTILE OBTAINED BY WARREN AND BRAGG

Sin θ	d	Obs. Int.	hk0	Sin θ	d	Obs. Int.	hk0
.0484	7.33	v.s.	200	.0310	12.0		110
.0968	3.67	v.s.	400	.0625	5.68		130
.1452	2.443	w.	600	.0990	3.58		150
.1936	1.832	w.	800	.0620	5.74	weak and	220
.2420	1.466	w.	1000	.0908	3.91	too diffuse	240
.2904	1.221	w.	1200	.1240	2.843	to be	260
.3388	1.047	w.	1400	.0752	4.75	identified	310
.3872	.916	w.	1600	.0925	3.84		330
.0772	4.60	w.	040	.1205	2.94		350
.2316	1.531	v.s.	0120	.1042	3.40		420
				.0386			020
				.1158	3.06		060
				.1544	2.29	not	080
				.1930	1.838	observed	0100
				.2702	1.313		0140

TABLE 13. DIFFRACTION PATTERN OF ANTHOPHYLLITE BY WARREN AND MODELL

Sin θ	d	Obs. Int.	hkl	Sin θ	d	Obs. Int.	hkl
.039	9.1	w.	200	.110	3.23	s.	440
.078	4.58	w.m.	400	.115	3.09	v.s.	610
.117	3.03	w.	600	.130	2.74	s.	630
.156	2.27	w.m.	800	.195	1.82	m.s.	1010
.234	1.51	s.	1200				
				.140	2.53	v.s.	202
.040	9.4	w.m.	020	.150	2.36	m.s.	302
.080	4.42	m.s.	040	.160	2.22	w.	402
.120	2.95	w.	060	.170	2.08	s.	502
.160	2.21	w.	080				
.201	1.76	w.	0100	.070	5.1	w.	011
.241	1.47	v.s.	0120	.091	3.91	w.	031
.281	1.26	w.	0140	.210	1.69	m.s.	033
				.225	1.58	s.	053
.045	7.9	m.s.	210	.245	1.45	m.s.	073
.070	5.1	w.	230	.270	1.32	w.	024
.090	3.95	w.	420	.280	1.27	w.	044

The very rich pattern of crocidolite from South Africa is given in Table 10. Powder patterns were obtained using Cu and Fe radiation and although the background was reduced using the latter radiation no additional reflections appeared. Here the film gave a far richer pattern which was undoubtedly due to a high degree to the greater efficiency of the Co radiation.

The pattern of Georgia anthophyllite given in Table 11 is comparable to the Chester chrysotile in sharpness. The pattern is rich and shows the lack of correspondence between the powder and film intensities expected.

The diffraction data for the Thetford chrysotile obtained by Warren and Bragg[3] is given in Table 12 for reference. The indices of the reflections, the observed intensities and sin θ are listed. The corresponding d values are here added. Values for the strongest lines for anthophyllite are given in Table 13 from the work of Warren and Modell[4]. It is evident from a comparison of Tables 3 and 12 for Thetford chrysotile that the agreement is close for the two sets of data. The absence of weak lines in the present film patterns can be readily attributed to the lower efficiency of the Co radiation compared to both Cu and Mo. It is obvious, however, that the effect of different radiations will be one of damping or enhancing for the pattern as a whole such that the relative intensities remain the same.

It is interesting to note that all powder patterns were also obtained using an alcohol smear of the powder on a glass plate. On the whole, the same relative intensities were maintained although the background increased. In the case of the very diffuse patterns of Zermatt and Nevada, the stronger lines were considerably enhanced. In the latter case particularly, the only self respecting powder pattern was obtained in this fashion; when the holder was employed and random orientation was nearly obtained, the lines were sufficiently weak to be lost in the background noise. Thus, in powdered mixtures, it may be necessary to prepare the specimen in this manner before any asbestos lines can be expected. In most cases, only the prominent lines will appear so that the data of the weaker lines become primarily of academic interest.

Conclusions

X-ray diffraction patterns are given for 10 different asbestos samples including chrysotile, crocidolite, and anthophyllite.

Patterns obtained for various chrysotile samples show considerable variation in the number, sharpness and d values of the reflections.

The salient features of the typical asbestos patterns for identification purposes are maintained whether the pattern is obtained from a powder or fiber sample. In some cases, it may be advisable to enhance the weak lines of a powdered sample by using an alcohol smear.

---

[3] *Zeit. Krist.*, **76,** 201–210 (1930).

[4] *Zeit. Krist.*, **75,** 161–178 (1930).

THE ALTERNATING LAYER SEQUENCE OF RECTORITE*

W. F. Bradley, *Illinois State Geological Survey, Urbana, Illinois.*

Abstract

Rectorite is a complex layer type hydrous alumino-silicate related to the better known mica-like minerals. The structural scheme of rectorite consists of contiguous pairs of pyrophyllite-like units separated by pairs of layers of water molecules. An equally apt description would be the alternation of one pyrophyllite unit with one vermiculite unit. The nature of the arrangement is confirmed by the preparation of the equivalent complex in which ethylene glycol proxies for water.

The recognition that random mixed layer growths occur in nature with considerable frequency among the clay and clay-like minerals (1, 2) has raised the question whether minerals might not exist which would be characterized by a specific regularly alternating epitactic intergrowth. In a sense this is precisely the case with well known minerals like the chlorites or the chrondrodite series. The present intention is to demonstrate that the principle extends to more complex instances.

Rectorite is included among the species of doubtful validity in *Dana's* Sixth Edition, and has since been omitted. A specimen of the original material (USNM #80607), obtained by R. E. Grim from W. F. Foshag of the United States National Museum, has been available for study. Analyses cited by Dana for material dried at 110° C. are:

	SiO_2	Al_2O_3	H_2O	Fe_2O_3	CaO	MgO	Na_2O	K_2O	H_2O (110° C.)
1.	52.72	36.60	7.76	0.25	0.45	0.51	2.83	0.26	8.78
2.	52.88	35.51	7.76						8.83

The specimen is preponderantly monomineral, having associated with it only a small proportion of a kaolinite group mineral. The weak kaolinite lines in the diagrams of Fig. 1 have simply been excluded from the analysis which follows. Excessive preferred orientation, occasioned by characteristic matted texture of the sub-parallel aggregates is also evident in the reproductions, and serves to emphasize the outstanding characteristic of the diagrams, which is the extended series of orders of diffraction from the basal periodicity.

The presence of a hexagonal array of prism diffraction lines reminiscent of those of clays immediately suggests that rectorite is some arrangement of the mica-type hydrous alumino-silicate layer, but the magnitude of the fundamental periodicity, about 25 Å, exceeds common values.

A valuable supplementary source of information in the study of layer silicates has been the observation that water layers (when present in such structures) may be displaced by other liquids, as ethylene glycol, with production of a new sequence of diffraction orders for an altered fundamental periodicity (1). The pair of sequences is then more amenable to interpretation than is a single sequence.

---

* Published with the permission of the Chief, Illinois State Geological Survey, Urbana, Illinois.

In Table 1 are summarized the data employed in interpretation of the diagrams of Fig. 1. From an earlier study of a number of layered associations of montmorillonite with organic liquids (3), arbitrarily reduced *F*-factor estimates and signs were available as comparison standards which could be assumed to apply in this present case if it were true that one mica, montmorillonite, or pyrophyllite layer were involved in the present structure. The numbers in the *F* columns of Table 1 were chosen by comparison of the intensities of the rectorite diagrams with those of reflections at comparable angles for various montmorillonite-liquid complexes.

TABLE 1. *X*-RAY DIFFRACTION DATA FOR RECTORITE IN 00*l* SERIES

Order	Relative Intensity natural configuration $d_{001}=25.0$Å	Estimated relative *F* importance	Sign for octahedral origin	Sign for interlayer origin	Relative intensity glycol complex $d_{001}=26.6$Å	Estimated relative *F* importance	Sign for octahedral origin	Sign for interlayer origin
1	SSS	10	+	+	SSS	10	+	+
2	SSS	6	+	−	SS	4	+	−
3	W	1	+	−	M	2	+	−
4	W	1	−	−	W	1	−	+
5	S	4	−	−	M	2	−	−
6		0			M	3	−	−
7	coincident with kaolinite	2	omitted		W	$1\frac{1}{2}$	+	+
8	SSS	15	+	−	SS	10	+	−
9		0			S	6	+	−
10		0			W	1	+	+
11	M	2	−	−		0		
12	M	2	−	+	W	1	−	−
13	S	4	−	+	M	2	−	+
14	M	2	−	−	S	4	−	+
15		0			W	1	−	−
16		0				0		
17	W	1	+	−		$\frac{1}{2}$	+	omitted
18						$\frac{1}{2}$	+	
19							+	
20						$\frac{1}{2}$	+	

Figure 2 represents the results of one-dimensional Fourier synthesis based on the *F*-values and signs so chosen. The traces from $z=0.0$ to 0.2 are typical for a three-component layer. The intervening space is occupied in both cases by five lesser maxima which lose definition in the glycol reaction. One suggestion is that this space includes a second three-component unit unsymmetrically displaced with respect to the conven-

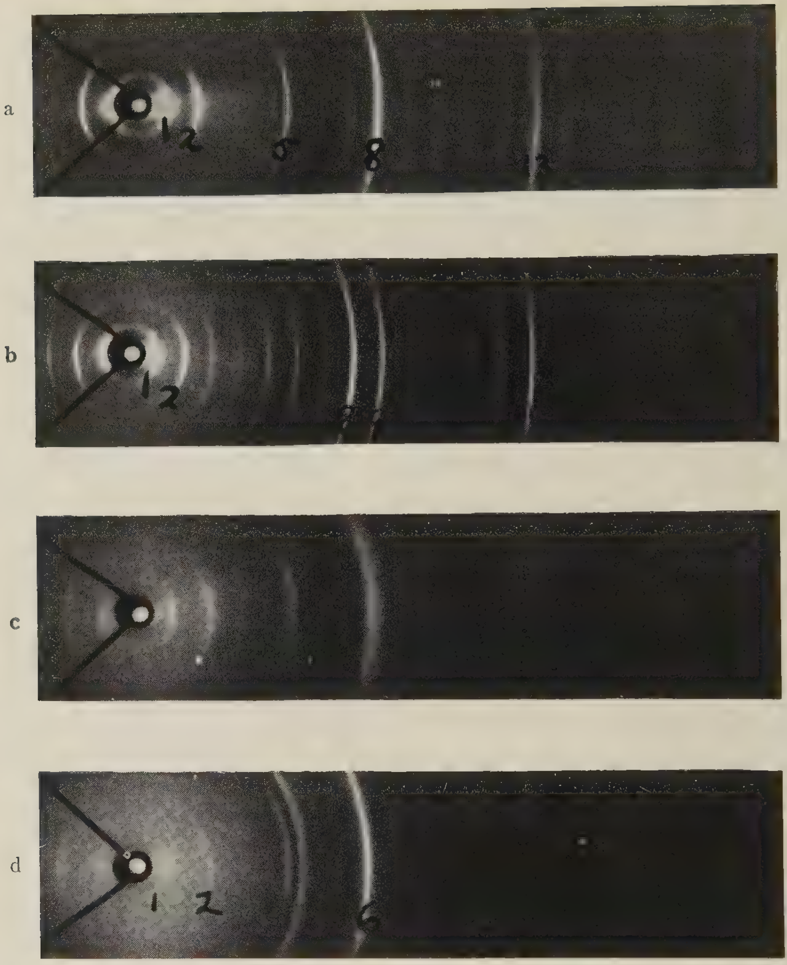

FIG. 1. *X*-ray powder diffraction diagrams of rectorite; (*a*) natural material, (*b*) complex with ethylene glycol, (*c*) natural material dried at 200° C, (*d*) natural material roasted at 600° C. Several important $00l$ orders are marked for reference.

tional origin. Rearrangement of signs to conform to an origin at the trough near $z=0.2$ affords the second pair of syntheses illustrated in Fig. 3. These traces are readily interpreted as contiguous pairs of three component, pyrophyllite-type layers, interleaved in the one case by double layers of water and in the other by double layers of ethylene glycol.

Rectorite does not swell or disperse in water. Specimens irradiated while bathed in water exhibit the same 25 Å periodicity as does the natural material. The molecular water layers are however removed by oven drying, after which a pyrophyllite-like dehydration product remains.

The condition of the dehydration product can be discussed in some detail. Thermal analysis (4) indicates that the molecular water is removed in three fractions. Two rather large unresolved endothermal effects center around 100° and 150° C., and a lesser ill defined trend extends to about 300° C. This character, together with the absence of

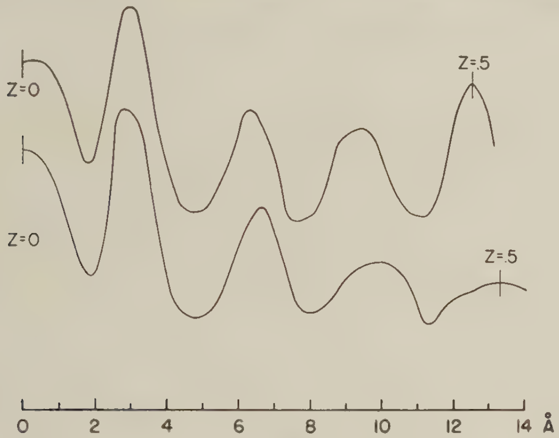

FIG. 2. Preliminary electron density projections from $z=0$ to $z=.5$ for rectorite (upper) and for the rectorite glycol complex (lower). The origin lies in an octahedral layer.

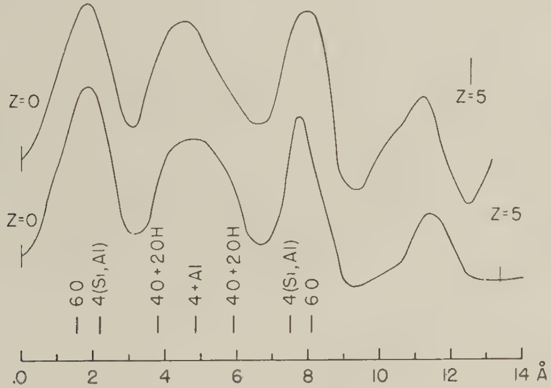

FIG. 3. Electron density projections from $z=0$ to $z=.5$ using interlayer origin for rectorite (upper) and for its glycol complex (lower). Levels of constituent atoms for the ideal structural model are marked.

swelling just noted, is suggestive of the vermiculite type of water layer rather than the montmorillonite type. Diffraction diagrams of partially dehydrated material, of which one is illustrated in Fig. 1, show distinct lack of homogeneity. Low orders are relatively sharp and at least approximately rational. Higher orders are complex and appear to consist of relatively sharp rational components with which there are associated more or less diffuse scattering maxima. For parallel to sub-parallel aggregates such as those with which we are here concerned, penetration of radiation into the aggregates is less for low angle diffraction than for the higher orders. The conclusion may therefore be made that for the par-

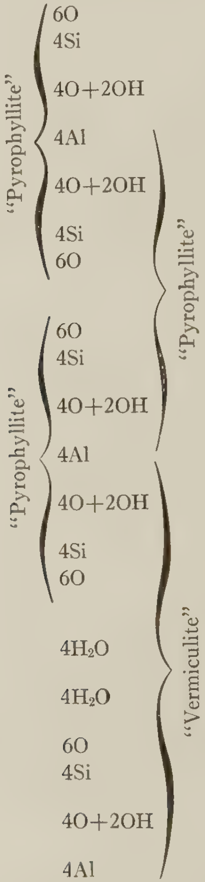

Fig. 4. Schematic representation of the sequence of atomic layers in rectorite.

tially dehydrated aggregates a surface skin of a certain number of dehydrated layers encloses interior layers with which water either may or may not still be associated, the interior sequence being a random array. The surface layer periodicity is about 19.5 Å and the interior average periodicity about 21 or 22 Å. Specimens heated to 600° C. have again become homogenous, and differ for the anhydrides prepared from montmorillonite or related minerals only in the persistence of a weak first order line for the doubled periodicity; that is about 19.5 Å. This order apparently signifies that the "pyrophyllite" neighbors which were originally together continue to stand closer to each other than to those neighbors which were previously separated by water, and are probably still separated by the not inconsiderable number of Na^+ ions of the cited analysis which were presumably associated with this water.

Chemically, this assemblage is in agreement with the analyses quoted by Dana if allowance be made for the 10 or 15 per cent of kaolinite which was probably present in the analyzed specimens. Optically, the refractivities are essentially the same as for Na-montmorillonite. The mean index would be about 1.50–1.52 with birefringence low. No observed index is cited by Dana.

In coordinating the *x*-ray diffraction information with the thermal character it can probably best be said that both alumino-silicate layers resemble pyrophyllite and that the water is in a condition comparable with that of the vermiculites. The structure then amounts to alternate piling of one pyrophyllite unit on one vermiculite unit. The schematic sequence is illustrated in Fig. 4. Alternative braces illustrate the ambiguity of origin which arises accordingly as one considers the layers to be geometrical or chemical entities.

The question of whether a study such as this can be said to validate the specific rank of rectorite as a mineral is probably one which should be deferred. The number of incompletely characterized doubtful species and variety names is too great to fairly estimate how many might be intergrowths of simpler systems.

REFERENCES

1. BRADLEY, W. F., Diagnostic criteria for clay minerals: *Am. Mineral.*, **30**, 704–713 (1945).
2. GRIM, R. E. & BRADLEY, W. F., The illite clays: *International Geological Congress*, vol. of titles and abstracts, London, pp. 127–128 (1948).
3. BRADLEY, W. F., Molecular associations between montmorillonite and some polyfunctional organic liquids: *J. Am. Chem. Soc.*, **67**, 975–981 (1945).
4. GRIM, R. E. & ROWLAND, R. A., Differential thermal analysis of clay minerals and other hydrous materials: *Am. Mineral.*, **27**, 811 (1942).

NOTES AND NEWS

NOTES ON ARCANITE, AMMONIAN APHTHITALITE AND OXAMMITE

Clifford Frondel, *Harvard University, Cambridge, Massachusetts.*

The name arcanite, originally proposed by Haidinger, has been held in a reserve status for natural K_2SO_4. This substance has not hitherto been identified with certainty in nature although it was at one time erroneously supposed to be represented by the aphthitalite, $(K,Na)_3Na(SO_4)_2$, of Racalmuto, Sicily. The only claimant to the name is the so-called arcanite of Eakle from the Santa Ana tin mine in Trabuco Cañon, Orange County, California. This substance occurred as thin, pseudohexagonal tablets which were interpreted as cyclic twins on (110) of orthorhombic individuals bounded by $\{001\}$, $\{101\}$ and $\{112\}$. The angles, for which only approximate measures were obtained, are close to those of both K_2SO_4 and aphthitalite. Chemical and physical data were not given for the mineral. The occurrence has not found general acceptance and the mineral was placed with aphthitalite by Hintze on geometrical grounds. Through the courtesy of Professor Adolf Pabst of the University of California the writer was enabled to examine the original specimen. The optical characters and the x-ray powder diffraction pattern proved to be identical with those of artificial K_2SO_4. Chemical tests indicated the presence of only K and (SO_4) as major constituents, and the mineral may hence be accepted as the first authentic natural example of arcanite.

The mineral taylorite was briefly described by Taylor in 1859 as a sulfate of potassium and ammonium from the guano deposits of the Chincha Islands off the coast of Peru. No further data have been published thereon. Chemical analysis indicated the formula to be $(K,NH_4)_2SO_4$ with $K:NH_4 \sim 5:1$. A small amount of Na_2O (1.68 per cent) also was reported. Crystallographic and optical data are lacking. The formula suggests that taylorite might be an ammonian variety of arcanite, especially since $(NH_4)_2SO_4$ and K_2SO_4 are isostructural and are known from studies of synthetic material to form a complete isomorphous series. Unfortunately, this question may never be settled since authentic specimens of taylorite from the Chincha Islands do not appear to be extant. The only specimen that could be located, in the collection of the U. S. National Museum (No. R5905), proved on examination to be a nodular mass of fibrous calcite. A number of reputed specimens of taylorite from a second, hitherto undescribed locality on the Guañape Islands—a group of guano islands off the coast of Peru about 400 miles northwest of the Chincha Islands—were found in the Harvard collection. This material comprised coarsely fibrous crusts and differs in this respect from the original taylorite which was said to occur as compact lumps or concretions with a crystalline structure. *X*-ray powder patterns of this material were virtually identical with that of aphthitalite (glaserite), $(K,Na)_3Na(SO_4)_2$. A chemical analysis of the mineral by F. A. Gonyer is cited below. The analysis yields

K_2O	$(NH_4)_2O$	Na_2O	SO_3	P_2O_5	H_2O at 95°	Organic	Total
33.87	5.68	9.65	48.62	0.70	0.21	present	98.73

the formula $(K,NH_4)_3Na(SO_4)_2$ with $(K,NH_4):Na=3.0:1$ and $K:NH_4=3.3:1$. The mineral thus is an ammonian variety of aphthitalite. The color is yellowish white and there is a distinct cleavage, presumably on $\{10\bar{1}0\}$. Fracture surfaces have a silky luster. Hardness $2\frac{1}{2}$. Specific gravity 2.51 (measured), 2.56 (calculated). Optically unaxial positive with $nO=1.498\pm0.002$ and $nE=1.503\pm0.002$. The powder pattern was indexed in terms of a hexagonal cell with $a_0=5.67$ *k*X and $c_0=7.34$ ($a_0:c_0=1:1.290$). These values are close to those of aphthitalite, which is hexagonal $-P$, scalenohedral ($\bar{3}\ 2/m$), with $a_0=5.65$ *k*X and $c_0=7.29$ ($a_0:c_0=1:1.294$) for material of unstated K:Na ratio, according to Gossner. Ammonian aphthitalite is soluble in water and has a saline and bitter taste. The material contains a small amount of organic matter and on heating turns brown or black and finally white. In these respects, and also in chemical composition, the present mineral resembles taylorite, and the two substances may perhaps be identical.

Another specimen of so-called taylorite from the Guañape Islands, contained in the collection of the American Museum of Natural History, has been described optically by Larsen. He found the mineral to be biaxial positive with 2V about 36°, $r>v$, and $nX=1.447$, $nY=1.448$, $nZ=1.459$. These values differ significantly from those for arcanite, ammonian arcanite or mascagnite, and doubtless refer to some other species, perhaps stercorite.

In the course of the above work specimens labeled guanapite, guanoxalate, and oxammite from the Guañape Islands were examined. One of the minerals present on the specimens was identified by optical and *x*-ray comparison with artificial material as ammonium oxalate monohydrate $(NH_4)_4C_2O_4\cdot H_2O$. This substance doubtless is oxammite, for which the formula $(NH_4)_4C_2O_4\cdot 2H_2O$ was originally given. The mineral formed opaque, yellowish, lamellar masses with a perfect cleavage on $\{001\}$. Optically biaxial negative with X perpendicular to the cleavage and $nX=1.440$, $nZ=1.593$, 2V medium large. The mineral was somewhat altered on the surface to a fibrous, unidentified substance.

REFERENCES

Haidinger, W., Handbuch der Mineralogie, Vienna, 492 (**1845**).
Eakle, A. S., *Bull. Dept. Geol. Univ. California*, **5**, 232 (1908).
Hintze, C., Handbuch der Mineralogie, **1**, Pt. 3B, 3695 (1929).
Gossner, B., *Jb. Min., Beil.-Bd.* **57**, 89 (1928).
Larsen, E. S., *U. S. Geol. Surv., Bull.* **679**, 142 (1921).
Taylor, W. J., *Proc. Acad. Nat. Sci. Philadelphia*, 309 (**1859**).

DEMONSTRATION OF THE DOUBLE REFRACTION OF ARAGONITE FOR RAYS TRAVELING IN THE NEIGHBORHOOD OF AN OPTIC AXIS

Reynolds M. Denning, *Michigan College of Mining and Technology, Houghton, Michigan.*

The purpose of this note is to call attention to the fact that the demonstration of "internal conical refraction" is facilitated by the use of the universal stage and that an unusually accurate axial angle determination can be made for both the primary and secondary optic axes.

The microscope has previously been used for demonstrating the behavior of rays of light passing through aragonite near an optic axis direction.[1]

With the aid of the universal stage, which today is available in most mineralogical laboratories, the demonstration of so-called internal conical refraction is greatly facilitated.

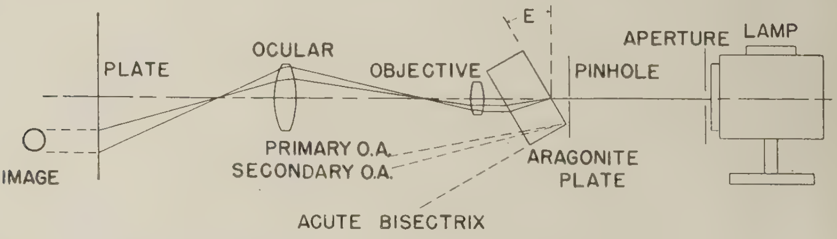

Fig. 1. Schematic diagram of the demonstration of "internal conical refraction".

Figure 1 shows schematically the essential features of the apparatus. The microscope, focused for projection of the pinhole image, is drawn as though made up of thin lenses. The plane of the drawing is taken as the axial plane of the crystal. To avoid confusion, only two rays, whose wave normals coincide with the primary optic axis, are shown. Rays traveling in such directions form a cone within the crystal and, because of their exact parallelism (in air), have zero intensity and contribute to the dark circles shown in Figs. 2 and 3. Each ray slightly inclined to those shown is doubly refracted and contributes light to point images. The points from the rays in a small cone which encloses the incident ray illustrated in Fig. 1 lie on the bright concentric circles, as can be demonstrated by Sylvester's construction.[2] Figure 2 shows the pinhole images for seven positions of the crystal. If the pinhole diameter is too large for the thickness of the crystal employed, the concentric rings are not resolved, and the pair is seen as a single ring. The light seen in either case has simply undergone double refraction. The rays which are truly conically refracted do not contribute to the image. The theory is correctly treated by Wooster[3].

---

[1] Clay, R. S., Treatise on Light, pp. 480–483, Macmillan & Co., Ltd. (**1911**).

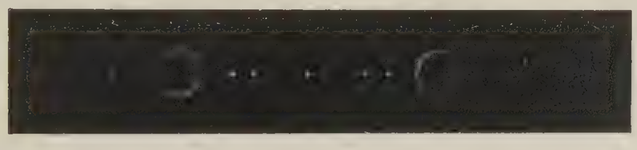

FIG. 2. Photograph of images of an illuminated pinhole as seen through an aragonite plate for seven selected positions of the crystal.

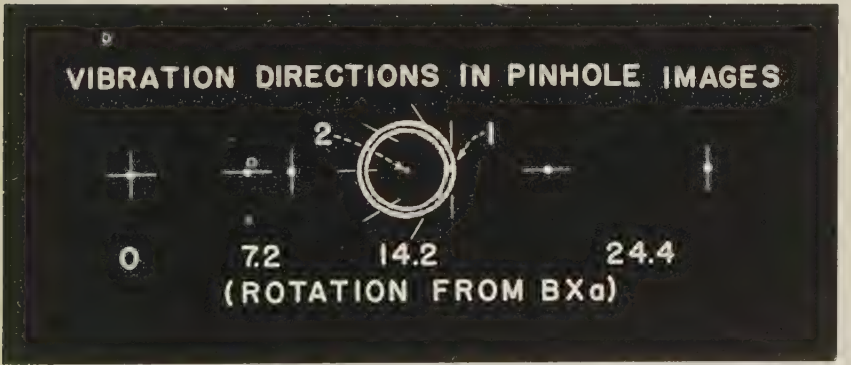

FIG. 3. Drawing of images of an illuminated pinhole as seen through an aragonite plate for four selected positions of the crystal. Straight lines indicate vibration directions. (1) Primary optic axis, (2) secondary optic axis.

To demonstrate the phenomenon, the polarizer and condenser were removed from the microscope, and a bushing was placed on the substage mount to permit a sheet of platinum foil, perforated by a small pinhole, to be located above the plane of the microscope stage. A thick plate of aragonite cut perpendicular to the acute bisectrix was mounted on a slide. The surfaces of the crystal plate were ground with 600 alundum, and a liquid film formed optical continuity between the usable central portion of the crystal and the slide. The edges of the crystal were cemented with Canada balsam. Also a thin cover plate was fastened to the upper surface of the crystal by means of a liquid of the same index as the β index of the crystal. The crystal assembly was mounted on the inner ring of the universal stage so that the east-west stage axis passed through the center of the crystal.

---

[2] Wooster, W. A., A Textbook on Crystal Physics, pp. 136–138, Cambridge University Press (**1938**).

[3] *Ibid.*, pp. 148–154.

The crystal is approximately oriented geometrically, the final adjustment being made by viewing the pinhole through the crystal. With the crystal in a general position two spots are seen. When the acute bisectrix coincides with the optical axis of the microscope, only one spot is seen. When the crystal is rotated from the acute bisectrix position about β through an angle approaching E, the two spots become crescents, and when the primary optic axis falls within the very small cone of wave normals within the crystal, the circles are seen.

The vibration directions of the light forming the images may be conveniently demonstrated by inserting a rotating analyzer or polarizer into the system. The results are shown in Fig. 3, which shows the images of the pinhole for four positions of the crystal, rotated about β from the acute bisectrix position by the angles indicated.

It should be noted that the appearance of the rings affords an extremely precise method for the determination of $2E$ for the primary optic axes. A series of ten measurements on one crystal yielded a value of $2E$ of $28.40 \pm 0.03°$ (probable error) at a temperature of 21° C. for D light.

With the aid of a calibrated filar micrometer, the cone angle (twice the angle between the primary and secondary optic axes) can be computed, the thickness of the crystal having been measured. On the crystal studied the cone angle was found to be 1.9°. Thus the angle $2E$ for the above stated conditions for the secondary optic axes is 26.5°.

The visual demonstration of the phenomenon is not particularly difficult. If aragonite is used, white light is satisfactory because of the relatively low axial dispersion. The photography of the phenomenon is, however, a patience-trying task. The following dimensions of apparatus may be of use as a guide to those who might care to set up the demonstration:

Lamp aperture 2 cm.
Lamp to pinhole distance 35 cm.
Pinhole diameter 24μ.
Pinhole to rotation axis of crystal 5 mm.
Thickness of crystal 9 mm. (A much thinner crystal may be used, especially with a smaller pinhole, but the effect is less striking.)

Diameter of unmasked usable portion of crystal 3 mm.
Objective, Leitz 35 mm. with iris stopped down to reduce scattered light.
Ocular, Leitz number 1.

The photograph was made by focusing the microscope for infinite image distance, using a camera having a 25 cm. lens focused for infinite object distance. Of course, the image could be projected to the plate by means of the ocular only. The exposure for each optic axis position with the sodium Lab-Arc was 20 minutes. The exposure for the acute bisectrix spot was 45 seconds. Fast panchromatic press film was used.

The writer wishes to thank Dr. C. B. Slawson, of the University of Michigan, for furnishing the excellent aragonite crystals used, and for making numerous pertinent suggestions.

MORDENITE FROM TINTIC, UTAH, AND THE DISCREDITED MINERAL ARDUINITE

Bronson Stringham, *University of Utah, Salt Lake City, Utah.*

Introduction

While mapping rock alteration in the Tintic Mining district, Utah, a small area was discovered in quartz latite which contained a zeolite originally thought to be arduinite (Stringham, 7). In order to make *x*-ray comparisons a sample of arduinite from the type locality in Italy was secured from the Harvard mineralogical collection, through Professor E. S. Larsen. The Tintic mineral proved to be identical to the type arduinite but it was finally found that the space group and unit cell of "arduinite" was identical with mordenite (Waymouth et al., 8); therefore, this study serves to discredit the species arduinite.

Arduinite was first found in the province of Val dei Zuccanti, Venecia, Italy, by E. Billows in 1912 who named and described it. His original paper could not be secured, but a review in the *Mineralogical Magazine* (5) states, "*Arduinite*, E. Billows, 1912. Two pamphlets both dated Padova 1912, entitled 'Analisi di alcuni minerali del veneto, Nota I, Arduinite, un nuovo Minerale,' one of 11 pages and the other of 14 pages. One of them is stated to be an extract from *Rev. Min. Crist. Ital.*, vol. **xli**; but the paper does not appear in that or in earlier volumes of that periodical." An analysis of arduinite was found in Appendix III to Dana's System of Mineralogy (2) together with a short description and it is here stated that Billows named the mineral after Giovani Arduino, a geologist of the 18th century. Doelter (3) gives the same analysis but states that it is an average of two analyses made by E. Billows. Later Barth and Berman (1) describe the mineral briefly and give optical data and provisional crystallographic data.

The early work was done with arduinite in mind and before *x*-ray equipment was available, hence the work done on mordenite, other than *x*-ray measurements, briefly presented here, is perhaps more extensive than necessary.

FIELD OCCURRENCE OF THE MORDENITE

At Tintic the mordenite occurs over an area about 150 by 50 feet in extent in quartz latite porphyry near the southeastern part of the district. The exact position is a considerable distance from any landmark. However, the road from the Tintic Standard mine to the Eureka Standard mine comes nearest the mordenite locality at a point about 1 mile south of the graveled "Valley" road junction. From here the area is about 300 yards north and 65 yards west and is situated near a low saddle on a very gently south sloping low hill.

The color of the unaltered mordenite is rusty red but microscopic work shows it to be truly colorless, and the red is apparently due to disseminated hematite dust. The individual crystals are long and slender, and packed in bundles which radiate from a central point giving a rosette appearance, the radii of which vary from around 2 mm. to 20 mm. Individual unit crystals are very small. One crystal fragment selected for *x*-ray work having dimensions of .5mm.×.2mm.×.05 mm. was apparently a single crystal when viewed under the microscope, but a rotation *x*-ray photograph showed it to be a bundle of 7 distinct units.

In thin section the rosettes are found to be entirely surrounded by quartz which replaces all constituents of the quartz latite. At the outer termination of the rosettes, mordenite needles replace and penetrate the quartz. Occasionally weathering has caused the hematite of some rosettes to alter to limonite and these appear rather brownish. The rosettes commonly are strung out along flow lines of the quartz latite, rarely forming a continuous chain, but usually disconnected with rock between. In several instances connected chains of rosettes were found to cross flow lines at approximately right angles. There seems little doubt that this mineral was formed during a post quartz latite hydrothermal stage.

OPTICAL DETERMINATION

Index of refraction of the arduinite and Tintic mordenite gave the following results: Mordenite, Tintic, $\alpha=1.474$, $\beta=1.475$, $\gamma=1.478$; "Arduinite," Italy, $\alpha=1.474$, $\beta=1.476$, $\gamma=1.478$*. The 2V, measured with the Universal stage was found to be near 76°. The optical orientation is, X parallel to *c* or long dimension of the crystal fragments, Y parallel to *a*, and Z parallel to *b*.

* Same values as Barth and Berman (1).

CHEMICAL ANALYSIS

The intimate association of quartz with mordenite necessitated the examination under a high power binocular microscope, of each fragment selected for analysis and apparently pure mordenite fragments were crushed and observed with the petrographic microscope. These precautions led to a final product which seemed to be essentially pure mordenite, except for the ever present hematite dust. A new mordenite analysis is here presented together with the original one by E. Billows for "arduinite."

TABLE 1

	Mordenite, Tintic Analyst; Lee C. Peck		"Arduinite," Italy Analyst; E. Billows (Doelter, 3)
SiO_2	64.95		49.40
Al_2O_3	11.71		14.57
Fe_2O_3	.62	(+MnO)	2.43
FeO	.41		
MgO	.11		
CaO	4.55		6.57
Na_2O	1.18		11.77
K_2O	1.71		1.54
H_2O+	6.25		13.85
H_2O-	6.20		
CO_2	1.04		
TiO_2	.03		
P_2O_5	.02		
MnO	.20		
	98.98		100.13

Billows' figures are considerably different and since both minerals are the same mineral structurally, their analysis should check more closely. If there had been enough of the type material available, a new analysis of it would have been made. The formula calculated from the Tintic analysis is $(Na_2,K_2,Ca)O \cdot Al_2O_3 \cdot 9SiO \cdot 6H_2O$, which is the same as that given for the type mordenite by How (4).

X-RAY DATA

Debye-Scherrer pictures were taken of Tintic and Italian material with identical patterns resulting. Weissenberg pictures of the Italian material were carried out to the 5th layer line giving information which could make the space group either $D^{17}{}_{2h}-Cmcm$ or $C^{12}{}_{2v}-Cmc$ and the orthorhombic unit cell dimensions $a_0=18.05$, $b_0=20.42$, $c_0=7.47$Å.

Subsequently these data were found to be identical to the space group for mordenite as measured by C. Waymouth et al. (8), and nearly the same orthorhombic cell dimensions given by them as $a_0 = 18.25$, $b_0 = 20.35$ $c_0 = 7.50$ Å. The fact that Pirsson (6) determined mordenite from Hoodoo Mountain, Wyoming, to be monoclinic encouraged the early belief that the Tintic material was truly arduinite. Some of the Hoodoo Mountain mineral was secured from Dr. Horace Winchell at Yale University and its *x*-ray powder pattern corresponded nicely to that of heulandite.

ACKNOWLEDGMENTS

Appreciation is offered to Dr. Dan McLachlan, Jr., of the University of Utah, Mineralogy Department for his assistance in the *x*-ray studies and to the Research Committee, University of Utah for the funds to defray expenses for the chemical analyses.

REFERENCES

1. BARTH, T. F. W., and BERMAN, H., *Chemie der Erde*, **5,** 22 (1930).
2. DANA'S *System of Mineralogy*, Third Appendix, p. 8, John Wiley.
3. DOELTER, C., *Handbuch der Mineral-Chemie*, Band II, Teil 2, p. 215, (**1921**).
4. HOW, H., *Jour. Chem. Soc.*, **17,** 100 (1864).
5. *Mineralogical Magazine*, "Review," **16,** p. 353 (1911–13).
6. PIRSSON, L., On mordenite: *Am. J. Sc.*, **40,** 232 (1890).
7. STRINGHAM, B., Arduinite from Tintic, Utah: (Abst.) *GSA Bull.*, **59,** 1383 (1948).
8. WAYMOUTH, C., THORNLEY, P. C., AND TAYLOR, W. H., An *x*-ray examination of mordenite (ptilolite): *Mineral. Mag.*, **25,** 212–216 (1938).

INDUSTRIAL DIAMOND DEVELOPMENT IN 1949

As in previous years the Industrial Diamond Information Bureau has compiled a report on the Industrial Diamond Development in 1949. The subject matter is sub-divided into: Scientific Aspects, Instruments Using Diamonds, Metallographic Polishing, Shaped Diamond Tools, Truing Tools, Diamond Dust, Diamond Grinding Wheels, Rock Drilling, Machining of Stone and Similar Materials, Grinding and Polishing of Diamond and Gemstones, Glass Machining, Art, Exhibitions. Copies of this report are available, free of charge, from the Industrial Diamond Information Bureau, 32–34 Holborn Viaduct, London, E.C.1. The mentioned literature can be obtained on loan, or in photostat copies, from the Bureau.

BOOK REVIEWS

PROBLEME DER NATURWISSENSCHAFTEN by Paul Niggli

Paul Niggli's Probleme der Naturwissenschaften erläutert am Begriff der Mineralart (Problems of the natural sciences illustrated by means of the conception of a mineral species) is published by Verlag Birkhäuser of Basel, Switzerland and sells for 18.50 Swiss francs. This beautifully printed, cloth-bound book of 240 pages may be regarded as an essay on the natural philosophy of crystallography. Part one, entitled Nature and Science, deals with the goals of natural science, the assumptions underlying the scientific conception of nature, and general methods of scientific research. Under the last heading Niggli defines two methods: the abstract-generalization, atectonic-imperative, factual-explanatory technique and the comparative-systematic, tectonic-normative, idealistic-illustrative technique. It is doubtful that more than a few American mineralogists and crystallographers will expend the time necessary to wade through this morass of abstruse "Germanology."

In part two the author discusses "Individuality, one of the foundations for the concept of species." Here is introduced, among other things, the notion of enteloprot—defined as the smallest unit of or for an individual which still contains the practical, entire individual character.

Parts three to ten are concerned with familiar crystallographic topics grouped under headings designed to emphasize the central theme—that of speciation in crystals. First are listed the fundamental factors in the definition of the crystalline form, such as vectors, symmetry, and zone laws. Thereupon follow descriptions of crystal structure, with NaCl used as an illustrative example, of the relations between structure and growth units, of the differences between ideal and real crystals, and of the notion of species in mineralogy.

Two sections contrast the variability of crystals—"inner" variability as related to the ideal crystallographic blueprint versus variability as a result of external conditions. Under the former belong such topics as isomorphous replacement, exsolution, defect structures, "vagabond" structural elements, adsorption, base exchange, and (growth) twinning. The second part deals, for example, with polymorphism, inversion, zonal structure, and plastic deformation. The book closes with a chapter on the principles governing mineral associations, including the phase rule, and a chapter entitled, "The subject of research determines the character of the science."

Niggli throughout emphasizes the analogy between mineralogy and biology, relating such units as individual, type, species, and assemblage across the two sciences. An interesting juxtaposition is his comparison of oriented mineral overgrowth with symbiosis. He might very well also have symbolized selective mineral alteration as an example of antipathetic symbiosis. By means of this fundamental analogy many "isolated" phenomena of crystal behavior and separately catalogued crystal characteristics may be interrelated in a natural crystallographic ontogeny. The book offers a refreshing approach to advanced mineralogical thought, which too often has been stagnated in the doldrums of indifferent systematology and haphazard presentation. The reviewer has for several years been using a similar analogy between mineralogy and biology, i.e. the separation of mineral characteristics into "environmental" and "hereditary" groups, as a basis for instruction in mineral paragenesis. There is no doubt that the advanced student receives this concept favorably. Niggli's book, which develops this theme in detail, is well worth the attention and appraisal of workers in our science.

E. Wm. Heinrich
University of Michigan

DIE JUNGEN ERUPTIVGESTEINE DES MEDITERRANEN OROGENS. (PART 2) DER CHEMISMUS DER POSTOPHIOLITISCHEN ERUPTIVGESTEINE BY CONRAD BURRI AND PAUL NIGGLI.

This paper-bound volume of 206 pages, which is published by Guggenbühl and Huber, Schweizer Spiegel Verlag of Zürich, Switzerland, stems from the Immanuel Friedlander Institute of Vulcanology of the Mineralogical-Petrographical Institute of the Eidgenossene Technische Hochschule of Zürich. It is a compilation of 2138 chemical analyses of Mediterranean-area igneous rocks, recalculated to the Niggli-Becke projection values—si, al, fm, c, alk, k, mg, ti, and p (see *Am. Mineral.*, **32,** 257–287, 1947). These values are listed, together with the rock name, locality, and magma-type according to Niggli's classification under three geographic sectors—the western, central and eastern Mediterranean. Three outline maps show the location of groups (called "tables") of analyses. A final section summarizes general statistical data derived from the compilation.

No doubt the volume represents an appallingly prodigious expenditure of time and effort in collecting and recalculating the analyses and grouping their projection values. American petrographers, in general, however, have made little use of the Niggli projections, and for them the work probably will be of ephemeral interest. It is unusually unfortunate that the original weight percentages of the rock analyses could not have been retained in the compilation, for such a collection would have served as a valuable source book in chemical petrography. According to the authors this was originally intended but was abandoned owing to increased size of the collection and increased printing costs.

E. WM. HEINRICH
University of Michigan

GEOLOGY AND ECONOMICS OF NEW MEXICO IRON-ORE DEPOSITS BY V. C. KELLEY.

The University of New Mexico recently has issued *Publication in Geology Number 2*—Geology and Economics of New Mexico Iron-Ore Deposits by V. C. Kelley, prepared in cooperation with the U. S. Geological Survey. This paper-bound, 246-page summary of existing knowledge of the economic and potentially economic iron resources of the state appears opportunely, just as western states are in the process of expanding an infant steel industry and as the United States mining industry as a whole is becoming concerned with the discovery and development of adequate iron ore to bolster dwindling reserves of the Lake Superior region. A handsome colored frontispiece showing magnetite and gangue minerals in the Fierro district graces the publication, which is profusely illustrated with 16 other plates and 46 figures, including 10 maps and sections in a rear pocket. The volume may be obtained from The University of New Mexico Press, Albuquerque, New Mexico for $3.00.

From 1906 to 1924 New Mexico ranked as the second largest producer of iron ore in the western states, and ore has been mined from 1889 to date, except for the period of 1932 to 1935. Nearly all production has gone to the Colorado Fuel and Iron Corporation at Pueblo, Colorado. The recorded output is 6,595,184 long tons of which about 18% was manganiferous iron ore. This is conservatively valued at $14,000,000 but represents less than 2% of the value of all other metals mined in the state.

Three main types of iron ore deposits occur: (1) pre-Cambrian iron-bearing quartzites and slates, (2) syngenetic deposits in sedimentary rocks, and (3) replacement deposits in sedimentary rocks. Type 1, or taconite, is of no present commercial interest. Type 2 is exemplified by beds of jaspery chert in the Magdalena group (Pennsylvanian) and oolitic hematite beds in the Bliss sandstone (Upper Cambrian), some of which are as much as 15 feet thick and contain 20–40% iron.

Nearly all production has been secured from pyrometasomatic ores (tactite-type) in sedimentary rocks (type 3), chiefly limestone or dolomite of Paleozoic age. The associated hypabyssal igneous rocks are intermediate in composition, commonly quartz-monzonitic to granodioritic and are of Tertiary age. Magnetite generally is the dominant ore mineral, occurring intergrown with ordinary hematite or less commonly specularite. Disseminated pyrite and chalcopyrite are common associates. Typical gangue minerals are carbonates, garnet, actinolite, serpentine, tremolite, epidote, wollastonite, phlogopite, and pyroxene. Tabular ore bodies with strongly banded structure parallel with replaced bedding are the rule. Structural features such as projections of sediments into the intrusive body, sharp bends in contacts, and crests and troughs of folds are in some districts responsible for localization of the ore masses.

Analyses of ores from 12 producing districts show an iron range of 48.1 to 58.2%, a phosphorus content of 0.030 to 0.115%, with sulfur varying from a trace to 0.91% and silica between 3.6 and 13.4%. Reserves for 8 southern counties are: (for 35–55% Fe) indicated ore, 24,573,000 long tons, inferred ore, 44,719,000 long tons. The principal reserves of 35–55% Fe ore are in the Fierro-Hanover district, which has produced over 5,000,000 tons of 50–55% ore. Large reserves of 25–35% Fe ore of the sedimentary type occur in the southern part of the Caballos Range in Sierra County.

The main part of the publication is concerned with detailed descriptions of some 30 main districts or groups of deposits. The work is unusually well organized and clearly and competently written. Illustrations are excellent throughout. In many ways the report sets standards of quality, both in the geologic work itself and in its presentation, for future compilations of this type.

E. Wm. Heinrich
University of Michigan

REPORT OF THE COMMITTEE ON THE MEASUREMENT OF GEOLOGIC TIME, 1948–1949.

The Report of the Committee on the Measurement of Geologic Time for 1948–1949 under the direction of John P. Marble, Chairman, has been published by Division of Geology and Geography, National Research Council. It may be obtained by sending a check, draft, or money order for $1.00 drawn in favor of the National Academy of Sciences to the above Division at 2101 Constitution Ave., N. W., Washington 25, D. C. The mimeographed, paper-bound volume of 139 pages presents the Summary Report of the Committee by its chairman and six summary reports (Exhibits A to F): (A) Japanese Analyses of Radioactive Minerals, 1936–1946 (Abstracted from "Chemical Analyses of Japanese Minerals II" by Zyunpei Harada, with comments by J. P. Marble. (B) Late Pleistocene Dates Derived from Radiocarbon Assay, by Richard F. Flint. (Reproduced from *Science*, **109**, 639, June 24, 1949). (C) Present Status of Absolute Age Measurements in Brazil, by John P. Marble. (D) Report to Committee on Measurement of Geologic Time, by L. H. Ahrens. (This deals with the strontium method, the decay constants of K^{40} and the possibility of a calcium age method, and the neighboring isobars, Sn^{115} and In^{115}.) (E) Some Problems of Age Measurements on Eastern North American Magnetites, by P. M. Hurley. (F) Annotated Bibliography of Articles Relating to the Measurement of Geologic Time, compiled by John P. Marble.

The Summary Report by John P. Marble brings together a great many miscellaneous pertinent details and comments, most of which would probably escape publication elsewhere. The annotated bibliography of 55 pages also is of considerable value, for it draws attention to many articles that have appeared in relatively obscure publications or in some not generally available.

E. Wm. Heinrich
University of Michigan

MINERALOGISCHE TABELLEN BY HUGO STRUNZ, second edition, Akademische Verlagsgesellschaft Geest & Portig KG. Leipzig C 1, 1949, pp. xiv+308. Price DM 21.

The first edition of this book (Leipzig 1941, Lithoprinted by Edwards Brothers, Ann Arbor, 1944) was reviewed and warmly praised by Professor Rogers in this journal in 1948. Though the contents as described by Professor Rogers remain much the same the new edition is about 25 pages longer and many improvements have been made.

Two subtitles, "Eine Klassifizierung der Mineralien auf kristallchemischer Grundlage" and "Mit einer Einführung in die Kristallchemie," clarify the aim and content of the book. Between the foreword (Vorwort) and the introduction (Einführung) a preface (Einleitung), ix–xiii, has been inserted. Here the author seeks to justify or explain his procedure in classifying minerals. He refers to his classification as crystallochemical and in summary says (p. xi–xii) that though it may at first glance seem to be purely chemical he has attempted to arrange and order (auszurichten) crystallochemically in every conceivable way.

The preface also contains a statement of the distribution of 1,124 "mineral species" whose symmetry is well established among the several crystal systems. The results, cubic 14.77%, hexagonal 7.83%, hexagonal-rhombohedral 8.99%, tetragonal 7.20%, orthorhombic 25.98%, monoclinic 29.72% and triclinic 5.51%, agree closely with the count made on 701 such "species" by Parker (*Fortschr. Min.*, **14,** 75, 1930). Finally there is in the preface a brief statement about the important matter of the relation of kX to Å units.

A great many changes have been made in the tables. For new data added since 1941 the author and year are mentioned though there are no direct references to original sources. For a few older data where a revised setting or interpretation is involved author and year are also given. All but two of the omissions noted by Rogers have been corrected.

For each mineral listed in the table formula, system, class, space group (both Schoenflies and Hermann-Mauguin symbols), cell dimensions and cell content are given where known. In the absence of cell dimensions morphological elements are given where available. Where needed the reconciliation of morphological and structural elements is indicated. A short statement on the structure or constitution is given for each major group.

Among the mineral groups whose treatment is revised in the new edition is tourmaline. Formerly placed among the nesosilicates (silicates with discrete SiO_4 tetrahedra) it is now found among the sorosilicates (silicates with limited groups of linked SiO_4 tetrahedra) and the formulas are written in conformity with the structure found by Hamburger and Buerger (*Am. Mineral.*, 1948) to whom reference is made.

Combined with the index is a list of the all too numerous obsolete and redundant mineral names. Each of these is elucidated very briefly.

The fragmentary and misleading list of mineralogical museums which appeared at the end of the previous edition has been eliminated. In its place appears a list entitled "Neuere Literatur zur Kristall- und Mineralkunde" in which are enumerated 44 books published since 1936. The selection is very uneven, omitting some important works and including others that are quite unworthy.

Lack of facility in reading German should be no bar to the use of this book. Its value lies in the comprehensive view it gives of the crystallochemical relations of minerals. It should be in the hands of every mineralogist who has any interest in these matters.

A. PABST
University of California

MINERALOGICAL SOCIETY (LONDON)

A meeting of the Society was held on Thursday, March 23, 1950, in the apartments of the Geological Society of London, Burlington House, Piccadilly, W. 1 (by kind permission). The following papers were read:

(1) The Clinopyroxenes of the Skaergaard Intrusion, E. Greenland.

By Mr. I. D. Muir.

A chemical and optical study has been made of the clinopyroxenes from the Layered Series of this intrusion. Fifteen new analyses of pyroxenes are presented. The augites form a long series ranging from normal diopsidic types in the lowest exposed rocks, to extremely iron-rich types, ferroaugites with practically no magnesia, in the extreme differentiates. Abrupt changes in the lime content of the clinopyroxenes are correlated with the absence of olivine in the Middle Gabbros and with its later reappearance in the Ferrogabbros. In the latest stages two distinct trends have been recognized, one being for the normal ferroaugites and the other for clinopyroxenes formed by inversion from iron-wollastonite. The replacements of the various ions in the pyroxene structure are discussed and an attempt has been made to correlate the optical properties of pyroxenes with their chemical composition.

(2) The Use of Diamond-Impregnated Tools for Rock-Slicing.

By Dr. K. C. Dunham.

A summary is given of the performance of diamond-impregnated cut-off discs and grinding laps during the past three years in the laboratories of the Petrographical Department of the Geological Survey and Museum. Details of a high-speed cutting machine incorporating a 12-inch 'Neven' copper-bonded diamond-impregnated saw, constructed by Government Training Centre, Letchworth, are included. A commercial machine based on this prototype will be exhibited.

(3) A Specific Gravity Balance.

By Sir James Walton.

The instrument described differs from an ordinary balance in that the arms instead of moving only a few degrees have to describe an arc of 90°, and the position of the centre of gravity has to be altered. The balance is suitable for specimens of 0.2 to 8.0 grams and enables a reading of specific gravity sufficiently accurate for most diagnostic purposes to be obtained in 1 to 2 minutes; it is particularly suitable for gemstones. Direct readings of weight are also obtainable.

(4) Collophane in Thames Gravel.

By Dr. G. F. Claringbull and Mr. S. E. Ellis.

A lenticle of fine sand in flood-plain gravel at the Concert Hall section, Waterloo (south bank of the Thames), yields a heavy residue containing collophane with a refractive index ranging from 1.53 to 1.62 and varying from isotropic to biaxial. Its origin (whether fossil or concretionary) is discussed.

The following papers were taken as read:—

(1) Some Unusual Alkali-Feldspars in the Central Australian Charnockitic Rocks.

By Mr. A. F. Wilson.

Two new analyses are discussed—one of a twinned microcline microperthite with misleading optical properties, and the other of a microcline microperthite with no cross-hatched twinning showing on (001). Attention is drawn to the abundance of triclinic untwinned alkali-feldspars in the charnockitic rocks.

Factors controlling inversion of orthoclase and development of twinning are discussed.

(2) FLUORESCENT FELDSPAR AND ZIRCON AS PETROLOGICAL AIDS.

By Mr. A. F. Wilson.

Stages in the feldspathization and magmatic injection of some Precambrian sediments may be demonstrated by a study of the fluorescence of potash feldspar and zircon. In certain crushed areas, mapping is facilitated by careful use of fluorescence.

A plea is made for widespread, but discriminating, use of the phenomenon, as an aid in correlation.

(*Titles and abstracts kindly submitted by G. F. Claringbull, General Secretary.*)

CONSTITUTION AND BY-LAWS OF THE MINERALOGICAL SOCIETY OF AMERICA*

CONSTITUTION

Article I. Name

This Society shall be known as the *Mineralogical Society of America.*

Article II. Object

The object of this Society shall be the advancement of mineralogy, crystallography, petrography, and allied sciences.

Article III. Officers

Section 1. The officers of the Society shall be a president, a vice-president, a treasurer, a secretary, and an editor, who shall be elected annually. There shall be an executive council consisting of the above officers, the retiring president, and four fellows at large, to be elected for terms of four years each.

Section 2. The Council shall be empowered to elect from time to time as honorary officers or fellows of the Society persons of eminence in the field of mineralogy, or some closely allied science, who shall serve for life.

Article IV. Membership

Section 1. The general membership of the Society shall be composed of fellows, members, and patrons. There may also be correspondents.

Section 2. (*a*) Fellows shall be persons who have published results of research in mineralogy, crystallography, or allied sciences, and who upon nomination by the Council shall have been duly elected to fellowship in the Society.

(*b*) Outstanding scientists of recognized scientific accomplishments in the field of mineralogy, crystallography, petrography and allied sciences, who are members of other scientific societies in the field of geology, such as the Geological Society of America, Society of Economic Geologists, American Institute of Mining and Metallurgical Engineers, American Association of Petroleum Geologists, and other similar scientific societies, may be nominated by the Council for fellowship in the Society.

Section 3. Members shall be persons not fellows who are engaged or interested in mineralogy, crystallography, petrography, or allied sciences.

Section 4. Patrons shall be persons who have bestowed important favors upon the Society. Election to patronship carries with it the rights and privileges of fellows.

Section 5. Fellows, members, and patrons shall be entitled to vote in the transaction of the regular business of the Society. Only fellows are eligible to office in the Society.

Section 6. Correspondents shall be persons who are distinguished for their attainments in mineralogy, crystallography, petrography, or allied sciences, and who are not resident in North America.

---

* The Constitution and By-Laws as here printed incorporate the amendments that have been voted by the Society from time to time as well as several new changes recommended by the Council. For the extent of these changes, reference should be made to *The American Mineralogist*, Vol. **25**, pp. 246–249 (1940). At the next election in October the general membership will be asked to vote on whether to accept or reject the Constitution and By-Laws as printed.

Article V. Amendments

Section 1. Amendments to the constitution may be proposed by ten (10) or more fellows who shall submit such amendments to the Council for presentation to the fellowship of the Society according to Article V, Section 2 of the Constitution.

Section 2. This Constitution shall be amended when the proposed amendment is favored by four-fifths of all the fellows voting upon it. A copy of the proposed amendment shall be published in the journal of the Society at least three months before the annual meeting. Voting shall be by mail ballot.

BY-LAWS

Article I. Membership

Section 1. Eligibility. Any person who has, in the opinion of the Council, contributed materially to the advancement of mineralogy, crystallography, petrography, or allied sciences, shall be eligible for fellowship in the Society. Any person interested in mineralogy, crystallography, petrography, or allied sciences, shall be eligible for membership.

Section 2. Election. (*a*) *Fellows.* Nominations for fellowship must be made by three fellows according to a form to be provided by the Council. Two of these fellows must be personally acquainted with the nominee and his qualifications. The Council will submit the nominations received by them, if approved, to a vote of the fellows in the manner provided in the By-Laws. The results will be announced at the next Council meeting, after which those elected will be notified by the Secretary. (*b*) *Members.* Any eligible individual may become a member by filling out an application blank obtainable from the Secretary or Treasurer, and paying one year's dues.

Section 3. Termination. A member's name will be dropped from the rolls if the annual dues are not paid by January 31.

Article II. Dues

Section 1. No person shall be accepted as a fellow of the Mineralogical Society of America unless he pays dues for the year within three months after notification of his election. The annual dues for fellows shall be five dollars ($5), payable in January.

Section 2. Fellows who have reached the age of seventy years, and who have paid dues for at least thirty (30) years, shall be exempt from further payment of dues.

Section 3. The annual dues for members shall be four dollars ($4), payable in January.

Section 4. An arrearage in payment of annual dues of four months shall deprive a fellow of the privilege of taking part in the management of the Society and of receiving the publications of the Society. An arrearage continuing over two (2) years shall be construed as notification of withdrawal.

Section 5. A single prepayment of an amount equaling twenty times the annual dues of a fellow of the Society shall be accepted as commutation for life for either fellows or members.

Section 6. Any person eligible under Article IV of the Constitution may be elected patron upon the payment of one thousand dollars ($1000) to the Society.

Article III. Duties of Officers

Section 1. Officers. The duties of the president, vice-president, treasurer, secretary, and editor of the Society shall be the usual ones performed by such officers. The treasurer, the secretary, and the editor shall make formal reports to the Society at least once a year. These reports shall be published in the journal of the Society.

Section 2. Executive Council. The Executive Council shall direct all affairs and activities of the Society not otherwise provided for by the Constitution, as well as perform those duties specifically assigned to it.

Section 3. Committees. The president shall appoint, with the approval of the Council, such committees as may further the objects of the Society, including a board of associate editors.

Article IV. Election of Officers and Fellows

Section 1. Nominations for office shall be made by the Council. The list shall be published in the journal of the Society at least three months before the annual meeting. Any ten (10) fellows or members may forward to the secretary other nominations for any or all offices. All such nominations reaching the secretary not later than three months prior to the annual meeting shall be printed, together with the names of the nominators, as special ballots. The regular and special ballots shall then be mailed to the general membership. The results shall be announced at the annual meeting, and the officers thus elected shall enter upon duty at the adjournment of the meeting.

Section 2. The list of nominations for fellowship in the Society shall be sent to the fellows at the same time as the nominations for officers. If ten per cent of the fellows voting on a given candidate cast opposing votes, the candidate shall be considered ineligible for fellowship.

Article V. Publications

Section 1. The Society shall publish a journal devoted to the advancement of mineralogy, crystallography, petrography, and allied sciences.

Section 2. The general membership of the Society shall be entitled to receive the journal.

Section 3. Corporations, libraries and institutions may subscribe to the journal at an annual rate equal to the dues of members.

Article VI. Affiliation with Other Scientific Organizations

The Council shall have the authority to arrange for affiliation with other scientific organizations, and, as the occasion may arise, to appoint fellows to represent the Society on the Councils of such organizations. In the case of the Geological Society of America, the representative so appointed shall also be a fellow of the Geological Society of America.

Article VII. Local Sections

Local sections of the Society may be formed in any locality, with the advice and consent of the Council, for the purpose of holding meetings and promoting coöperation. The affairs of such local sections shall be entirely in their own hands.

Article VIII. Meetings

There shall be an annual meeting of the Society and such other meetings as may be called by the Council. The annual meeting shall be held, whenever practicable, at the same time and place as that of the Geological Society of America.

Article IX. Revision of the By-Laws

After recommendation by the Council, by-laws may be enacted, amended or suspended by a two-thirds vote, by ballot, of those voting. Those by-laws affecting fellows only shall be voted on only by fellows. All others shall be voted on by the general membership.

NOMINATIONS OF OFFICERS FOR 1951

President: Adolf Pabst, University of California, Berkeley, California.
Vice-President: Michael Fleischer, U. S. Geological Survey, Washington, D. C.
Secretary: C. S. Hurlbut, Jr., Harvard University, Cambridge, Massachusetts.
Treasurer: Earl Ingerson, U. S. Geological Survey, Washington, D. C.
Editor: Walter F. Hunt, University of Michigan, Ann Arbor, Michigan.
Councilor (1951–54): George T. Faust, U. S. Geological Survey, Washington, D. C.

The above Fellows have been nominated by the Council as officers of the Mineralogical Society of America for 1951. They will be voted on at the election in October 1950.

C. S. Hurlbut, Jr., *Secretary*

A new geochemical journal, *Geochimica et Cosmochimica Acta*, is being published by Butterworth-Springer, 436 Strand, London, W.C.2, England, under the editorship of Professor L. R. Wager. The journal is international in scope and the plan is to give prompt publication to geochemical papers from all over the world. They will be published in English, French or German, with English summaries. Authors are to be given 75 reprints free of charge. Manuscripts should be sent to Earl Ingerson, U. S. Geological Survey, Washington 25, D. C., who is American editor for the new publication.

Subscription prices have not yet been announced, but the American agent is the Academic Press, Inc., 125 East 23rd Street, New York 10, New York, to whom inquiries should be addressed.

A natural occurrence of portlandite, $Ca(OH)_2$, has been found on the American Continent for the first time, at Cerro de La Corona, State of Morelos, Mexico. The mineral has been identified by geologists of the Instituto de Geologia of Mexico and of the U. S. Geological Survey. It occurs in a metamorphosed aureole in limestone around an extrusive basalt vent, probably of late Pleistocene age. A detailed mineralogic report by George T. Faust, Eduardo Schmitter, and Carl Fries, Jr., describing the occurrence and origin of the mineral, as well as the results of optical, chemical, x-ray, and thermal-analysis studies, will appear at a later date.

Dr. Duncan McConnell of the Gulf Research and Development Company has accepted a position as Professor of Mineralogy at the Ohio State University and will assume duties there at the beginning of the 1950–51 session.